Carderock Division
Naval Surface Warfare Center
West Bethesda, MD 20817-5700

CARDIVNSWC-TR-61-99-18 September 1999

Survivability, Structures, and Materials Directorate
Technical Report

ADVANCED MEASURES TO CONTROL GALVANIC CORROSION IN PIPING SYSTEMS

by

David A. Shifler

CARDIVNSWC-TR-61-99-18 ADVANCED MEASURES TO CONTROL GALVANIC CORROSION IN PIPING SYSTEMS

REPORT DOCUMENTATION PAGE

Form Approved
OMB No. 0704-0188

1. AGENCY USE ONLY (Leave blank)	2. REPORT DATE	3. REPORT TYPE AND DATES COVERED
	August 1999	Research and Development

4. TITLE AND SUBTITLE
ADVANCED MEASURES TO CONTROL GALVANIC CORROSION IN PIPING SYSTEMS

5. FUNDING NUMBERS
NSWCCD: 1-613-766
1-613-866

5. AUTHOR(S)
David A. Shifler

7. PERFORMING ORGANIZATION NAME(S) AND ADDRESS(ES)
Carderock Division
Naval Surface Warfare Center
9500 MacArthur Blvd.
West Bethesda, MD 20817-5700

8. PERFORMING ORGANIZATION REPORT NUMBER
CARDIVNSWC-TR-61-99-18

9. SPONSORING/MONITORING AGENCY NAME(S) AND ADDRESS(ES)
Dr. A. John Sedriks
Office of Naval Research
Code 332
800 N. Quincy Street
Arlington VA 22217-5660

10. SPONSORING/MONITORING AGENCY REPORT NUMBER

11. SUPPLEMENTARY NOTES

12a. DISTRIBUTION/AVAILABILITY STATEMENT
Approved for public release; distribution is unlimited

12b. DISTRIBUTION CODE
Statement A

13. ABSTRACT (Maximum 200 words)

Mixtures of piping materials have been used in several piping systems during ship retrofitting . The use of dissimilar alloys may initiate galvanic corrosion of the more anodic member which could lead to piping failures. Several control methods have been applied which may introduce secondary corrosion and require periodic inspection and replacement. This study investigated several newer galvanic corrosion control (cathodic protection, barrier coatings, bi-electrode) methods, by the use of mockup piping tests to monitor their effectiveness and performance in flowing, natural seawater from 6 to 20 months. Use of a space spearator, cathodic protection, the bi-electrode, and the application of an organic or sealed anodized coating on the cathodic member of the couple were effective to varying degrees (30 to 99% effectiveness) in controling galvanic corrsoion. These newer methods may provide alternative galvanic corrosion control techniques that may allow selective use of mixed piping systems with a minimization of shutdowns for removing, inspecting, and replacing system components.

14. SUBJECT TERMS
Corrosion, galvanic corrosion, 70/30 Cu-Ni, piping, Alloy 625, titanium, bi-electrode, marine corrosion, corrosion control, cathodic protection

15. NUMBER OF PAGES
91

16. PRICE CODE

17. SECURITY CLASSIFICATION OF REPORT	18. SECURITY CLASSIFICATION OF THIS PAGE	19. SECURITY CLASSIFICATION OF ABSTRACT	20. LIMITATION OF ABSTRACT
Unclassified	Unclassified	Unclassified	Unclassified

TABLE OF CONTENTS

LIST OF TABLES

LIST OF FIGURES

ABSTRACT

Mixtures of piping materials have been used in several piping systems during ship retrofitting. The use of dissimilar alloys may initiate galvanic corrosion of the more anodic, electronegative member which could lead to piping failures. Several control methods have been applied which may introduce secondary corrosion and require periodic inspection and replacement. This study investigated several newer galvanic corrosion control methods (cathodic protection, space separation of the anodic and cathodic members of the couple, barrier coatings, bi-electrode), by the use in mockup piping tests to monitor their effectiveness and performance in flowing, natural seawater from 6 to 20 months. Use of a space separator, cathodic protection, the bi-electrode, and an organic and anodized coating on the cathodic member of the couple were effective to varying degrees (30 to 99% effectiveness) in controlling galvanic corrosion. These newer methods may provide alternative galvanic corrosion control techniques that may allow selective use of mixed piping systems with a minimization of shutdowns for removing, inspecting, and replacing system components.

ADMINISTRATIVE INFORMATION

This project was funded under the Surface Ship Materials Technology Program sponsored through Dr. John Sedriks of the Office of Naval Research (ONR) under Element 62234N. Work was conducted in the Marine Corrosion Branch under the direction of Mr. Robert J. Ferrara.

ACKNOWLEDGEMENTS

The author would like to thank David East and Jim Chrzan of the LaQue Center for Corrosion Technology - under the direction of Mr. Dennis Melton - who constructed the test loops and conducted the testing of the piping mockups. Scott Marshall of LCCT performed the SEM and EDS analysis of the organic and anodized coatings. David Greenlaw conducted the pipe thickness measurements at CDNSWC after the mockup exposures. I would also like to recognize Dr. Harvey P. Hack who was the initial project engineer and provided advise after his departure from CDNSWC.

INTRODUCTION

The coupling of dissimilar alloys in conducting, corrosive solutions such as seawater can lead to accelerated, galvanic corrosion of the more anodic, electronegative alloy and protection of the more cathodic, electropositive alloy. The driving force for galvanic corrosion is the potential difference between two or more metals or alloys in a conductive medium that generates current flow between the anodic and cathodic members. The extent of galvanic corrosion between two or more coupled dissimilar alloys depends on other, sometimes very localized, factors such as the effective area ratio of the anodic versus cathodic members, solution conductivity, mass transport, solution flow characteristics, temperature, component geometry, the stability of passive films, the magnitude of the potential difference between the dissimilar alloys, oxygen content of the solution, and the cathodic efficiency and polarization characteristics of the more noble metal or alloy [1, 2].

Any metal or alloy immersed in a given conductive electrolyte and allowed to reach steady state conditions has a distinct potential. When two different alloys are coupled together, the alloy with the more negative potential undergoes anodic dissolution. This oxidation process results in an excess of electrons, which flow through the metallic path to the more positive alloy. On the surface of the more positive alloy, these excess electrons are consumed by a cathodic reaction that, in seawater, is usually oxygen reduction. The Galvanic Series is a list of corrosion potentials for various alloys and metals in a given electrolyte under defined conditions [3]. It is useful as a first attempt for predicting the possibility of galvanic corrosion and possible driving force of galvanic corrosion when two or more alloys are coupled in the same environment. The Galvanic Series is useful for predicting which metal/alloy will be anodic and which will be cathodic when the two alloys are coupled in the same environment.

Use of dissimilar pipe alloys for cooling system piping on ships has the potential to cause corrosion at each change-of-material interface. Current design of ship classes includes an inspection/waster piece at the most corrosion prone area of each interface. These waster pieces are thicker than normal gauge piping, are inspected periodically, and replaced when excessive corrosion has occurred. This process is expensive and requires shutdown of critical ship systems.

The use of the present waster pieces does not eliminate the possibility of corrosion-induced wall thinning in piping systems. Galvanic isolation and electrically isolated separator pieces may not always be viable corrosion control options due to the complexity or limited available space of the piping systems.

There are several basic techniques of mitigating galvanic corrosion: (1) selection of materials close to one another in the Galvanic Series; (2) change of environment; (3) break the conductive path between the coupled alloys; (4) design junctions to minimize crevices and promote advantageous geometry and area ratios; and (5) alter the respective overall cathodic or anodic reactions by coatings or cathodic protection [4]. In controlling galvanic corrosion in piping systems several issues must be considered. First, the selection of alternative alloys for Naval systems is often not practical due to their differing general corrosion resistances or incompatible mechanical properties. Second, a change of environment effected by adding inhibitors or deaerating seawater is not practical because they often require continuous application leading to high operational costs. Third, electrical isolation of dissimilar alloys must eliminate all alternative electrical pathways to be effective. Fourth, avoid threaded joints, particularly with materials far apart in the Galvanic Series. Brazed or welded joints are preferred to avoid crevices. The total cathodic and anodic currents must be equal i.e. $i_c A_c = i_a A_a$ where i_c and i_a are the current densities of the cathodic and anodic reactions respectively, and A_c and A_a are the cathodic and anodic areas. Fifth, coatings on the cathodic member are effective by promoting a favorable cathodic to anode area ratio. The cathodic currents generated by the smaller effective cathode area are spread over a much larger anodic area ($i_a = i_c A_c/A_a$ where $A_c/A_a <<< 1$). Coatings of the anodic member of a galvanic couple should be avoided because unfavorable area ratios may occur if the coating on the anodic member develops holidays. Galvanic relationships between different alloys may be altered in sulfide-polluted seawater [5]. Uncoupled copper-nickel alloys exposed to flowing, sulfide-polluted seawater have experienced increased pitting and accelerated corrosion [6,7].

Previous work on galvanic corrosion control measures has been preformed by CDNSWC. A study for up to 2 years was conducted to determine the long-term effects of coupling a titanium

alloy to several common marine machinery and structural alloys in quiescent and flowing seawater [8]. Commercial copper alloys when coupled to a titanium alloy in both quiescent and flowing unpolluted seawater showed increased corrosion by factors of 2 to 20. Nickel-based alloys 625 (UNS N06625) and C-276 (UNS N10276) experienced no measurable pitting, either uncoupled or coupled to a titanium alloy under flowing or quiescent conditions. Copper-nickel piping when coupled to a titanium condenser led to unacceptable, accelerated galvanic corrosion [9]. Use of short 70:30 copper-nickel or alloy 625 2-in. diameter (5-cm) piping sections, which are electrically isolated on either side between the dissimilar alloys, reduced galvanic corrosion by increasing the electrical resistance of the seawater, ionic current path. Three-foot (100 cm) separators reduced metal loss by 50 to 60 percent in 2-in. (5-cm) diameter piping [10].

Alternative galvanic control methods that could eliminate the need for inspection, improve safety, and control corrosion in piping systems were investigated. Mitigation of galvanic corrosion would provide ship designers with more materials options within piping systems. Several possible candidate methods for controlling galvanic corrosion were investigated: (1) coating the cathodic member of the couple (alloy 625 or titanium) to reduce the overall cathodic reaction; (2) use of a dielectric or metallic spacer placed between the cathodic to the anodic members of the couple; (3) cathodic protection applied to the more anodic member of the galvanic couple; and (4) use of a bi-electrode device between the anodic and cathodic piping members of the dissimilar alloy interface.

This report summarizes the effectiveness and performance of calcareous, organic, and anodized coatings applied on titanium piping, increasing the resistance path between dissimilar alloys, cathodic protection, and the use of a bi-electrode device in controlling galvanic corrosion when coupled to 70/30 copper-nickel piping. The use of rapid polarization has been routinely used for offshore structures in connection with cathodic protection systems because of the formation of calcareous deposits that act as a natural coating and reduce current demand. The application of an initially high cathodic current density to steel has resulted in the formation of very protective calcareous deposits in natural seawater [11-17]. These deposits require lower subsequent long-term current densities to maintain adequate protection to the steel components than if lower initial current densities were first applied. An optimum potential of -1.00 V(SCE)

provided adequate protection. While hydrogen is generated at potentials < -0.7 V(SCE), the calcareous deposits may protect against hydrogen adsorption by titanium and form a barrier to galvanic corrosion by reducing the effective cathodic area involved in the galvanic couple. A commercial organic coating and a thick anodized titanium oxide coating were also evaluated for their effectiveness in controlling galvanic corrosion. Some of the results have been published previously [18,19].

Cathodic protection has been used extensively in controlling corrosion in many environments. Galvanic corrosion is controlled by driving the potential of the more active member of the galvanic couple electronegatively into its cathodic region. A new, unique design for controlling galvanic corrosion involves using a ring anode and a ring cathode in a spool piece located between dissimilar pipes. An external power supply is used to adjust current in the bi-electrode device (from the anode to the cathode) to cancel the electric field gradients caused by the galvanic potential difference between the piping materials, thereby reducing or eliminating galvanic corrosion between the piping materials. The bi-electrode also can be used as a cathodic protection device, by making both ring electrodes anodic relative to the surrounding piping.

THEORY OF OPERATION OF THE BI-ELECTRODE

The bi-electrode concept was conceived at CORROSION/95 during discussions of a paper [20] between Dr. John Beavers and Dr. H.P. Hack.

When two dissimilar metal pipes are electrically connected in seawater, the potential difference between them causes a galvanic current to flow through their connection. To complete the galvanic circuit and maintain charge neutrality, an equal ionic current must flow through the seawater path that separates them. The flow of current through the slightly resistive seawater creates an IR drop between the anodic pipe and the cathodic pipe, resulting in a potential gradient between the piping segments in seawater.

A bi-electrode device (BED) is a pair of ring electrodes which is inserted between the anodic and cathodic pipes, and electrically isolated from both. A schematic of the device is shown in

Figure 1. A current is applied between the electrodes of the BED, generating a potential gradient which counters the ionic current from the galvanic couple. By proper adjustment of the bi-electrode current, the total potential gradient between the anodic and cathodic pipes can be made equal to the difference in their freely corroding potentials. The anodic pipe is exposed to the potential of the cathodic pipe plus the bi-electrode-induced potential gradient, the sum of which has been adjusted to be the same as the anodic pipe's free corrosion potential. The anodic pipe will therefore not have any driving force for galvanic corrosion, as the cathodic pipe has been "screened" from it by the bi-electrode potential gradient.

The advantages of a bi-electrode are: (1) it does not require that the anodic and cathodic pipes be mechanically separated to remove the electrical connection; (2) it does not require a physical separation between anodic and cathodic pipes apart from that introduced by the presence of the bi-electrode itself; (3) it does not "throw" current into the anodic or cathodic pipes and so does not have a limited area that it can protect; and (4) it requires no electrical connection to the anodic or cathodic pipes themselves.

The disadvantages of the bi-electrode are that it must be physically placed between the anodic and the cathodic pipes, it requires an external power supply, and it will cause corrosion if hooked up backwards (like a cathodic protection system) or if operated at too high a current.

A major goal of this investigation was to test the feasibility and efficacy of the bi-electrode concept on a full scale piping system. The purpose of this study was to investigate the effectiveness of this and other newer countermeasures in controlling galvanic corrosion in piping systems. This was to be achieved by determining the magnitude and distribution of galvanic corrosion of 70:30 copper-nickel piping when coupled to Alloy 625 or titanium piping.

EXPERIMENTAL PROCEDURE

Mockup Loop Construction

A series of piping mockups was constructed to simulate the most probable geometry and environmental conditions in the piping system of interest. Twelve piping mockups were initially designed with either Alloy 625 or titanium coupled to 70:30 copper-nickel piping as shown in

Figure 2. These mockups were constructed and tested at the LaQue Center for Corrosion Technology (LCCT), Wrightsville Beach, NC. Most of the mockups were operated for a period of one year. A schematic of the initial mockup loops is illustrated in Figure 3.

Ten-foot, 2-in (5-cm) diameter pipe sections of each material were procured. For 70:30 copper-nickel, type 1 seamless tubing was procured in accordance to MIL-T-16420K, grade 1 [21], except that the wall thickness and inside diameter were required to be that of 2-in. diameter pipe. Titanium piping was procured according to ASTM B-337 Grade 2 specifications [22]. Alloy 625 welded piping was procured to ASTM B705-82, class 2 [23] specifications. The thickness of all nominal 2-in pipes was Schedule 40.

The main seawater supply to the mockup assembly was nominal 6-in. (15 cm) polyvinyl chloride (PVC) pipe. Service to the individual piping loops was accomplished by tapping the 6-in manifold PVC pipe with 4-in. (10 cm) tee connectors. Nominal 2-in. (5 cm) PVC globe valves were used, along with nominal 4-in. by 2-in.(5 cm) reducers, to regulate the seawater flow to each mockup. A rotameter (Figure 4) was inserted in the discharge end of each mockup and examined daily to monitor seawater flow and help maintain flow at 6 fps (1.8 m/s) during the entire test period. Seawater flow was once-through and independent for each mockup loop. Ambient seawater temperature flowing through the piping mockups at Wrightsville Beach ranged from 7 to 28 °C. In addition to temperature, other seawater variables during the duration of the exposure tests such as dissolved oxygen content, pH, and salinity were monitored as shown in Figures 5 and 6.

The original twelve piping mockups were designed with either 10-foot (300 cm) sections of titanium or alloy 625 coupled to 10-foot lengths of 70:30 copper-nickel (Figures 1 and 2). The piping legs of six mockup loops were electrically isolated with a 0.25-in (0.6 cm) length of PVC 2-in diameter pipe to allow ZRA measurements between the pipes. In the other six loops a 10-in long PVC spacer or the bi-electrode device of the same length was placed between the piping sections. The various connections between the dissimilar alloy sections are shown in Figure 7. A coal tar epoxy coating was applied on about 6 inches (15 cm) of the outer pipe surfaces of both the inlet and outlet ends and covered by a piping sleeve to minimize seawater exposure and

mitigate any corrosion that would otherwise generate galvanic currents within possible crevice sites. A 2.5-in. (6.4 cm) diameter nylon-reinforced black rubber hose was placed over each of the pipe ends, and connected to the piping sections and the PVC spacers. The sleeves were secured with care by two band clamps for each joint to minimize the formation of crevices and ensure leak free connections. PVC spacers about 10-in. (25 cm) long were placed at the discharge to compensate for the difference of spacer length between the dissimilar alloy piping sections. Each piping condition with or without an applied galvanic corrosion countermeasure was tested in duplicate.

The bi-electrode device was initially conceived to be two platinized titanium rings embedded in a 10-in (25 cm) section of 2-in PVC pipe prevent local flow disruptions (Figure 3). The platinized ring electrodes were 4-in wide and spaced 2 in apart. Wires on the outside were connected to an external power source so that the device could act as either a cathodic protection device or as a bi-electrode capable of stopping the galvanic current flow. In the cathodic protection (CP) mode, a cathodic current of 200 μA was initially applied; eventually, after 12 days 20 mA was applied between both ring electrodes in parallel and the copper-nickel pipe section to examine the effects of cathodic protection applied to dissimilar metal piping couples. In the bi-electrode mode, current was applied from the ring anode to the ring cathode of the bi-electrode of sufficient magnitude to reduce and eliminate the galvanic ionic current flux between the Alloy 625 and the 70-30 copper-nickel pipes. Two separate piping mockups loops used the bi-electrode in this way.

Calcareous deposits were formed on two titanium pipes in slowly flowing natural seawater (<1.0-fps) by connecting two 10-foot (300 cm) sections of titanium pipe to zinc anodes for a period of two weeks. Enamel paint was sprayed on the outside titanium surfaces to minimize current demand on the anodes and to prevent deposits from forming on the exterior. Two anodes were used, one on the upstream end and the other on the downstream end. The mixed potential of the titanium pipe/zinc couple was -1.045 V(SCE).

After approximately one year, tests of ten of the twelve piping mockups were terminated. Two piping mockups continued for another 8 months: pipe loop #1 was bare titanium coupled to

70/30 copper-nickel while pipe loop #8 had a calcareous deposit coating on the titanium piping section that was coupled to a 70:30 copper-nickel pipe.

Two new piping mockups were designed with either 8 or 10-foot (240 or 300 cm) sections of titanium coupled to 8-foot lengths of 70:30 copper-nickel (see Table 1). A titanium pipe was coated with an organic, urethane-based Ticomp™ 10 coating and another titanium section was coated with an anodized TiO_2 (Tiodize™ Type IV). Both of these piping loops were exposed for 6 months. The piping legs of all the pipe sections near the couple were covered with a coal tar epoxy coating over about 6 inches (15 cm) of both the inlet and outlet ends of the outer pipe surfaces to minimize seawater exposure and mitigate any corrosion that would otherwise generate galvanic currents in a possible crevice area. A 2.5-in diameter nylon-reinforced black rubber hose was placed over each of the pipe ends, and connected the piping sections and the PVC spacers. The sleeves were secured with care by two band clamps for each joint to minimize the formation of crevices and ensure leak-free connections.

The organic, urethane-based (Ticomp™ 10)[1] and anodized titanium oxide (Tiodize™ Type IV with an inorganic PTFE-based Tiolon™ X-40 final coat/sealer conforming to AMS 2488C specifications [24]) coatings were applied by Tiodize Co., Inc. (Huntington Beach, CA) on titanium piping sections previously exposed for one year in flowing seawater. Prior to placing the respective coating on the titanium sections, the pipes were thoroughly cleaned. After cleaning and prior to applying the organic coating, the titanium pipe was grit blasted with 120 mesh abrasive, abraded with Scotch-brite™[2], and a primer applied. Prior to anodizing the other titanium pipe, it was degreased with a hot alkaline soap and rinsed. The organic urethane-based coating was applied on both inside and outside pipe surfaces, while the other titanium pipe was masked on the outside and anodized coating applied only on the inner pipe surface. A complete listing of the fourteen piping mockups is summarized in Table 1.

[1] Tiolon, Ticomp, and Tiodize are registered trademarks of Tiodize, Co., Inc.
[2] Scotch-brite is a registered product of 3M Corporation.

Galvanic Current Measurements

Galvanic current measurements were made between the outer surface of the 70:30 copper-nickel and the titanium pipe or Alloy 625 sections on all piping mockups via connections on each pipe. A zero-resistance ammeter (ZRA) was used for all current reading measurements. Current measurements were made daily during the first week and then weekly over the remainder of the mockup exposure. The ZRA was connected only when the readings were actually taken. Otherwise, the dissimilar outer pipe sections were electrically coupled by external wiring. To avoid current flow interruptions while connecting the ZRA, the ZRA was first connected in parallel to the regular wiring system. Then the normal wiring was disconnected while the current

Table 1 – Mockup Piping Configurations (Flow Rate - 6 fps (1.8 m/s))

Piping Mockup Designation	Pipe Condition, Length	70:30 CuNi Length	Exposure Time
Pipe 1	Titanium Bare, 10 ft. (300 cm)	10 ft.(300 cm)	637 days
Pipe 2	Calcareous Deposit on Titanium, 10 ft	10 ft	365 days
Pipe 3	Bare Alloy 625 –10 ft, CP with bi-electrode	10 ft	340 days
Pipe 4	Bare Alloy 625 –10 ft, bi-electrode operation	10 ft	343 days
Pipe 5	Bare Alloy 625 –10 ft 10-in PVC spacer	10 ft	379 days
Pipe 6	Bare Alloy 625 –10 ft	10 ft	379 days
Pipe 7	Bare Titanium, 10 ft.	10 ft.	379 days
Pipe 8	Calcareous Deposit on Titanium, 10 ft	10 ft.	623 days
Pipe 9	Bare Alloy 625- 10 ft, CP with bi-electrode	10 ft	340 days
Pipe 10	Bare Alloy 625 –10 ft, bi-electrode operation	10 ft	343 days
Pipe 11	Bare Alloy 625 –10 ft 10-in PVC spacer	10 ft	379 days
Pipe 12	Bare Alloy 625 –10 ft	10 ft	379 days
Pipe 13/3	TI-COMP™ 10 coating, Titanium 8 ft. (240 cm)	8 ft. (240 cm)	188 days
Pipe 14/9	Tiodized™ Type IV anodized coating, 10 ft.	8 ft.	188 days

flow was measured by the ZRA. The regular wiring was reconnected before the ZRA wiring was disconnected after the measurement.

The applied current of the bi-electrode was manually adjusted to maintain a galvanic current between Alloy 625 and 70:30 copper-nickel section below 5 μA. During one two-week period, the galvanic currents in the bi-electrode mockups were monitored daily to evaluate the effectiveness of more frequent applied current corrections with the bi-electrode.

Potential Measurements

Potential measurements versus distance along the piping sections were made several times during the exposure on all of the mockups. The measurements were made in 1-ft increments (30-cm) from the seawater inlet end of the titanium or Alloy 625 pipe along most of its length. For loops with only the 0.25-in spacer between the dissimilar pipes, the potential was measured in one-inch (2.5 cm) increments over a span of about 6 inches (15 cm) of the titanium or Alloy 625 outlet and 6 inches (15 cm) along the copper-nickel inlet; measurements were made in 1-ft (30 cm) increments over the remainder of the copper-nickel section to the discharge end. In the loops with the bi-electrode or the 10-in long PVC spacer, the one-inch increments coincided mostly with the PVC spacer or the bi-electrode.

The potential measurements were made using a Luggin-Haber probe with an Ag/AgCl reference electrode. The probe was inserted in a mockup by opening a piping plug on the seawater inlet end and replacing it with the probe. This was accomplished without disturbing the flow to the other mockups.

The selected mockup was individually isolated by shutting off the inlet water of the selected mockup with the globe valve. Once the Luggin probe was installed, seawater flow was resumed and after the mockup had stabilized, the potentials were measured. Initially, potentials were measured by traversing the mockup length from inlet to outlet ends of both cathodic and anodic piping section, respectively, but a second traverse was made to verify that the probe intrusion during the first traverse had not influenced the potential readings.

Post Mockup Test Examinations

The mockup loops were examined periodically and photographed at the titanium or Alloy 625 section outlets and/or copper-nickel inlets if heavy deposition or corrosion were noted. After the conclusion of the piping exposures, the pipe mockups were disassembled and visually examined for the presence of corrosion product films and fouling. The orientations of the pipe sections were marked for later reassembly. Two-foot (60-cm) sections from the inlet end (end adjacent to the titanium or Alloy 625) of the copper-nickel piping were cut and analyzed at CDNSWC for determination of the material losses from galvanic interactions. From earlier examinations the two-foot (60-cm) copper-nickel sections were significantly longer than the observed effective galvanic length and area where material losses and corrosion were noted. Each copper-nickel pipe section was split longitudinally to expose the top and bottom sides as they had existed during mockup testing. First, the split piping sections were photographed to document their appearance in the 'as received' condition. The waterside surface deposits and scales on the copper-nickel piping were cleaned with a 10 % nitric acid solution followed by rinsing with hot tap water. The wall losses were mapped by compiling micrometer measurements in a grid pattern marked by every 0.5" (1.25 cm) along the pipe length and circumferentially every 0.63" with 0.00" corresponding to the top, 12 o'clock orientation of the pipe. These rather coarse surface grids missed some deeper pits and corrosion sites, but the locations of these more severe surface losses were recorded separately using the same grid location system. In general, the pipe thickness was not uniform around the pipe circumference. In most cases, the micrometer measurements were compensated linearly for the copper-nickel pipe samples.

Physical measurements were made to map the distribution and depth of corrosion attack along the pipe interiors. Both the urethane-based and anodized titanium oxide coatings were examined after the six-month exposures by scanning electron microscopy (SEM) and analyzed by X-ray energy dispersive spectroscopy (EDS) to determine the elemental and adherence characteristics of the coatings to the titanium substrate after seawater exposure.

RESULTS

Mockup Current Measurements

The galvanic currents of the couples between uncoated titanium and 70:30 copper-nickel piping sections (loops 1 and 7) were initially below 100 μA, as shown in Figure 8. The effective length of galvanic interaction was both unknown and changed with time as biofilms, deposits, and environmental changes occurred during the current measurements, therefore the currents were not normalized by area. The currents gradually increased during the first month of exposure. After one month, a sharp rise in the galvanic currents occurred - peaking at over 6000 μA after 50 days' exposure. Loops 1 and 7 displayed decreasing galvanic currents after 50 days and approached steady-state values of about 1000 μA and 2000 μA respectively after 12 months exposure. An additional 8 months (day 379 to day 637) of exposure of mockup loop 1 maintained steady state galvanic currents of about 1000 μA despite changing seawater temperatures, salinities, and oxygen contents.

The galvanic currents measured between the titanium pipe sections with calcareous deposits and the 70:30 copper-nickel piping sections were relatively high (56-312 μA) during the first month, but quickly settled to 25 to 40 μA after 36 days' exposure (Figure 9). The currents eventually decreased to 8-11 μA when the flowing natural seawater temperature was 7-10 °C. When the seawater temperatures increased, the resultant galvanic currents gradually increased from 8 μA to 164 μA in loop 2 and from 11 μA to 96 μA in loop 8. These increasing currents may have been caused by calcareous deposits flaking from the titanium surface, decreased calcareous deposit thickness due to an increased deposit solubility in warmer seawater, or enhanced O_2 diffusion through the calcareous deposits. After a one-year exposure, the galvanic currents were 167 μA and 38 μA for loops 2 and 8, respectively. After 12 months, titanium piping with calcareous deposits coupled to copper-nickel piping displayed decreased galvanic currents by a factor of 15 to 40 as compared to initially bare titanium/copper-nickel couples.

The exposure of loop 8 was continued for another 8 months (day 365 to 623) to evaluate the influence of the calcareous deposits for a longer exposure time. The galvanic currents remained low until day 475 after which the galvanic current began to rise slowly with increasing water

temperature. As Figure 9 shows, the galvanic currents continue to increase until the galvanic currents from loop 8 (calcareous titanium coupled to 70:30 copper-nickel piping) were similar to bare titanium coupled to copper-nickel (loop 1).

The galvanic currents from the interaction between Alloy 625 and 70:30 copper-nickel are presented in Figure 10. There was a general current increase from 100 μA after 1 hour exposure to over 1500 μA after 50 days for both loops 6 and 12. The behavior of loops 6 and 12 differed after 60 days exposure. The measured galvanic currents from loop 6 quickly increased from 1800 μA by day 64 to 5700 μA after 72 days exposure and gradually decreased to 3700-3900 μA after 246 days. Afterwards, the galvanic currents fluctuated between 3600 and 5200 μA from 246 days to day 379. On the other hand, the measured galvanic currents of loop 12 gradually increased from 718 μA after 64 days exposure to 4800 μA after 162 days. Galvanic currents from loop 12 never reached a steady state condition over the 379 days that the mockup was operational; the currents fluctuated between 3600 and 6700 μA.

The measured galvanic currents versus time from the Alloy 625 and 70:30 copper-nickel piping sections were coupled, but separated by a 10-in PVC spacer (loops 5 and 11) are displayed in Figure 11. The currents increased gradually to 1000 μA during the first 35 days of exposure in the mockup testing loops. The currents rose abruptly to 4400-4800 μA in day 37 in both mockups and gradually decreased to 1900-2200 μA after exposures of 190 days. Currents slowly increased to 2800 and 3600 μA in loops 5 and 11 respectively as the seawater became warmer. From 220 to 379 days the currents fluctuated between 2000 and 3000 μA in loop 5 while in loop 11 the measured galvanic currents undulated between 2500 and 3500 μA. The 10-in.(25 cm) PVC spacer decreased the average galvanic currents by about 20 to 50 percent as compared to the Alloy 625/Cu-Ni couples of loops 6 and 12 where the longer dielectric spacers were absent.

Cathodic protection was applied to the 70:30 copper-nickel segment of mockups loops 3 and 9 using the bi-electrode as an impressed current anode between the piping segments. Application of 200 μA for 12 days reversed the natural galvanic currents in seawater from copper-nickel to Alloy 625. However, this was short-lived, as the galvanic currents from the 625/70:30 copper-

nickel couple gradually increased with time, as shown earlier. The galvanic currents eventually exceeded the impressed current supplied by the bi-electrode. During exposure day 12, the impressed cathodic protection current was increased to 20 mA. The resultant currents measured after cathodically protecting the Alloy 625-70/30 copper-nickel galvanic couples are shown in Figure 12. The currents measured between the copper-nickel and Alloy 625 piping sections slowly increased after raising the protection current to 20 mA. During day 12 the galvanic currents were about 5700 μA and mostly increased with time for both mockup loops 3 and 9. The maximum currents between Alloy 625 and 70:30 were 15800 and 14600 μA in loops 3 and 9 respectively, but appeared to be settling to about 11000 to 12000 μA at 340 days exposure.

Current was applied from an external source to the bi-electrode device (BED) to establish a potential gradient and form an electric field which opposed the natural galvanic ionic current flux. The attempt was to keep the resultant galvanic current at or near zero (± 5 μA) by manually adjusting the current between the bi-electrodes at prescribed time intervals. Usually adjustments were done weekly. The current applied to the bi-electrodes is shown in Figure 13. The applied currents between the bi-electrodes varied with time. The initial applied currents required to provide zero resultant current between the Alloy 625-70/30 copper-nickel were 7.5 mA and 9 mA for mockups 4 and 10 after 20 and 15 days, respectively. The applied bi-electrode currents in mockup 4 increased to a maximum of about 34 mA at day 252 before reverting to lower applied currents over the final three months. The bi-electrode applied currents on loop 10 were 25.5 mA during day 252 and gradually increased in the final three months (to day 343) to 31 mA. This demonstrated that control of the galvanic currents was dependent on various, often very localized, factors that required frequent bi-electrode adjustments.

The net galvanic currents between the Alloy 625 piping section and the 70:30 copper-nickel with the bi-electrode fluctuated as shown in Figure 14. One-week exposure after the last manual current correction generally led to relatively high resultant galvanic currents of 5-890 μA. Adjusting the applied bi-electrode current returned the resultant galvanic current to within the test range goal of ± 5 μA. Galvanic currents from Loop 4 was more variable than loop 10. At one time, Loop 10 exhibited stability during one 2-month period while loop 4 required almost daily alteration of the applied bi-electrode currents. After 210 days of exposure, the required

applied currents for the bi-electrodes were 35 mA and 28.5 mA for loops 4 and 10 respectively. Increasing the frequency of current monitoring and modification of the applied bi-electrode currents from weekly to daily reduced the resultant galvanic current fluctuations (Figure 15). The resultant current changes during the daily monitoring were 0 to 51 μA. More frequent manual control indicated the importance of developing automated control of the BED to optimize galvanic corrosion control.

The galvanic currents generated between the Ticomp™ 10 (urethane-base) coated titanium and the coupled 70:30 copper-nickel piping as a function of exposure time are shown in Figure 16. The currents remained below 5 μA during the first 100 days. Currents increased after 100 days, but remained between 10 and 15 μA until the conclusion of the test (188 days). The currents from this coated titanium/70:30 copper-nickel piping couple were 1.5% or less than the steady-state galvanic currents generated from bare titanium/70:30 copper-nickel piping couples.

The galvanic currents of the titanium section with a thick anodized titanium oxide (Tiodize™ Type IV) on titanium section coupled to 70:30 copper-nickel versus exposure time are shown in Figure 17. The overall currents were ≤ 10 μA over the entire exposure period of 188 days and exhibited no evidence of increasing over that duration.

Mockup Potential Distribution Measurements

The potential profile along the bare titanium/70:30 copper-nickel piping mockup loops 1 and 7 vs. time are shown in Figures 18 and 19, respectively. Unless the segments have a different length (see Table 1), the 0 to 10-foot distance from the inlet in the potential profile figures are the Alloy 625 or titanium cathodic members of the piping loops and the 10 to 20-foot segments are the 70:30 copper-nickel segments. When the 10-in PVC spacer or the bi-electrode are utilized the copper-nickel sections are transposed downstream by about one foot (30 cm). The potential difference between the titanium and copper-nickel sections of loops 1 and 7 during the first 2 days exposure was less than 100 mV. The potential of the titanium leg at the inlet end was -133 to -143 mV(Ag/AgCl) while the potential of the copper-nickel leg was -190 to -213 mV. The potential profile of the mockup loops changed abruptly on exposure day 14. The potential of the

titanium section during day 14 reached a maximum of +284 mV for both loops 1 and 7 respectively. At day 14, about 4 ft (1.2 m) of the titanium pipe contributed to the galvanic couple while about 5 to 6 feet (1.5 to 1.8 m) of copper-nickel pipe was affected by the galvanic interaction. The potential difference between the titanium and copper-nickel sections was about 500 mV. The ennoblement of the titanium segment is likely due to the formation of biofilms [25-30]. At about 150 days and later, the potential of the entire 10-ft (300 cm) length of titanium was influenced by the galvanic interaction while the length of copper-nickel pipe affected by the couple was 4 to 5 feet (120-150 cm). The increase in the cathodic to anode area ratio could lead to greater dissolution of the copper-nickel alloy from the galvanic interaction.

The maximum potential of the titanium leg generally decreased with time, likely due to thicker organic films, slime, and deposits forming over the inner surface, since titanium is not inherently resistant to biofouling. The maximum titanium potential measured during the potential profile survey at 247 days was +82 mV. The potential of the copper-nickel piping at the interface with titanium was +95 mV during day 14. At day 451 the maximum titanium potential was +20 mV, and by day 637, the maximum potential was -40 mV. The minimum, most electronegative, copper-nickel potential usually varied from -70 to -120 mV after day 190 to the end of the exposure tests. Most of the galvanic corrosion damage from the couple, as discussed in a later section, occurred in the first 12-18 inches (30-45 cm) of the copper-nickel piping. The potential at the titanium/Cu-Ni junction also declined with time - the potential from 51 to 157 days diminished from 44 to 11 mV. At 247 days the potential at the junction of the couple was -95 mV. At day 247 the potential at the junction of the couple was -95 mV. During the period between day 157 and 247, a potential dip of 20 to 30 mV was observed in the copper-nickel leg about 1-2 feet (30-60 cm) from the junction with titanium. The reason for this potential drop is unknown at this time.

By day 351, the potential profile of the titanium/70:30 copper-nickel couples no longer displayed an reverse S-shaped curve, but was relatively flat and linear along the combined 20-ft (6 m) long titanium and copper-nickel piping sections. This flat potential profile between the titanium and copper-nickel sections continued through day 637 when the piping loop was disassembled. The potential difference from the titanium section inlet to the copper-nickel outlet

sections was 40-80 mV from day 351 to the end of the test (637 days). At that time, the potential of the titanium section was about –0.040 V (Ag/AgCl) and the copper-nickel section was –0.080 V. Although the copper-nickel may be at an electropotential in its anodic range, the formation of deposits on the titanium surface may effectively limit the cathodic reaction and subsequently the anodic reaction on the copper alloy. Lastly, the potential profile was dependent on flow velocity. The potential during day 157 was higher than measurements both before and afterwards due to a failure in the seawater supply pipe which had caused loss of flow for 4-10 hours before repair was completed.

The potential profile for calcareous deposit coated titanium coupled to 70:30 copper-nickel piping (loops 2 and 8) is illustrated in Figures 20 and 21, respectively. Initially, potentials along both the entire coated titanium and copper-nickel segments are depressed as compared to bare titanium coupled to 70:30 copper-nickel. The calcareous deposit appeared to reduce the effective cathode surface area and/or reduced the cathodic efficiency by diminishing the current flow through the barrier coating from oxygen or water reduction reactions. Since the total current derived from the cathode (titanium pipe area) must equal the total anodic area represented by the copper-nickel surface, the resultant galvanic corrosion was lower on the 70:30 copper-nickel pipe sections coupled to calcareous deposit coated titanium than if coupled to the bare titanium of the same overall area. The lower cathodic currents reduced the corresponding anodic currents from the copper-nickel piping surface substantially. The potential profiles also tended to be linear over the entire titanium/copper-nickel mockup length with the maximum potentials at the titanium inlet and the minimum at the copper-nickel outlet, suggesting that the calcareous deposits acted as a barrier to the ionic current diffusion to the titanium surface.

There appeared to be a gradual degradation of the calcareous barrier with time. This may have been due to some flaking of the deposit or because the deposit had thinned due to increased solubility as the seawater temperature increased. The potential at the calcareous deposit/copper-nickel junction of loop 2 increased from -309 mV after 1 hour exposure to -160 mV at 1-2 days, to -144 mV on day 119, to -99 mV after 233 days, although excursions to approximately 0 mV were measured at days 143 and 210. The junction potential of Loop 8 increased from -217 mV

after 1 hour to between -147 and -191 mV during 1 to 233 days exposure (the lone exception being day 206 when the measured junction potential was -61 mV). The potential profile measurements would suggest that higher galvanic currents and corresponding galvanic corrosion of the copper-nickel pipe would be expected on mockup loop 2 than on loop 8. The current measurements of loops 2 and 8 confirm this observation.

The potential profile of loop 8 remained somewhat linear for 437 days; on day 437 the potential ranged from -60 mV(Ag/AgCl) at the titanium inlet to -65 mV 20 ft (600 cm) downstream at the copper-nickel outlet. On day 532, the titanium leg became ennobled (-30 mV) relative to the copper-nickel piping section; a potential difference between the dissimilar piping sections was 30 mV. The potential difference between the titanium and copper-nickel piping sections continued to increase from day 437 until the end of the mockup testing (day 623), primarily because the measured potential in the copper-nickel pipe dropped to about -110 to -120 mV. On day 623 the potential difference between the titanium and 70/30 copper-nickel segments was 80 mV, thus providing a possible increased driving force for enhanced galvanic corrosion.

The potential profile of an Alloy 625/70:30 copper-nickel mockup (loops 6 and 12) are illustrated in Figures 22 and 23. Little polarization of the copper-nickel section by the alloy 625 was observed during the first two days of exposure. Initially, the potentials of the 625 legs were from -110 to -200 mV while potentials of the copper-nickel piping sections stayed around -210 mV. However by day 14, the potential difference between the two dissimilar alloys in loop 6 was about 430 mV (+250 mV at the 625 segment versus –180 mV at the copper-nickel section) and The potential profile of the Alloy 625/copper-nickel couple began to resemble a reverse S-curve. The potentials of the Alloy 625 in both loops were unstable in flowing seawater during the next 50 days, ranging from -150 to +260 mV. The potentials of Alloy 625 in flowing seawater appear to have settled at day 100 to day 379 into a range of from +170 to +230 mV. The length of galvanic interaction along the 625 pipe was 6-7 feet (180-210 cm) while 5-7 (150-210) feet of copper-nickel piping was affected by the couple. The potential of the copper-nickel pipe leg tended to rise with time, although there was some fluctuations between -20 and -150 mV. Loop 12 behaved similarly, but the potential differences between alloy 625 and 70/30 copper-nickel

piping sections were never as great as loop 6; the maximum difference was about 390 mV at day 100 and decreasing until the potential difference was approximately 260 mV at day 379.

A 10-in long PVC spacer was placed between the Alloy 625 and 70:30 copper-nickel pipe sections of mockups 5 and 11. The potential profiles of the mockups are shown in Figures 24 and 25. The 10-in PVC spacer did not alter the shape of the potential profile between of the Alloy 625 and copper-nickel legs with exposure time as compared to the directly coupled (0.25" spacer) 625/70:30 copper-nickel loops described earlier. The potential of the 625 segments coupled to copper-nickel using a 10-in. spacer tended to be 20-60 mV lower than the 625 leg galvanically coupled to 70:30 (loops 6 and 12) with only the minimal 0.25-in PVC spacer. The longer PVC spacer tended to generate smaller potential differences between the dissimilar alloys in loops 5 and 11 than the 625/copper-nickel couples in loops 6 and 12.

The potential profile of the coupled Alloy 625/70:30 copper-nickel piping mockups under cathodic protection (loops 3 and 9) are presented in Figures 26 and 27. In this case, both of the electrodes of the bi-electrode device were used as impressed current anodes to apply current to the Alloy 625 and copper-nickel pipe. Initially, 200 μA were applied to the copper-nickel pipe which did not alter the potential profile from that observed in the other coupled Alloy 625/70:30 mockups during the first days exposure in flowing seawater. Increasing the impressed current to 20 mA during day 14 or day 16 (loops 3 and 9, respectively) resulted in a deep potential trough between the Alloy 625 and the copper-nickel piping sections. The potential minimum occurred at the bi-electrode/CP device. Initially, 20 mA of impressed current dropped the minimum potential at the bi-electrode to –630 to -670 mV versus Ag/AgCl. The depth of the potential well decreased and the minimum potential increased with time with the fixed 20 mA impressed current. The minimum potentials after 210 days were -320 to -335 mV for the two piping mockups under cathodic protection. Cathodic protection affected both dissimilar alloy legs by depressing the potential below their free corrosion potentials. Initially, the alloy 625 inlet potential was -150 mV, but gradually increased to +150 to +170 mV after 120-210 days. The potential at the copper-nickel outlet also increased from -240 mV initially to -60 mV for loop3 after 250 to 314 days and –20 mV for loop 9 after 315 days. At first, CP depressed the potential of the 625 segment over its entire 10-ft (300 cm) length, but after about 100 days exposure, only

6-7 (180-210 cm) feet were influenced by CP. Cathodic protection consistently affected about 5 feet of the 70:30 copper-nickel pipe. The rise in the minimum potential with time at a fixed impressed current led to shorter lengths of the copper-nickel piping being adequately protected; after 210 days only about two feet of the copper-nickel pipe was at or below its free corrosion potential.

The potential profiles (loops 4 and 10) caused by the bi-electrode on the galvanic couple between Alloy 625 and 70:30 copper-nickel is illustrated in Figures 28 and 29. The galvanic ionic current flux left from the more anodic member of the couple (copper-nickel) and flowed upstream towards the cathodic 625 pipe. A current was applied between the bi-electrodes so that an offsetting potential gradient generated an electric field between the two ring electrodes and countered the natural galvanic current flux between each BED electrode and its adjacent piping segment, thereby resulting in a zero net galvanic current flux. As mentioned previously, manual adjusting of the applied current between the bi-electrodes was required to counter the galvanic currents. The potential of the respective Alloy 625 and copper-nickel piping increased with time, which in turn, tended to increase the galvanic currents. This required applied current adjustments to the bi-electrode. The potential drop across the bi-electrode was typically very sharp - a potential decrease of nearly 400 mV could occur over a span of 7-8 inches (18-20 cm). The applied bi-electrode current on loop 4 was decreased from about 35 mA at day 225 to 22 mA by day 343 in order to maintain a zero net galvanic current flow. The effective galvanic lengths of dissimilar alloys interacting with one another is a dynamic process. As shown in the potential profiles of both loops 4 and 10, the potential of the alloy 625 section adjacent to the bi-electrode is generally more electropositive than at the inlet, while the potential of the 70:30 copper-nickel alloy is more electronegative near the bi-electrode device than several feet away from the device. This indicates that the applied current to the device electrode nearer the cathodic segment becomes a more effective cathode that the Alloy 625 so that an offsetting current flows from 625 cathode to the electrode nearest that alloy. The current applied to the device electrode nearest the 70:30 copper-nickel pipe becomes anodic to the copper alloy so that an induced current flux from this BED electrode to the copper-nickel alloy is generated and counters the galvanic ionic current flow from the copper-nickel alloy towards the cathodic pipe.

The potential profiles versus exposure time of the urethane-based Ticomp™ 10) and anodized titanium oxide (Tiodize™ Type IV) coated titanium/70:30 copper-nickel piping couple are shown in Figures 30 and 31, respectively. The potential profiles of both coated loops were linear over the entire 188-day exposure period. The initial potentials (after 1-hour exposure) of the titanium and copper-nickel piping sections were -200 to -220 mV(Ag/AgCl). After 2 days the potential of the titanium and copper-nickel piping sections became more noble by about 30 mV for the organic coated titanium loop while the anodized titanium oxide coated titanium mockup (loop 14/9) ennobled by 10 mV. The organic coated titanium/70:30 copper-nickel piping mockup (loop 13/3) displayed the most electropositive potential at day 97 (-100 to -90 mV from titanium inlet to copper-nickel outlet). The potential of loop 13/3 shifted to -145 to -135 mV just prior to termination of the mockup test at day 188. The potential of loop 14/9 increased at days 97 and 188 to -120 mV. The potential ennobled about 40 mV in the copper-nickel section at day 97; the reason for this potential change is not known at this time. These coatings appeared to be superior to the calcareous-deposit-coated titanium loops at similar exposure times.

Visual Examination

After exposure of the mockup loops was completed at LCCT, 2 or 4 feet from selected Alloy 625 or titanium sections were cut and sent to CDNSWC for visual examination. All copper-nickel sections were sent to CDNSWC where 1 to 2-foot section sections were cut. Both cathodic and anodic piping sections were cut into the top (T) and bottom (B) sections based on the positioning during the exposure tests.

As viewed in Figure 32, the 70:30 copper-nickel segment adjacent to the calcareous deposited titanium displayed no visual evidence of pitting or other unusual surface conditions after one year of seawater exposure. This is in stark contrast to the copper-nickel section couple to bare titanium (Loop 7). Apparent corrosion was found along the first six inches of the bottom half (Figure 32). The 70:30 copper-nickel sections coupled to bare Alloy 625 piping sections displayed very heavy copper alloy corrosion products along a one-foot segment adjacent to the cathodic piping member (Figure 33). As shown in Figure 34, several corrosion sites appear to

coincide with the heavy deposits at the copper-nickel inlet. Visually, the presence of the 10-inch long, nonconductive PVC spacer between the cathodic and anodic piping members decreases the degree of corrosion penetration and associated copper alloy corrosion products (Figure 35). The magnitude of seawater flow was insufficient to prevent macrofouling of the Alloy 625 piping section loop 11 (Figure 36).

Figure 37 shows the condition of the 2-foot inlet end sections (loops 3 and 9) of the 70:30 copper-nickel piping under the influence of cathodic protection. A tight scale has formed over much of the surface. After some cleaning (Figure 38), the piping sections indicate calcareous deposits have formed and that no inherent corrosion had occurred during the one-year exposure. Figures 39 and 40 displays the distribution of the calcareous deposits on both the top and bottom halves of the copper-nickel piping 9 to 16 inches away from the CP device. The calcareous deposits are not uniformly formed on either the top or bottom piping halves. However, as long as the cathodic protection system is operative and the potential below the free corrosion potential of 70:30 copper-nickel, the calcareous deposit will decrease the demand of the CP system. Figure 41 show the morphology of the calcareous deposit at those sites where it is present.

Copper-nickel piping sections (loops 4 and 10) under the influence of the bi-electrode operation exhibits very little scaling on the waterside surfaces (Figure 42) in the contrast to the copper-nickel surfaces under CP.. In addition to no scaling of the 70:30 copper-nickel, Figure 43 shows that no pitting or corrosion is found on the waterside surfaces.

Macrofouling occurred in many of the Alloy 625 and titanium piping sections. Both cathodic alloys are not natural antifoulants or biocides to marine organisms. The recommended velocities for the use of either Alloy 625 or titanium in natural seawater is above 6 m/s (20 fps) which is also about 30% above the maximum recommended (15 fps) velocity of straight sections of 70:30 copper-nickel piping. Figure 44 shows the level of macrofouling at one end of the titanium piping after one-year exposure. Upon opening that titanium piping section, Figure 45 displays macrofouling along two feet at the inlet end. The macrofouling on the titanium piping, shown in Figure 46, is tightly adherent. The outlet end of a Alloy 625 piping section also displays biofouling (Figure 47). Most of the macrofouling settled along the bottom half of the

piping (Figure 48). The cross-section of the macrofouling of a titanium pipe restricted water flow to about 25 to 35% of intended flow volume (Figure 49). This can cause flow disturbances and velocity permutations sufficient to cause erosion corrosion.

As mentioned before, one calcareous deposit-coated titanium piping loop was continued for an additional 8 months exposure so that the total exposure period was 20 months. During that additional, 8-month period, the measured galvanic currents increased to nearly the levels of the bare titanium/70:30 copper-nickel couple. Figure 50 shows the condition of the titanium pipe after 20 months exposure. It appears that the calcareous deposit is still present along the titanium interior piping surfaces. Though not present after 12 months, macrofouling had occurred during the 12-20 exposure period (Figure 51). Heavy mussel growth was observed on the bottom pipe half that could have been caused erosion of the calcareous deposits from the titanium surface. Increasing galvanic currents may also have been caused by decreased calcareous deposit thickness due to increased its solubility in warmer seawater or by enhanced ionic diffusion through the calcareous deposits.

Some thinning and flaking of the calcareous deposit (Figure 52) appeared to have been experienced during the additional 8 months of exposure which probably led to increased cathodic currents from the oxygen reduction reaction and associated increased anodic currents from the copper-nickel section. Clams or mussels formed on the bottom of the titanium pipe were about 3-5 months old (Figure 53); the flowing seawater was reportedly strained during the entire exposure period.

As mentioned earlier, some titanium pipe sections were reused after thorough cleaning to apply either an organic or an anodized coating. Figure 54 shows the pre-exposure condition of the organic urethane-based TI-COMP™ 10 coating that had been applied on both inner and outer surfaces of titanium pipe 13/3 (Figure 54). After six months exposure, only some loose silt was found along the interior pipe surfaces (Figure 55). Figure 56 shows a different view of the loose deposit on the organic-coated titanium piping. These deposits were easily removed to reveal a smooth and intact coated pipe surface (Figure 57). The 70:30 copper-nickel section at the inlet end displayed a small site where biofouling had occurred, but exposed no visible signs of pitting

or waterside corrosion (Figure 58). Loose deposits were located on the anodized pipe 14/9 after 6 months exposure in flowing natural seawater (Figures 59). The copper-nickel piping section coupled to the anodized-coated titanium section exhibited no visible corrosion (Figure 60).

After the exposure period of the mockup piping loops using the bi-electrode in its intended mode, the device was examined. Figure 61 shows configuration of the bi-electrode used in these tests. The device consisted of two 4-inch long platinized (I.D. only) titanium pipe nipples. These nipples were then connected to a 2-inch PVC coupler. Each electrode end of the bi-electrode device displayed some interesting characteristics after the 343 days of exposure. The electrode end oriented adjacent to the Alloy 625 piping section displayed calcareous deposits and macrofouling along the entire length of this electrode and the PVC coupler as shown in Figure 62. This is not too unexpected because platinum does not have biocidal capabilities. The calcareous deposits formed on this electrode indicate that it acted as the cathode of the bi-electrode device. The electrode adjacent to the 70:30 copper-nickel section is devoid of any deposits, silt, slime, or biofouling (Figure 63). This electrode acted as the anode of the bi-electrode device where oxidation processes occurred. The effect of applied current to a BED placed between titanium and 70:30 copper-nickel piping sections was determined. The results are shown in Figure 64. The current applied to the bi-electrode at 0, 1/3, 2/3, and full power corresponded to 0, 15.2, 30.2, and 48.2 mA, respectively. Full power completely counteracted the normal galvanic current flow. As the applied current was increased the ZRA current reading decreased from +850 μA at no power to +538 μA at 1/3 power, +379 μA at 2/3 power to -5 μA at full power. As the power to the bi-electrode is increased, the potential of the titanium adjacent to the BED becomes more electropositive than steady state potential of titanium and the copper-nickel adjacent to the BED becomes more electronegative than the steady state potential of copper-nickel. This indicates that as the power to the BED electrodes is increased, the electrode adjacent to the cathodic titanium piping section becomes more cathodic than the cathode piping alloy and the electrode adjacent to the copper-nickel becomes more anodic than the copper alloy itself. When the electrode become either sufficiently more cathodic or anodic than the piping materials, induced currents are generated between the cathodic BED electrode and the pipe cathode and between the anodic BED electrode and the piping anode that flow counter to the

normal galvanic current flux. The resultant galvanic currents are zeroed when the induced currents at each electrode completely counter the normal ionic current flow. A schematic of the operation of the bi-electrode based on these visual observations and that observed during the mockup tests are shown in Figure 65.

Piping Thickness Measurements and Topography Mapping

After splitting, cleaning, and rinsing, the material losses on the copper-nickel pipe sections were mapped according to orientation and distance from the copper-nickel inlet (the inlet was separated from the titanium pipe by a 0.25-in. (0.63 cm) PVC insert). Figure 66 shows the surface topography of the copper-nickel pipe loop 1 after a one-year exposure coupled to bare titanium. As expected the heaviest material losses occurred within the first 3 inches (7.5 cm) and along the top of the pipe section. Pits as deep as 0.012" (0.030 cm) were measured. The extent of the galvanic interaction was about 5-6 pipe diameters (10-12 in.; 25.5-30 cm). The top portion of the pipe is more susceptible since surface deposits, silt, biofilms, and slimes are more apt to settle on the bottom of the titanium pipe. Pipe loop 7 displayed similar corrosion behavior with a maximum pitting depth of 0.013" (0.033 cm) (Figure 67).

Figure 68 displays the surface topography of the 70:30 copper-nickel pipe 2 that was coupled to the calcareous deposit coated titanium pipe for 365 days. No corrosion related to the seawater exposure test was observed. Several sites that were 2-3 mils deep were generated by scraping the pipe surface during sample preparation after exposure. Figure 69 displays the surface topography of the 70:30 copper-nickel pipe 8 that was coupled to the calcareous deposit coated titanium pipe for 623 days. Despite the higher anodic currents measured over the last 150 days, little surface damage was observed along the copper-nickel pipe. Scattered pits 0.002" deep were found along the bottom of the pipe about 2 to 11 inches (5-28 cm) from the titanium/copper-nickel couple.

The surface topography of the copper-nickel inlet segment of Alloy 625/70:30 copper-nickel piping loop 6 after 379 days of flowing seawater exposure is shown in Figure 70. As observed with titanium as the cathodic member, the extent of the galvanic interaction was about 5-6 pipe diameters (10-12-in.; 25.5-30 cm). Although the topography map indicates a maximum

corrosion depth of 0.012", several sites outside of the grid had pits that were 0.022 to 0.066" deep at distance up to 5 inches from the inlet. The nominal wall thickness of the copper-nickel Schedule 40 piping is 0.180-inch. The surface topography of the copper-nickel inlet segment of Alloy 625/70:30 copper-nickel piping loop 12 after 379 days in flowing seawater is shown in Figure 71. The maximum pit depths were 0.032 to 0.060" along this copper-nickel leg at distance up to 3 inches from the inlet.

The presence of the dielectric PVC spacer decreases the effective length of galvanic interaction of the copper-nickel alloy with Alloy 625. In both piping loops 5 (Figure 72) and 11 (Figure 73), the effective length is about 3 piping diameters (3-in; 7.5 cm) from the inlet with the most serious pittng.extending over only the first 2 inches of the copper alloy pipe. The maximum pit depths were 0.018" and 0.010" for piping loops 5 and 11, respectively.

Figure 74 shows the copper-nickel surface topography of piping loop 3 after its 340 day exposure to cathodic protection. No corrosion was found along the copper-nickel pipe surface. As mentioned in the experimental section, the pipe thickness measurements were compensated linearly to account for variations in piping thickness around the circumference. The method worked in most instances, but the topography profile of copper-nickel piping loop 9 under cathodic protection did not give a true indication of the surface profile. Subsequent visual observation and measurement by an alternative procedure did not indicate any waterside corrosion.

The surface topographies of the copper-nickel pipes under the influence of the bi-electrode in piping loops 4 and 10 (Figures 75). The 70:30 copper-nickel sections from both piping loops displayed no measurable corrosion despite the topography view in piping loop 4. The bi-electrode was effective in preventing the anodic dissolution of the copper-nickel alloy.

Figure 76 displays the typical surface topography of the copper-nickel piping sections adjacent to the urethane-based or anodized titanium piping sections. In both of these galvanic couples, the copper-nickel showed no measurable corrosion. Both of these coatings were

effective in reducing the cathodic reaction substantially and generating, correspondingly, lower galvanic corrosion of the copper-nickel piping section.

SEM Examination and X-ray Analysis

The organic, urethane-based and anodized titanium coated sections were examined after the 6-month exposure tests by scanning electron microscopy (SEM). Figures 77 and 78 shows the SEM cross-sectional micrographs of the coatings. The urethane-based organic coating (Figure 77) is 410-420 μm thick, while the anodized coating is about 4 μm thick (Figure 78). Both coatings show no discernible porosity or defects. Adherence of both coatings to the titanium pipe substrate also appeared to be good; no delamination was observed. Mapping via X-ray energy dispersive spectroscopy of the urethane-based coating is shown in Figure 79. Fluorine appears to be concentrated at the titanium/coating interface and at the coating/water interface.

The elemental x-ray maps of the anodized titanium pipe 14/9 are viewed in figures 80 and 81. Despite the expectation of a titanium oxide layer, there was little indication of titanium in the anodized coating on the piping surface. The analysis did identify the presence of phosphorus, chromium, oxygen, and fluorine in this anodized layer. This would suggest that the anodizing occurred in a phosphate acid solution and the inherently porous anodized layer was likely sealed in chromate acid sealing treatment and teflon final seal coat.

DISCUSSION

The total amount of galvanic current from the 70:30 copper-nickel pipe (anode) when connected with titanium or Alloy 625 (cathode) of similar diameter under moderate seawater flow was lower than might be expected from separation of the anodic and cathodic alloys as listed in the Galvanic Series in flowing seawater [3]. Test results indicate that in some non-critical areas, these couples may need no corrosion protection at all, or it may be sufficient to perform occasional inspection to monitor the degree of corrosion.

The titanium and Alloy 625 pipes all had similar potentials and caused similar galvanic currents when in similar configurations. This is to be expected, as neither of these materials

corrodes or has a thick protective film. Thus both should act as oxygen electrodes, yielding similar cathodic behavior. Similar long-term cathodic polarization behavior of these alloys in seawater has also been observed, which is consistent with similar galvanic currents [31].

All the bare titanium and Alloy 625 piping segments experienced ennoblement of several hundred millivolts between 14 and 65 days, with the exception of the material with calcareous deposits. It appears that the calcareous deposits prevented the ennoblement phenomenon, by a mechanism currently unknown. The galvanic current increased 7-14 days after ennoblement occurred, indicating a probable cause/effect relationship. Ennoblement of the cathode increased the potential difference between the anode and the cathode; the larger potential difference between the dissimilar alloys enhanced the driving force for increased galvanic corrosion of the more anodic, copper-nickel sections. The phenomenon of ennoblement is likely caused by microbial action that increases the cathodic kinetics, which would shift the cathodic polarization curves to higher currents, thus increasing galvanic currents from the anode [25-30].

Calcareous deposits were highly effective initially in lowering galvanic currents to very low levels during the first year of exposure. Galvanic currents increased later in the test, possibly due to thinning of the calcareous deposits or increasing due to seasonal changes in seawater temperature or dissolved oxygen.

Galvanic currents increased after 475 days in the mockup piping loop where the titanium was coated with calcareous deposit. After about 600 days the measured galvanic currents from loop 8 approached the current measured from bare titanium/70:30 copper-nickel piping couple. Heavy mussel growth observed on the bottom pipe half could have caused erosion of the calcareous deposits from the titanium surface. The removal of the barrier coating would expose the titanium and subsequently increase galvanic currents. Enhanced galvanic currents may also have been caused by decreased calcareous deposit thickness due to increased solubility of the deposit in warmer seawater or by enhanced diffusion of reaction species through the calcareous deposits.

The use of a 10-in spacer between the anode and cathode pipes in the couples resulted in a 40-50% reduction in galvanic current. In a similar type test conducted earlier, a similar 1-ft spacer was not effective in reducing galvanic current, while a 3-ft spacer was required to get similar current reduction [31]. Longer spacers were shown in this previous study to have increased effectiveness in reducing galvanic corrosion due to the increased seawater IR drop introduced for longer spacers. The reason for the increased effectiveness of the spacer in this exposure test versus the previous one is unknown at this time.

Use of the bi-electrode as a pair of impressed current anodes for cathodic protection was effective in shifting the potential of the copper-nickel enough to suppress the anodic corrosion reactions. At the applied current used (20 mA) during the cathodic protection of the Alloy 625/70:30 copper-nickel piping couples, the applied current density on the platinized titanium electrodes was 0.25 mA/cm^2 or 0.025 $\mu A/m^2$. This would amount to an electrode consumption rate of 0.78 $A\text{-}yr/m^2$ or less than 0.04 mg consumption of the platinized electrode material per year [32]. The cathodic protection usually shifted the potential far more than was required. Thus, more current was supplied than was needed to do the task of protection. Since the cathodic protection was set up under constant current, the control of this system was simple and operation was safe and stable.

Use of the bi-electrode (BED) in its intended mode was very effective in countering the galvanic current fluxes generated from 70:30 copper-nickel by its couple with a more cathodic metal or alloy through the establishment of an offsetting electric field. The applied currents to the BED required in this test was 10 to 35 mA or 0.012 to 0.042 $\mu A/m^2$ of applied current density. This is far below the typical anode current density of this electrode material of 540-1080 A/m^2 [32]. The BED prevented galvanic corrosion of the 70:30 copper-nickel pipe couple to Alloy 625. When the bi-electrode was properly adjusted, the copper-nickel potential was flat across the entire pipe length, even near the BED anode, indicating that the copper-nickel did not appear to be affected directly by the presence of the cathodic material at all. The cathode pipe potential was also flat, indicating that it there was not influence from the anodic pipe section. The BED system, when the applied current is adjusted correctly, worked to stop galvanic corrosion. Issues regarding "throwing power" do not occur in the BED mode as would arise if

cathodic protection were used. Control of the bi-electrode was difficult however. Daily manual adjustments were far more effective at keeping galvanic current low than weekly adjustments.

Control of the bi-electrode was difficult however. Daily manual adjustments were far more effective at keeping galvanic current low than weekly adjustments. In practice, this type of control is not possible, as the anode and cathode pipe would be shorted through common structure and pipe hangers, so galvanic current could not be measured. Another method of control must be sought. Just as hooking up a cathodic protection system backwards can accelerate corrosion, improper control of the bi-electrode can also accelerate corrosion. Thus, the issue of control must be resolved before this device can find use.

The organic, urethane-based coating and the anodized titanium oxide coating both reduced the effective cathodic area in the galvanic piping couples. Both coatings acted as a barrier coating which could either slow the oxygen reduction rate or reduce the active sites for oxygen reduction. Since the overall cathodic currents must equal the total anodic currents, a decrease of two orders of magnitude in the measured currents, spread over the same effective galvanic length of copper-nickel, will result in corrosion rates approaching uncoupled corrosion rates of 70:30 copper-nickel in seawater. The success of these coatings, without loss of bond strength after 6 months exposure, may lead to an increased usage of dissimilar piping for naval systems. The passive nature of this galvanic control measure does not require external power sources or electrical devices that may have a finite life. However, further testing of coating compatibility and adhesion on heat-affected surfaces from welding and evaluation of these possible control measures by long-term exposure tests needs to be performed. The behavior of the anodized titanium pipe without PTFE may be significantly different from the piping section with a PTFE final coat/sealer.

CONCLUSIONS

Titanium and Alloy 625 behaved similarly as the oxygen reduction cathode surfaces in the galvanic couples with 70:30 copper-nickel piping. The ennoblement of both titanium and Alloy 625 that occurred between 14 and 65 days resulted in an increase in galvanic current. Pretest applied calcareous deposits were highly effective in lowering galvanic currents to negligible

levels. The use of a 10-in. spacer between the anode and cathode pipes in the couples also resulted in a 30-50% reduction in galvanic current.

Use of the bi-electrode device as a pair of cathodic protection anodes was effective in shifting the potential of the copper-nickel enough to prevent galvanic corrosion, and control of the cathodic protection system was simple. However, in the present tests, the device usually supplied more current than was needed to do the task of protection. In contrast to cathodic protection, BED use does not form calcareous-type scales on the 70:30 copper-nickel piping.

Use of the bi-electrode device in its intended BED mode was very effective in preventing galvanic corrosion by establishing of an electric field sufficient to counter the ionic current flux flowing from the anodic member to the cathodic alloy. The applied currents required for control were small. The applied current to the device electrode nearer the cathodic segment becomes a more effective cathode that the Alloy 625 so that an offsetting current flows from the 625 cathode to the BED electrode nearest that alloy. The current applied to the device electrode nearest the 70:30 copper-nickel pipe becomes anodic to the copper alloy so that an induced current flux from this BED electrode to the copper-nickel alloy is generated and counters the galvanic ionic current flow from the copper-nickel alloy towards the cathodic pipe.

Control of the bi-electrode was difficult however. More frequent adjustments of the bi-electrode applied current reduced the galvanic current fluctuations. Just as hooking up a cathodic protection system backwards can accelerate corrosion, improper control of the bi-electrode could also accelerate corrosion.

The use of coatings on the titanium cathodic member of coupled titanium/70:30 copper-nickel galvanic piping sections was effective in reducing the magnitude of galvanic currents by 95 to +99%. Galvanic currents permanently increased after 475 days on a copper-nickel pipe section coupled to calcareous-deposit-coated titanium. These increasing currents may have been caused by calcareous deposits flaking from the titanium surface, decreased calcareous deposit thickness due to increased solubility of the deposit in warmer seawater, or enhanced diffusion through the calcareous deposits, thus delay the ennoblement of the titanium leg.

Both the 420 μm thick, organic, TICOMP™ 10 urethane-based coating and the 4 μm thick TIODIZE™ type IV, anodized coating with a PTFE sealer/final coat on titanium piping sections coupled to 70:30 copper-nickel piping were effective for over 6 months in preventing galvanic corrosion in seawater flowing at 6 fps (1.8 m/s). Both of these coatings showed no defects or loss of adherence at the coating/titanium substrate interface after completion of the six-month exposure. Other coating may be equally effective, but should be tested in natural seawater.

REFERENCES

1 - J. W. Oldfield, "Electrochemical Theory of Galvanic Corrosion," Galvanic Corrosion, STP 978, H. P. Hack, ed., ASTM, West Conshohocken, PA, p. 5, (1988).

2 - R. Francis, "Galvanic Corrosion of High Alloy Stainless Steels in Sea Water," *British Corrosion Journal*, Vol. 29, p. 53, (1994).

3 - F.L. LaQue, Marine Corrosion: Causes and Prevention, Wiley-Interscience, New York, 179 (1975).

4 - M. G. Fontana, Corrosion Engineering, 3rd ed., McGraw-Hill, New York, 48 (1986).

5 – H.P. Hack, "Galvanic Corrosion of Piping and Fitting Alloys in Sulfide-Modified Seawater", Galvanic Corrosion, STP 978, H. P. Hack, ed., ASTM, West Conshohocken, PA, p. 339, (1988).

6 - J. P. Gudas, H. P. Hack, "Sulfide-Induced Corrosion of Copper-Nickel Alloys," CORROSION/77, paper 93, NACE International, Houston, TX (1977).

7 - J. P. Gudas, *et al.*, "Accelerated Corrosion of Copper-Nickel Alloys in Polluted Water," CORROSION/76, paper 76, NACE International, Houston, TX (1976).

8 - I.L. Caplan, H.P. Hack, "The Galvanic Effects of Titanium Coupled to Various Marine Alloys in Seawater", Report CDNSRDC-SME-80/54, NSWC, (October 1980).

9 - H.P. Hack, W.L. Adamson, "Analysis of Galvanic Corrosion Between a Titanium Condenser and a Copper-Nickel Piping System", Report No. 4553, DTNSRDC, NSWC (January 1976).

10 - H.P. Hack, W.L. Wheatfall, "Evaluation of Galvanic and Stray Current Corrosion in 70/30 Copper-Nickel/Alloy 625 Piping Systems", CARDIVNSWC-TR-61-94/15 (July 1995).

11 - S. L. Wolfson, W. H. Hartt, *Corrosion*, Vol. 37, p. 70, 1981.

12 - W. H. Hartt, C. H. Culberson, S. W. Smith, *Corrosion*, Vol. 40, p. 609, 1984.

13 - S.-H. Lin, S. C. Dexter, *Corrosion*, Vol. 44, p. 615, 1988.

14 - J. E. Finnegan, K. P. Fischer, "Calcareous Deposits: Calcium and Magnesium Ion Concentrations," CORROSION/89, paper 581, NACE International, Houston, TX.

15 - K. P. Fischer, J. E. Finnegan, "Cathodic Protection Behavior of Steel in Sea Water and the Protective Properties of the Calcareous Deposits," CORROSION/89, paper 582, NACE International, Houston, TX.

16 - J. S. Luo, R. U. Lee, T. Y. Chen, W. H. Hartt, S. W. Smith, *Corrosion*, Vol. 47, p.189, 1991.

17 - K. E. Mantel, W. H. Hartt, T. Y. Chen, *Corrosion*, Vol. 48, p. 489, 1992.

18 - D.A. Shifler, H.P. Hack, D. Melton, "New Techiniques for Galvanic Corrosion in Piping Systems", paper 706, NACE International, Houston, TX (1998).

19 - D.A. Shifler, D. Melton, "Control Measures to Mitigate Galvanic Corrosion", paper 319, NACE International, Houston, TX (1999).

20 - H. P. Hack, W. L. Wheatfall, "Evaluation of Galvanic and Stray Current Corrosion in 70/30 Copper-Nickel/Alloy 625 Piping Systems," CORROSION/95, paper 272, NACE International, Houston, TX.

21 – U.S. Department of Defense Military Specification MIL-T-16420K, "Tube, Copper-Nickel Alloy, Seamless and Welded (Copper Alloy Numbers 715 and 706)" April 14, 1978 (Amendment 1: September 16, 1988).

22 - ASTM Standard Specification B-337-95, "Seamless and Welded Titanium and Titanium Alloy Pipe", West Conshohocken, PA: ASTM (1995).

23 - ASTM Standard Specification B-705-94, "Nickel-Alloy (UNS 06625 and N08825) Welded Pipe", West Conshohocken, PA: ASTM (1994).

24 - Aerospace Material Specification 2488C – "Anodic Treatment, Titanium and Titanium Alloys", SAE International, Warrendale, PA, (December 1994).

25 – V. Scotto, R.d. Cintio, G. Marcenaro, *Corrosion Science*, v. 25, 185 (1985).

26 – R. Johnsen, E. Bardal, *Corrosion,* v. 41, 296 (1985).

27 – S.C. Dexter, G.Y. Gao, *Corrosion,* v. 44, 717 (1988).

28 – M. Eashwar, S. Maruthamuthu, S. Sathiyanarayanan, K. Balakrishnan, *Corrosion Science*, v. 25, 1169 (1995).

29 - J. P. LaFontaine, S.C. Dexter, "Effect of Marine Biofilm on Galvanic Corrosion", Proceedings of the 1997 Tri-Service Conference on Corrosion, Session 6, Tri-Service Committee on Corrosion, Wrightsville Beach, NC (November, 1997).

30 – V. Scotto, M.E. Lai, *Corrosion Science*, v. 25, 1007 (1998).

31 - H. P. Hack, "Atlas of Polarization Curves for Naval Materials in Seawater," Report CARDIVNSWC-TR-61-94/44, NSWC, April 1995.

32 – D.A. Jones, Principles and Prevention of Corrosion, 2nd ed, Prentice Hall, Upper Saddle River, NJ, 463, (1996); also R.H. Heidersbach, Metals Handbook: Corrosion, vol. 13, 9th ed, ASM International, Materials Park, OH, 471 (1987).

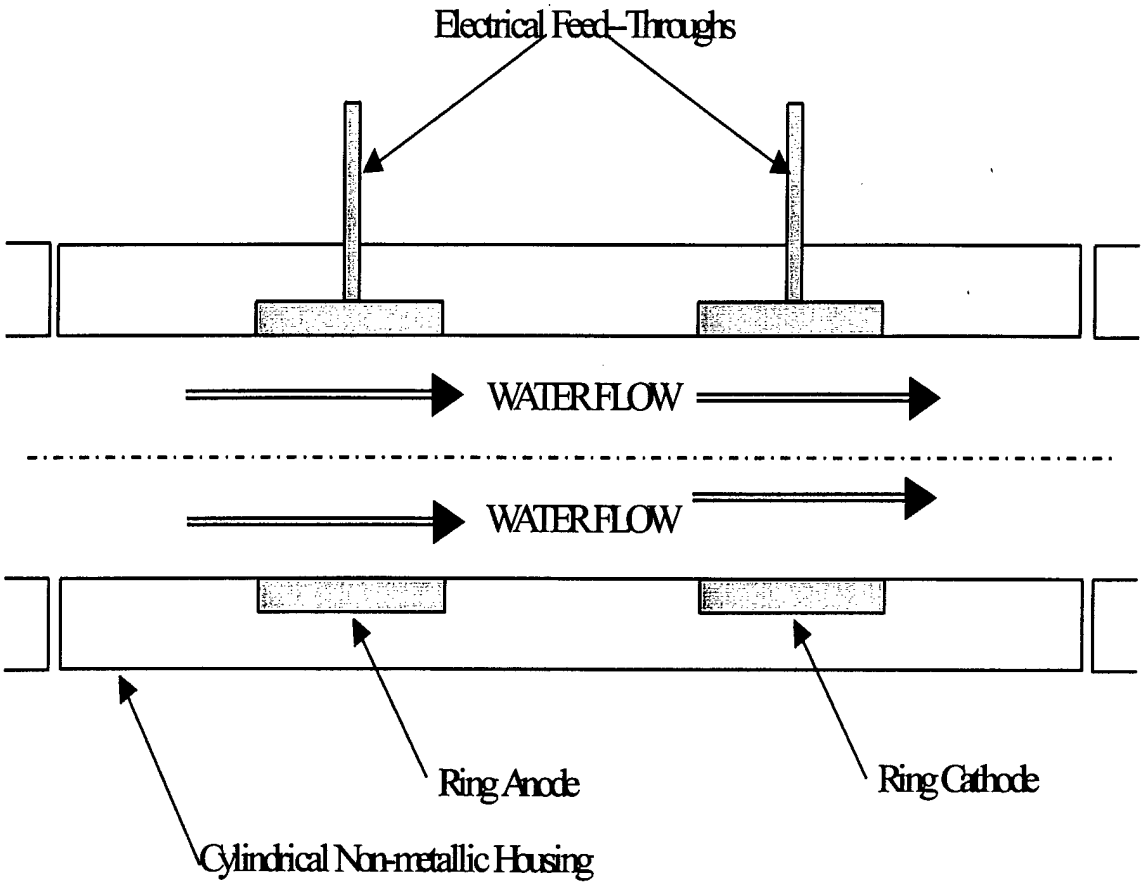

Figure 1 - Schematic of the Bi-electrode Device

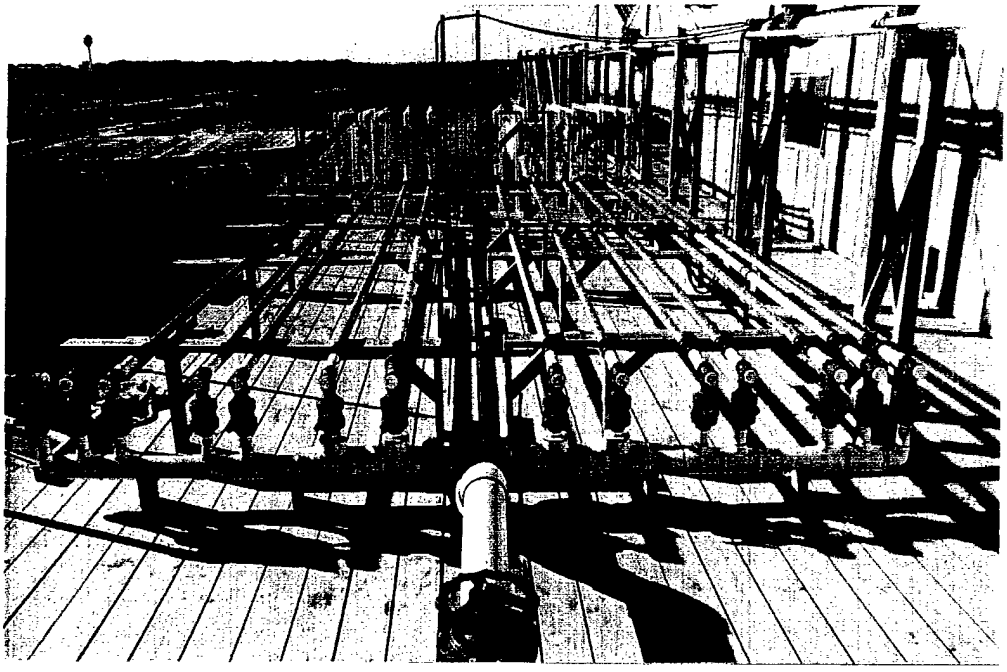

Figure 2 - Overall view of operating seawater piping mockups at LCCT.

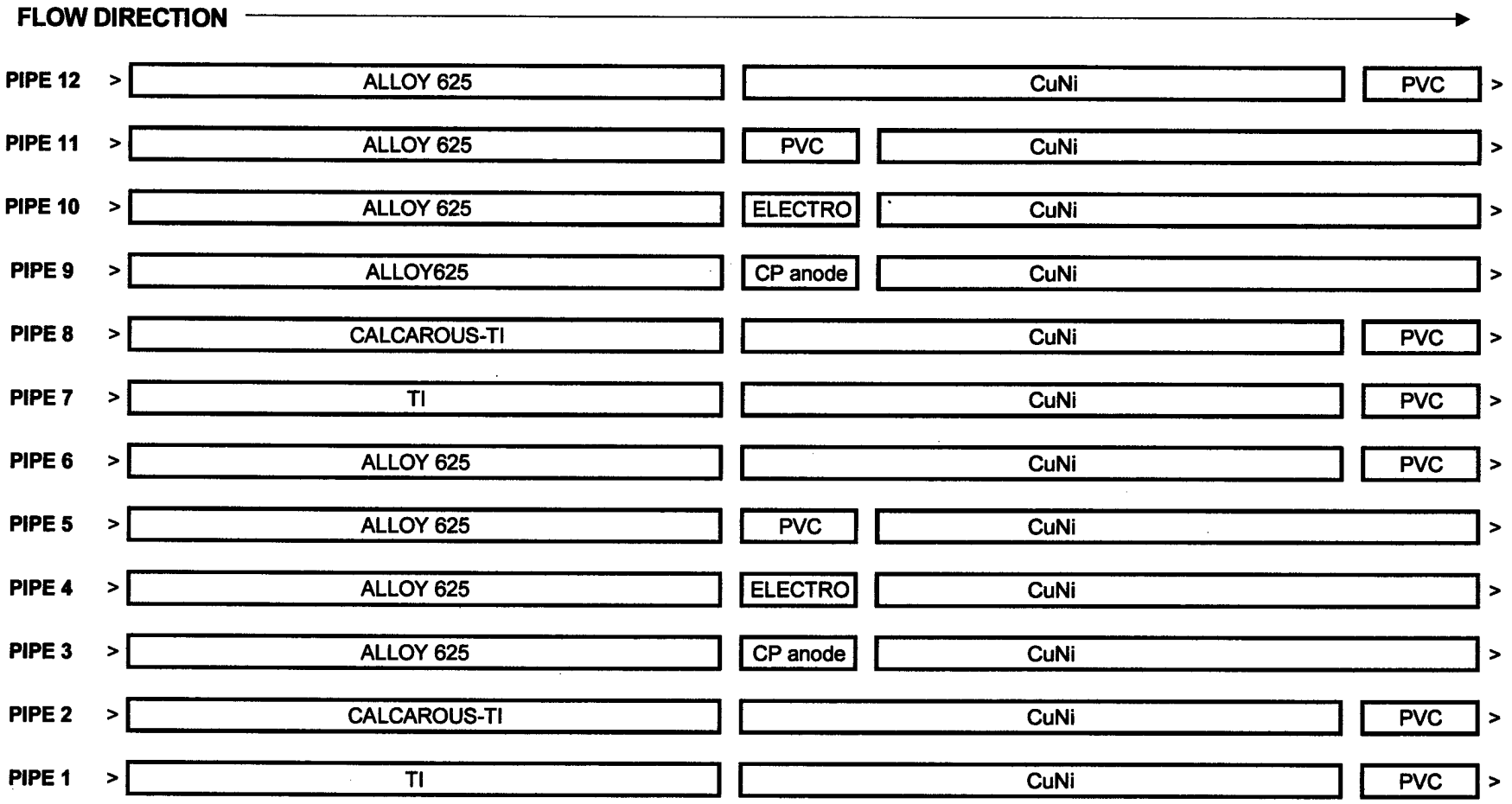

Figure 3 - Schematic of Mockup Loops

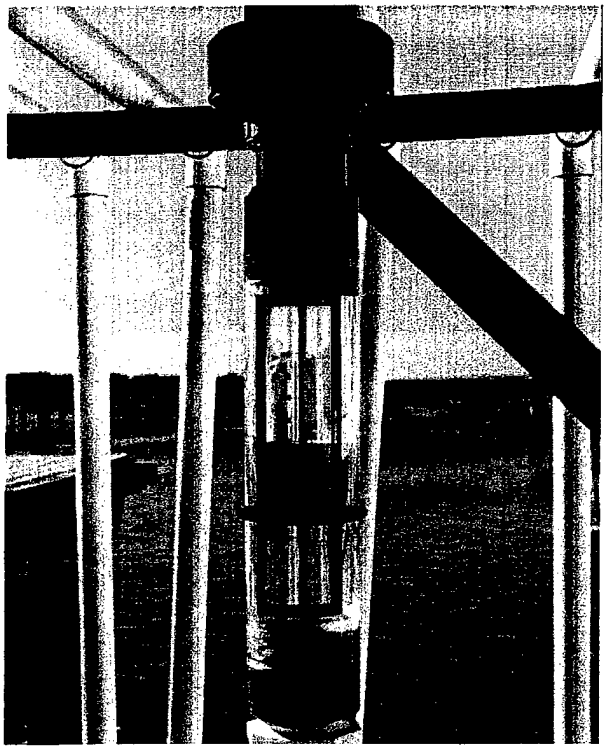

Figure 4 - Rotometer used to control the seawater flow daily through each mockup loops.

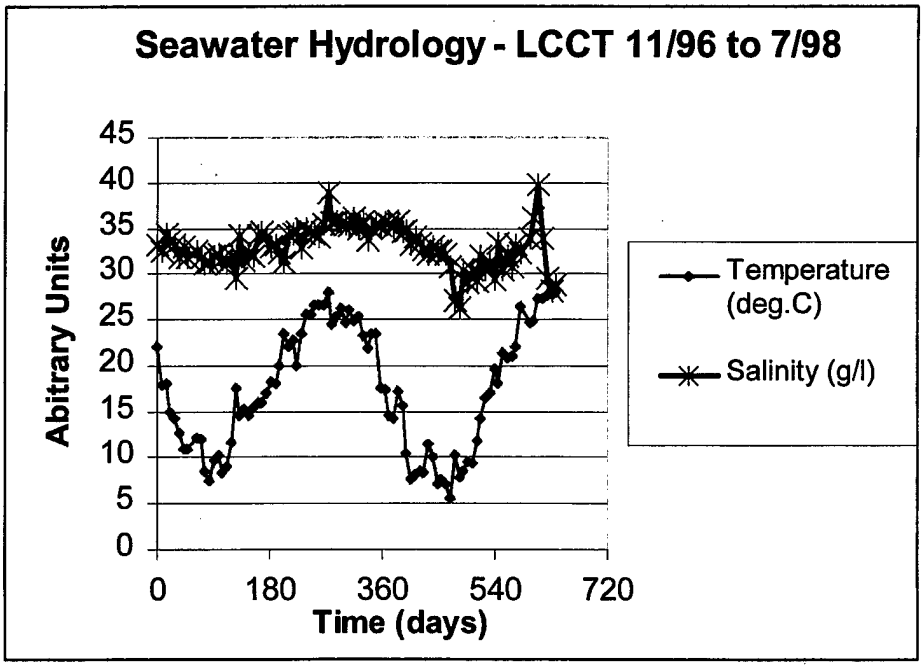

Figure 5 - Temperature and salinity variation during exposure tests.

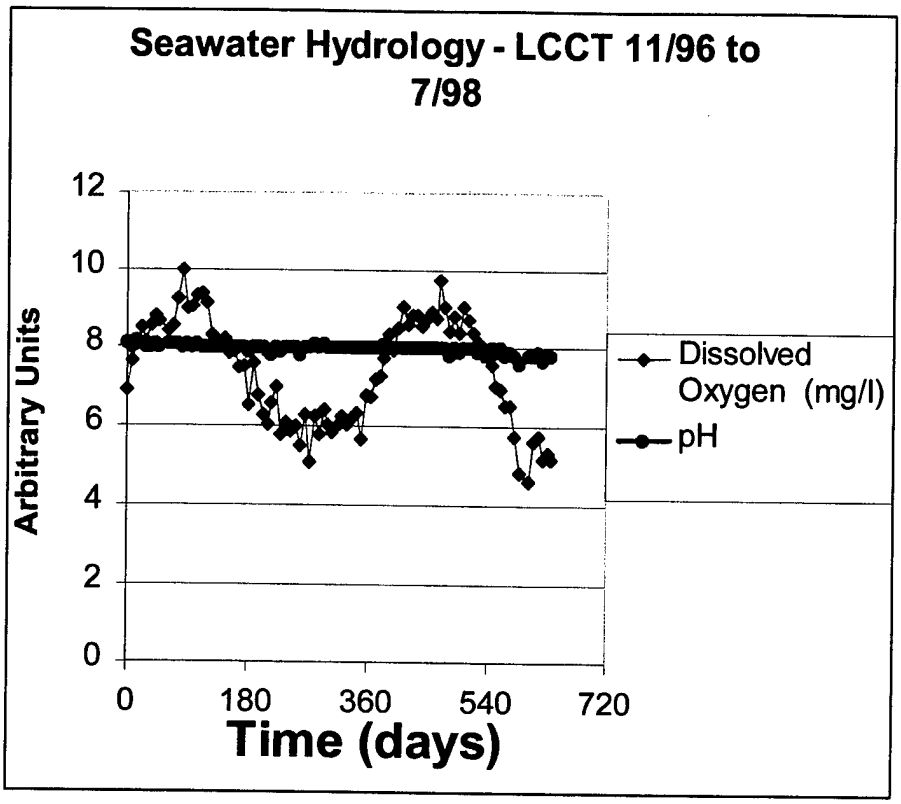

Figure 6 – Dissolved oxygen and pH variations during exposure tests.

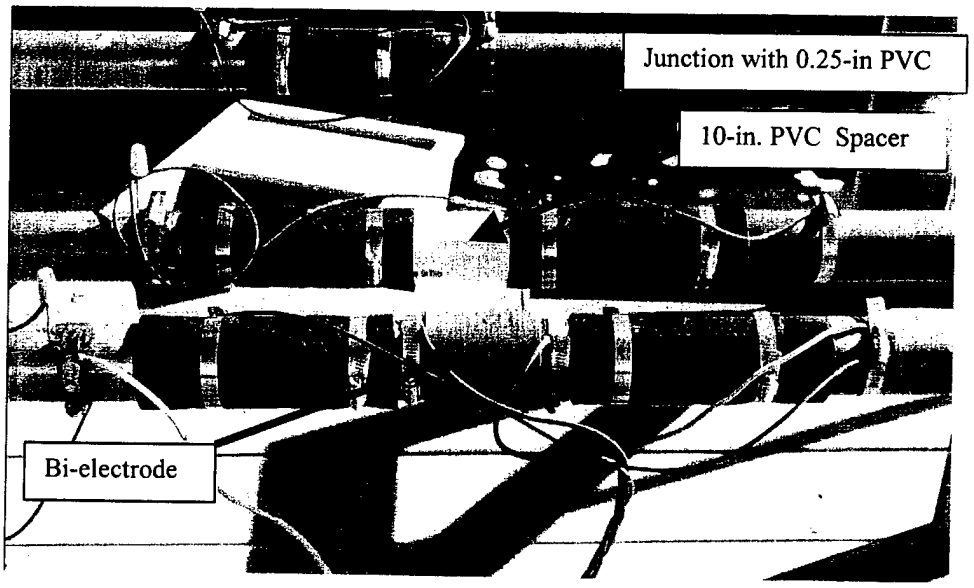

Figure 7 - Bi-electrode, 10-in. long PVC spacer, and short 0.25 spacer as used in the various mockup loops.

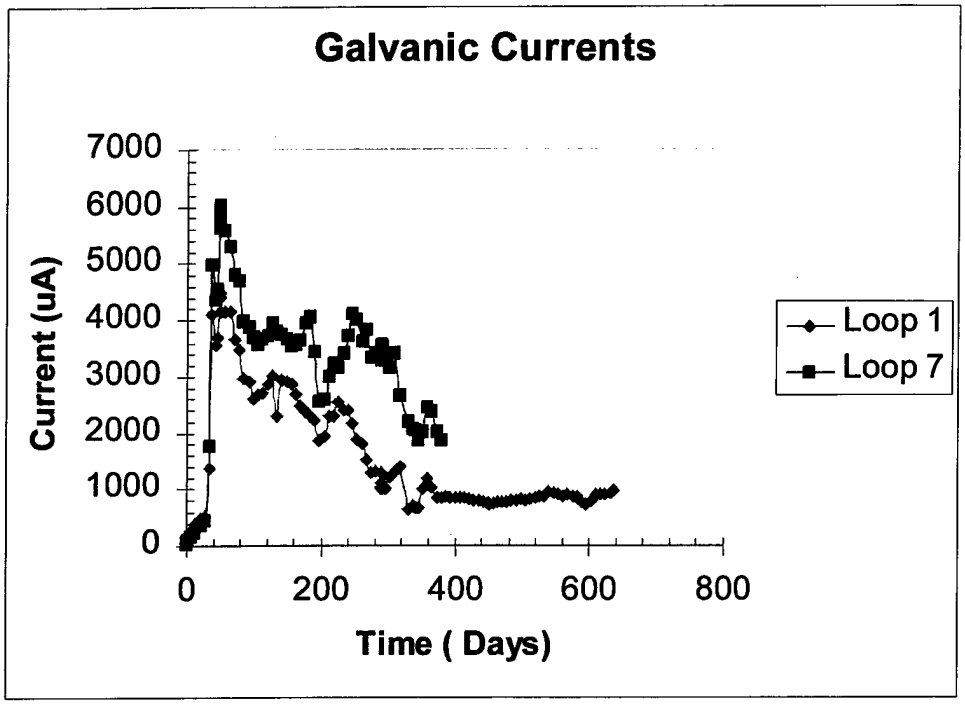

Figure 8 – Titanium/70:30 Copper-Nickel Piping Couples – measured galvanic currents as function of exposure time (Loops 1 and 7).

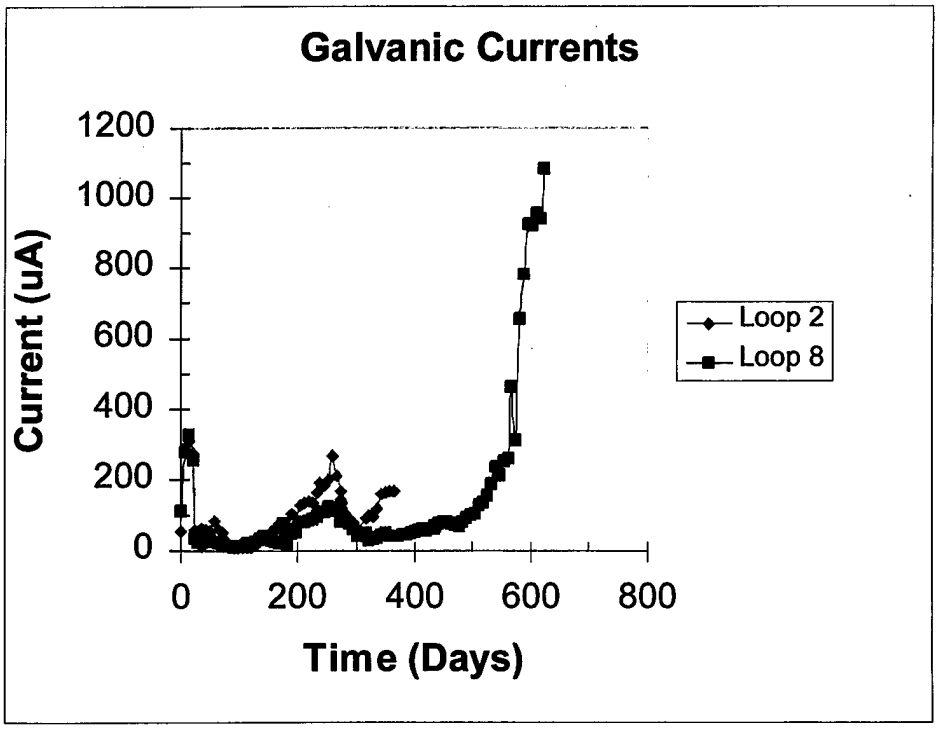

Figure 9 – Titanium with calcareous deposit coating/70:30 Copper-Nickel Piping Couples – measured galvanic currents as a function of exposure time.

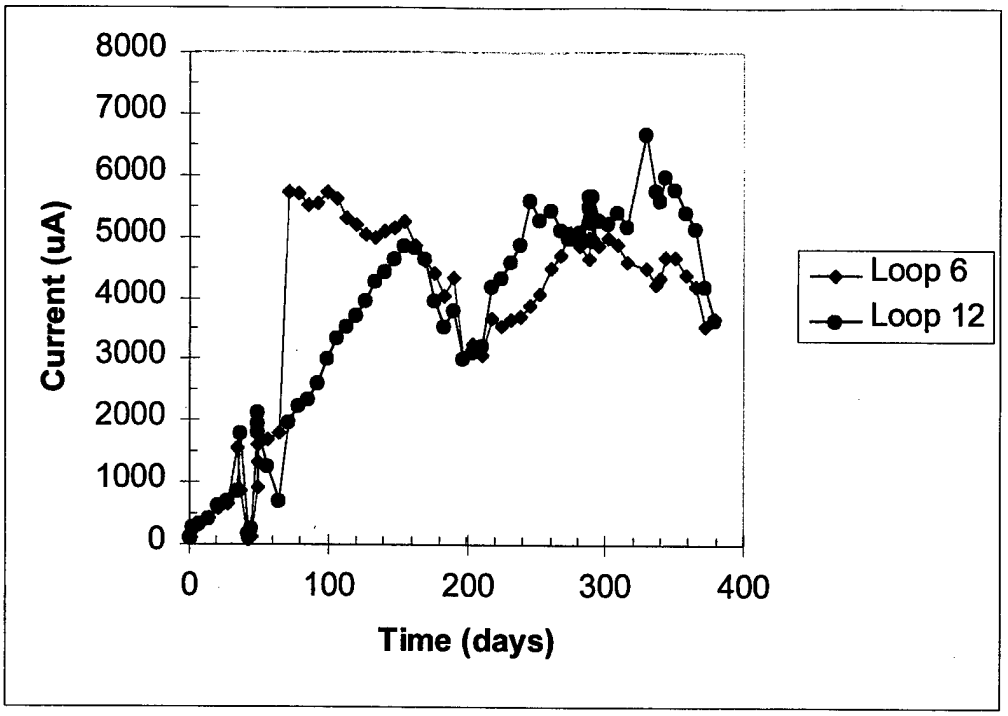

Figure 10 - Alloy 625/70:30 Copper-Nickel Piping Couples – measured galvanic currents as a function of exposure time (Loops 6 and 12).

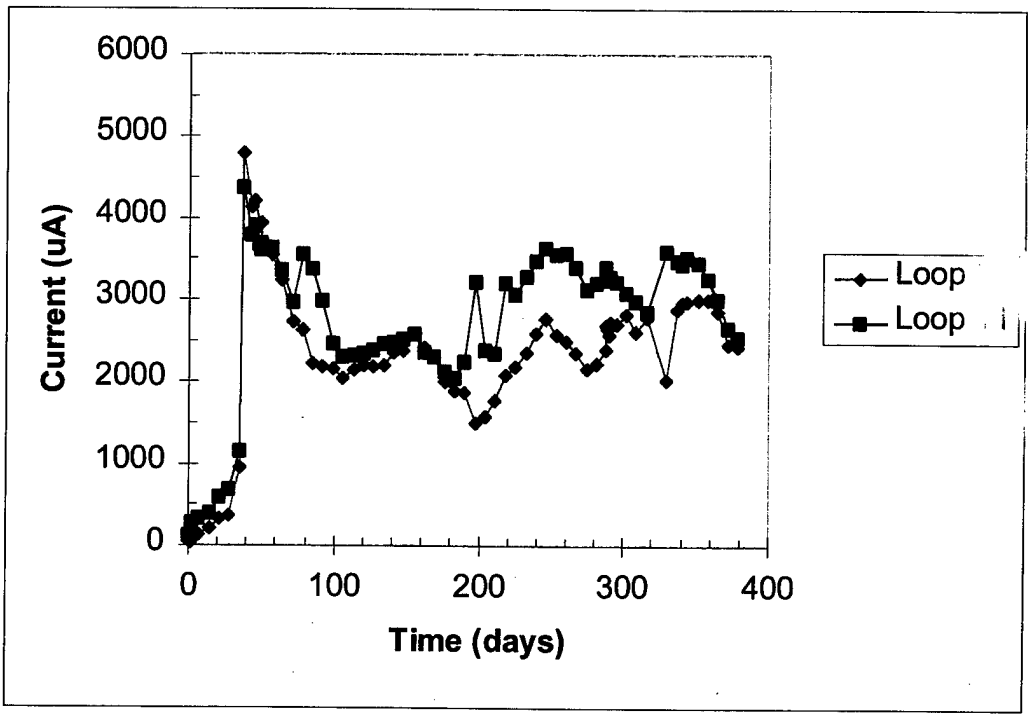

Figure 11 - Alloy 625/70:30 Copper-Nickel Piping Couple separated by 10-in PVC spacer – measured galvanic currents as a function of exposure time.

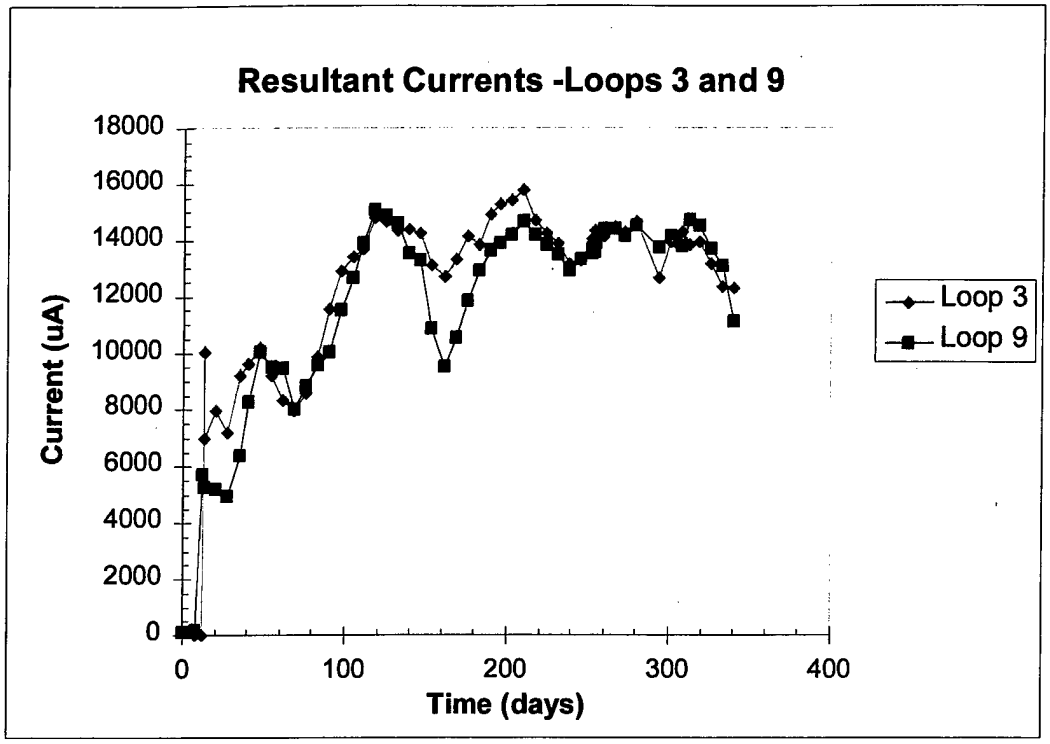

Figure 12 - Alloy 625/70:30 Copper-Nickel Piping Couple with bi-electrode used in the cathodic protection mode – measured resultant currents as a function of exposure

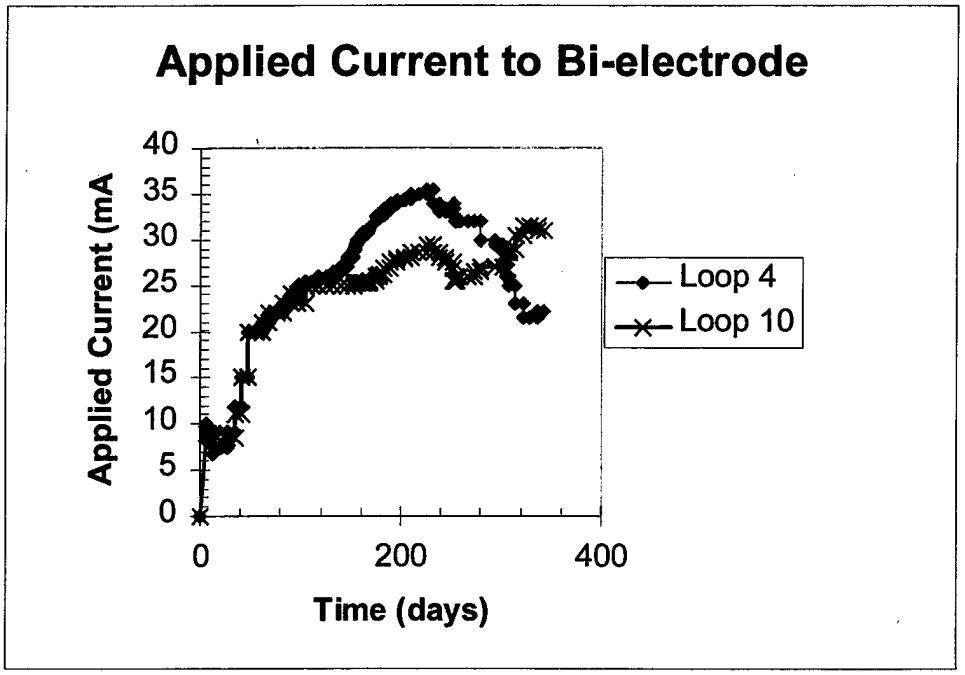

time.

Figure 13 - Current applied to the bi-electrode for Alloy 625/70:30 copper-nickel piping couples (Loops 4 and 10).

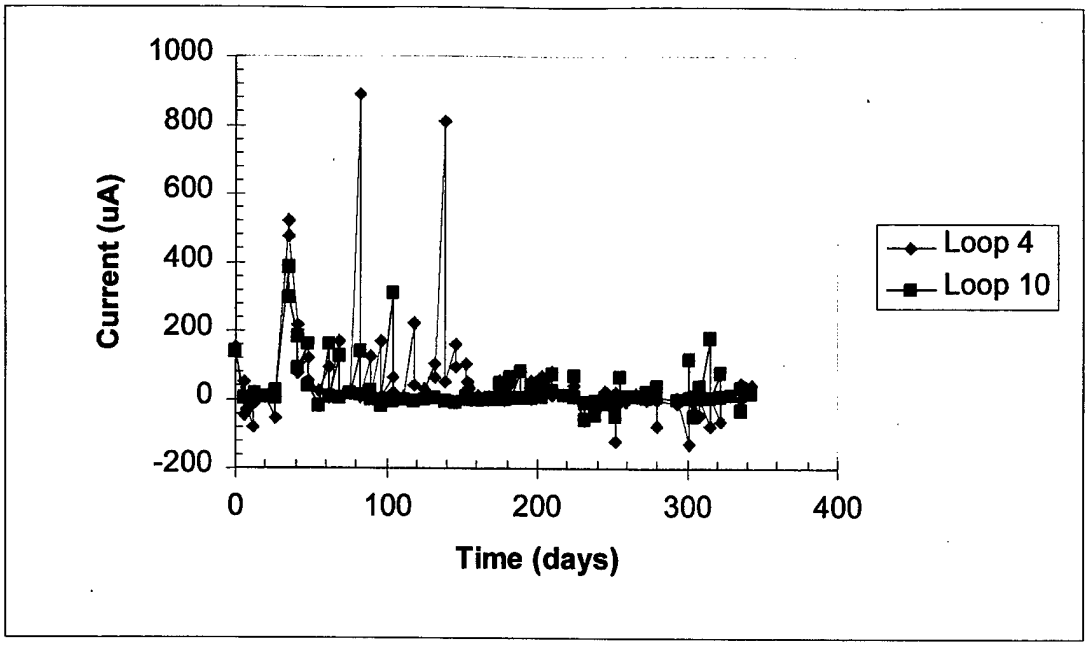

Figure 14 - Measured galvanic currents between Alloy 625/70:30 copper-nickel piping couples (Loops 4 and 10) as a function of exposure time using the bi-electrode device. Bi-electrode adjusted weekly.

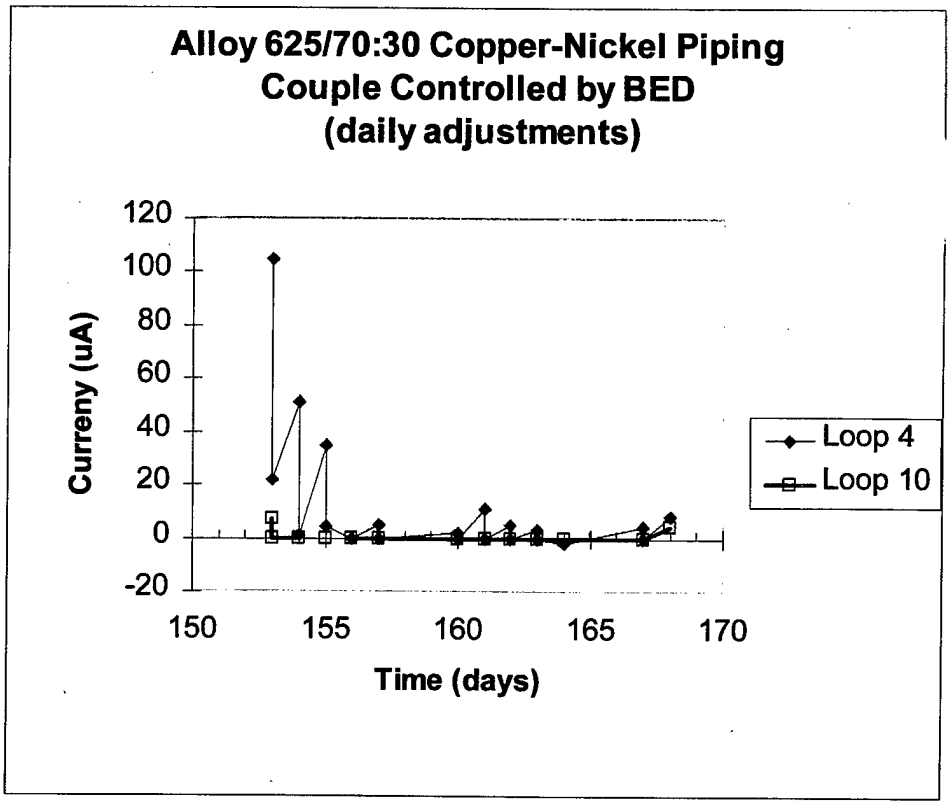

Figure 15 - Measured galvanic currents between Alloy 625/70:30 copper-nickel piping couples as a function of exposure time and daily bi-electrode adjustments.

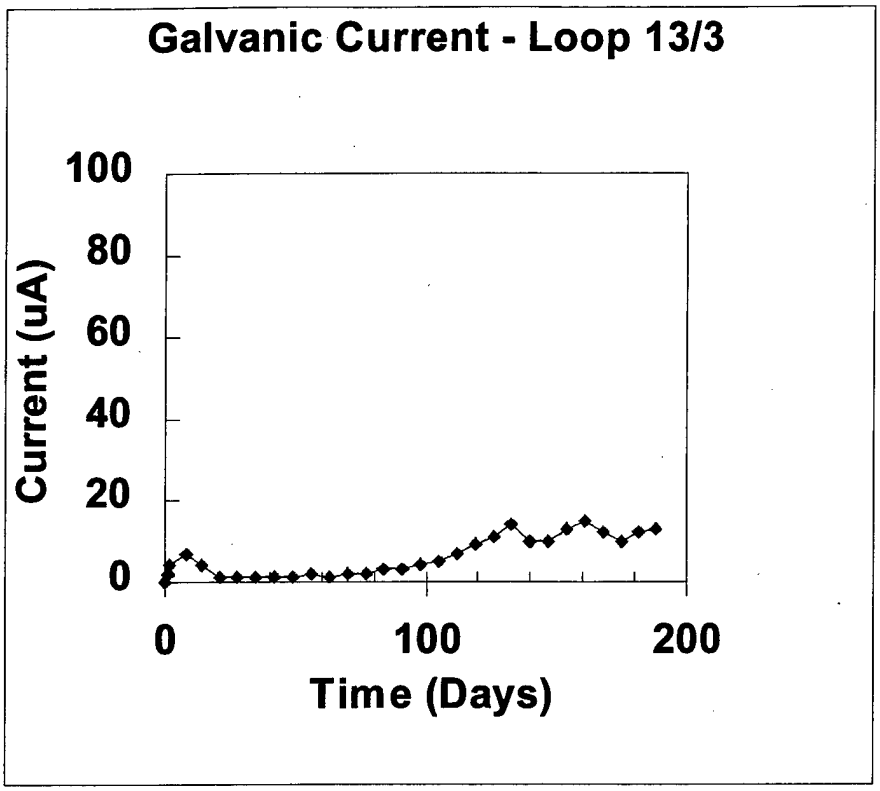

Figure 16 – Urethane-based coated Titanium/70:30 Copper-nickel Piping Couple – measured galvanic currents as a function of exposure time (Loop 13/3).

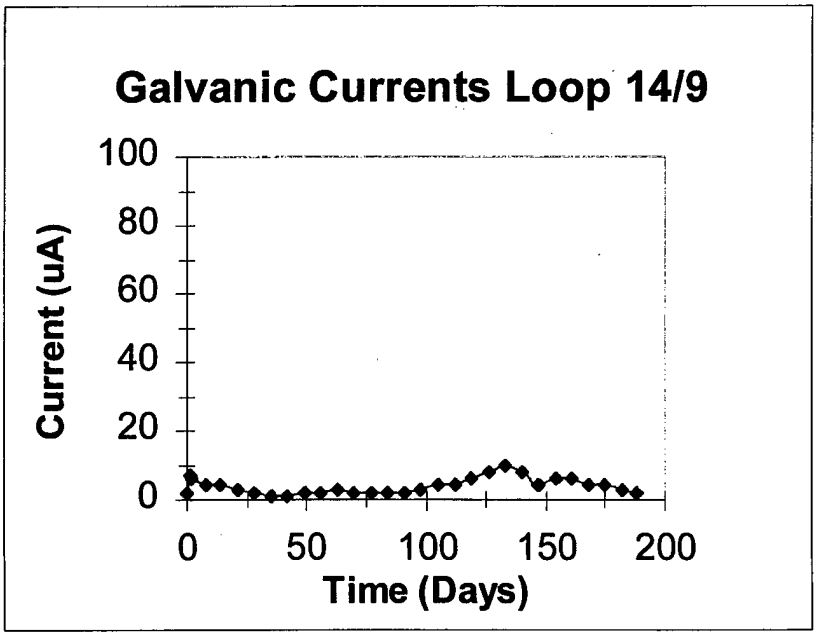

Figure 17 – Anodized Titanium/70:30 Copper-Nickel Piping Couple – measured currents as a function of exposure time (Loop 14/9).

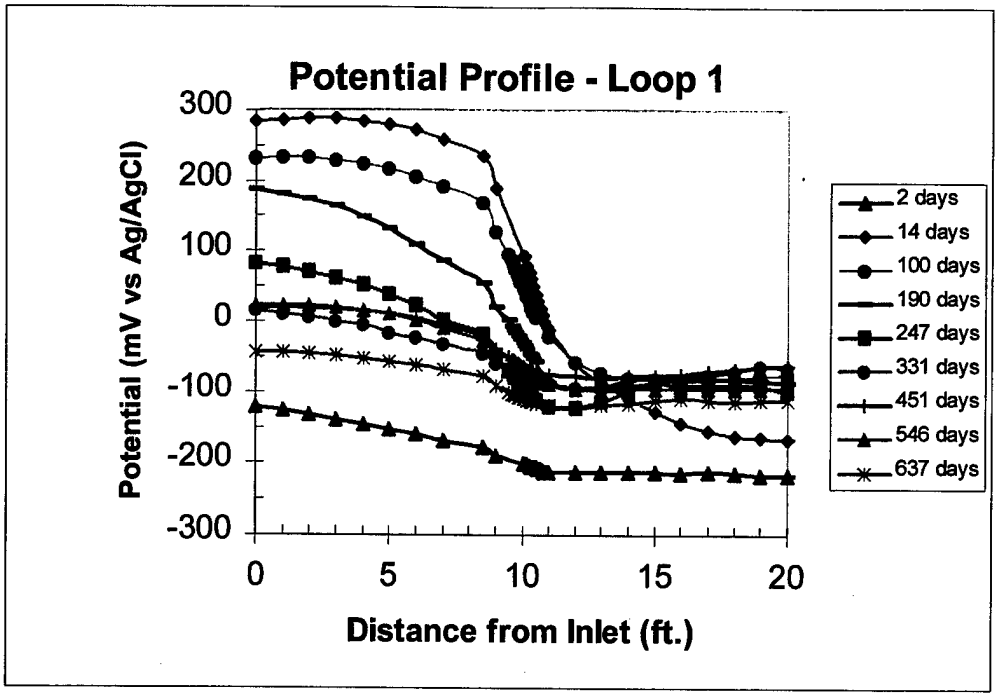

Figure 18 - Titanium/70:30 Copper-Nickel Piping Couple – potential profile of Loop No. 1as a function of time and location along the pipe (Loop 1).

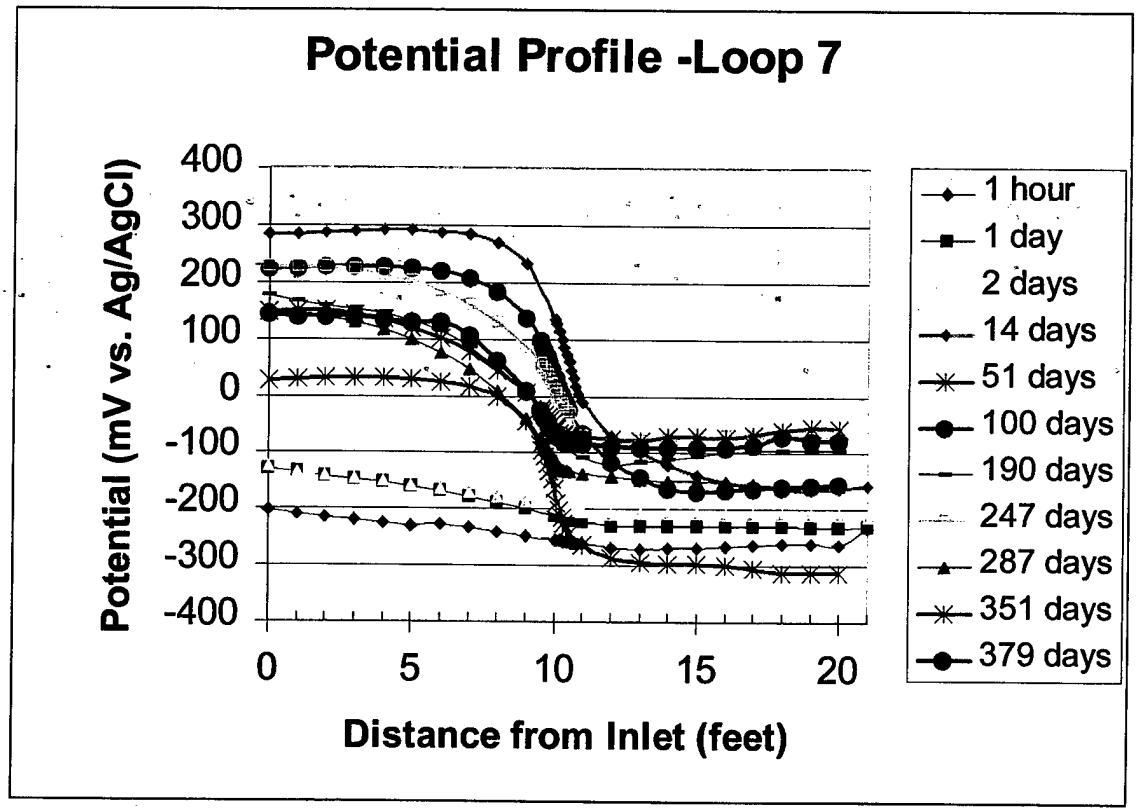

Figure 19 - Titanium/70:30 Copper-Nickel Piping Couple – potential profile as a function of time and location along the pipe (Loop 7).

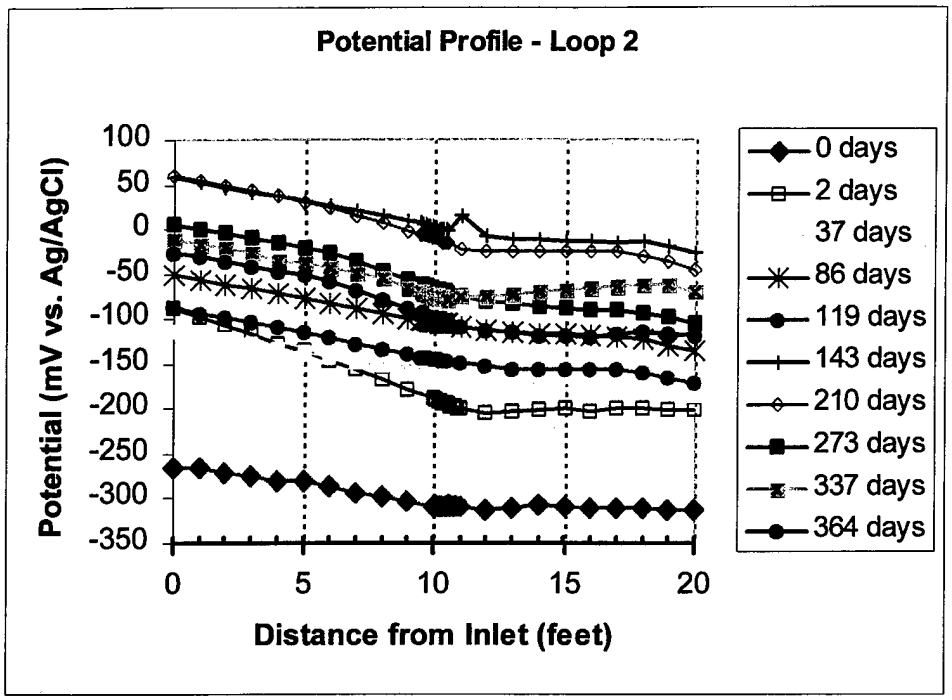

Figure 20 - Calcareous-deposit-coated Titanium/70:30 Copper-Nickel Piping Couple – potential profile as a function of time and location along the pipe (Loop 2).

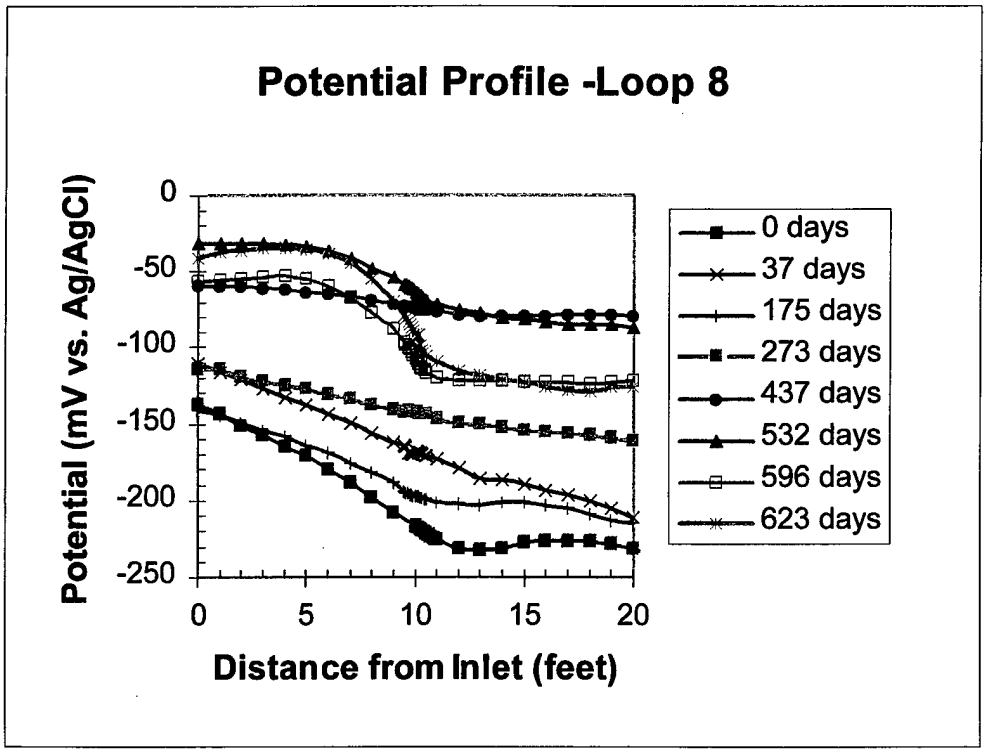

Figure 21 - Calcareous-deposit-coated Titanium/70:30 Copper-Nickel Piping Couple – potential profile as a function of time and location along the pipe (Loop 8).

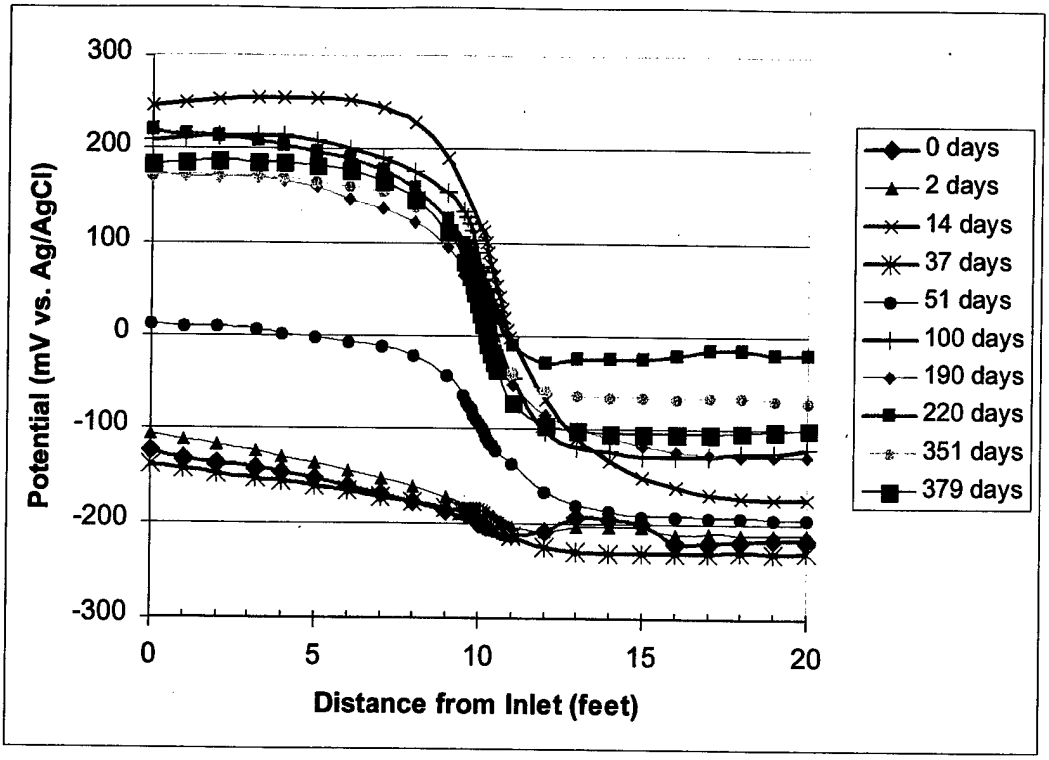

Figure 22 - Alloy 625/70:30 Copper-Nickel Piping Couple – Loop 6. Potential profile shown as a function of time and location along the pipe.

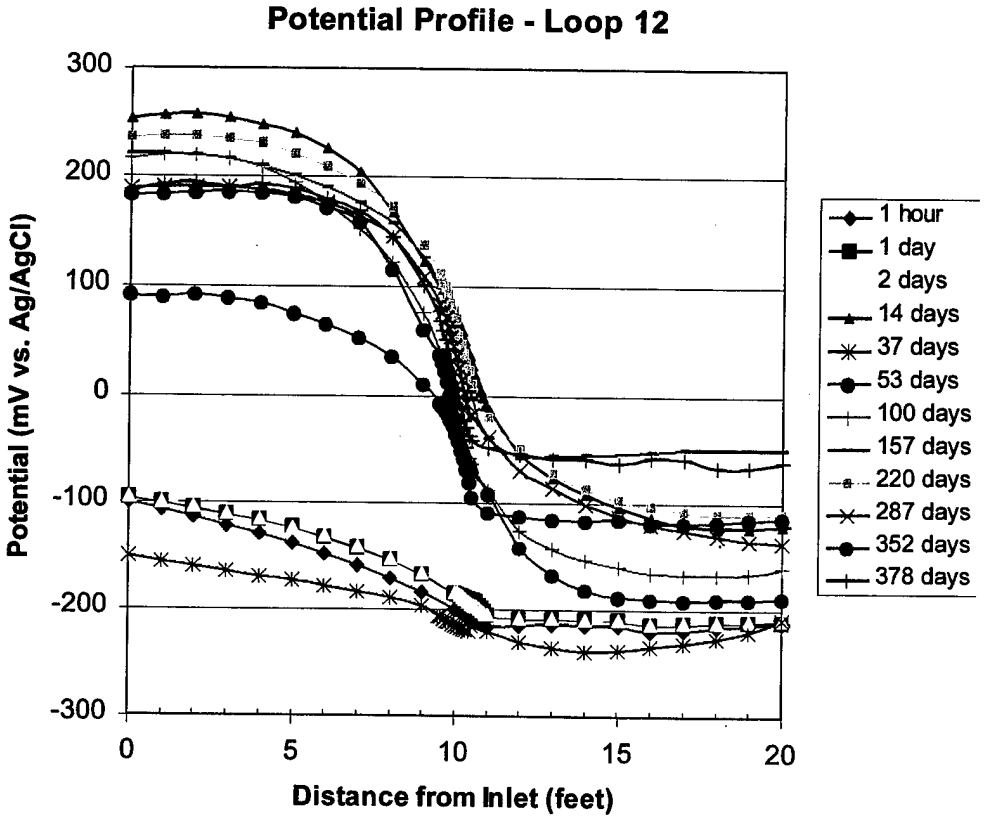

Figure 23 - Alloy 625/70:30 Copper-Nickel Piping Couple – Loop 12. Potential profile shown as a function of time and location along the pipe.

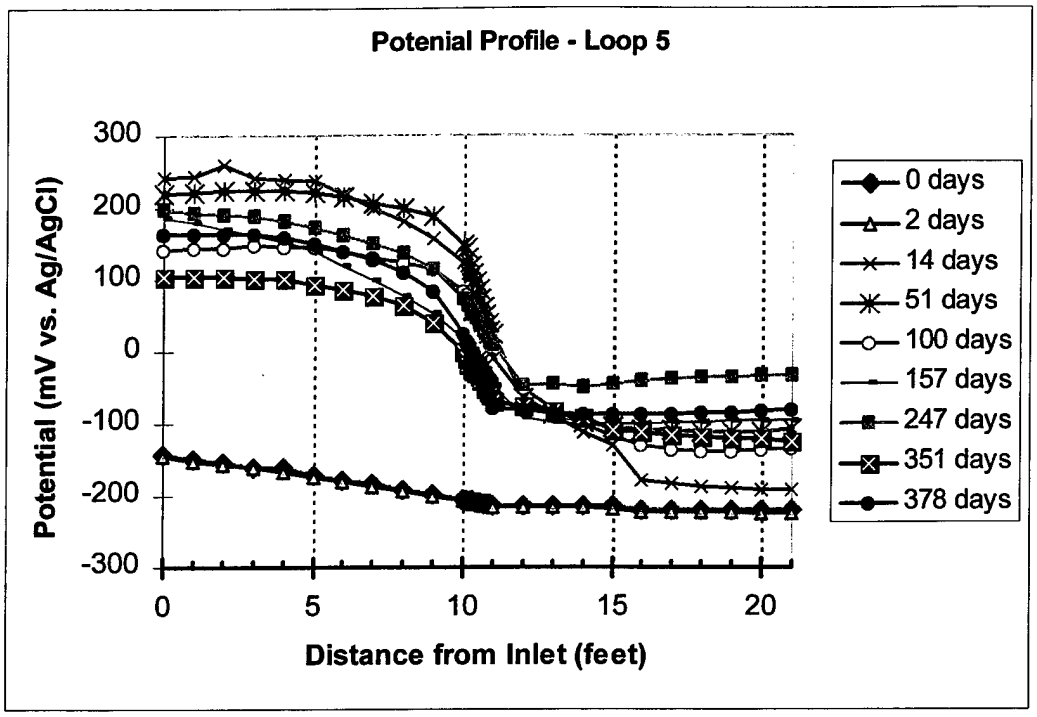

Figure 24 - Alloy 625/70:30 Copper-Nickel Piping Couple separated by a 10-in long PVC spacer – Loop 5. Potential profile shown as a function of time and location.

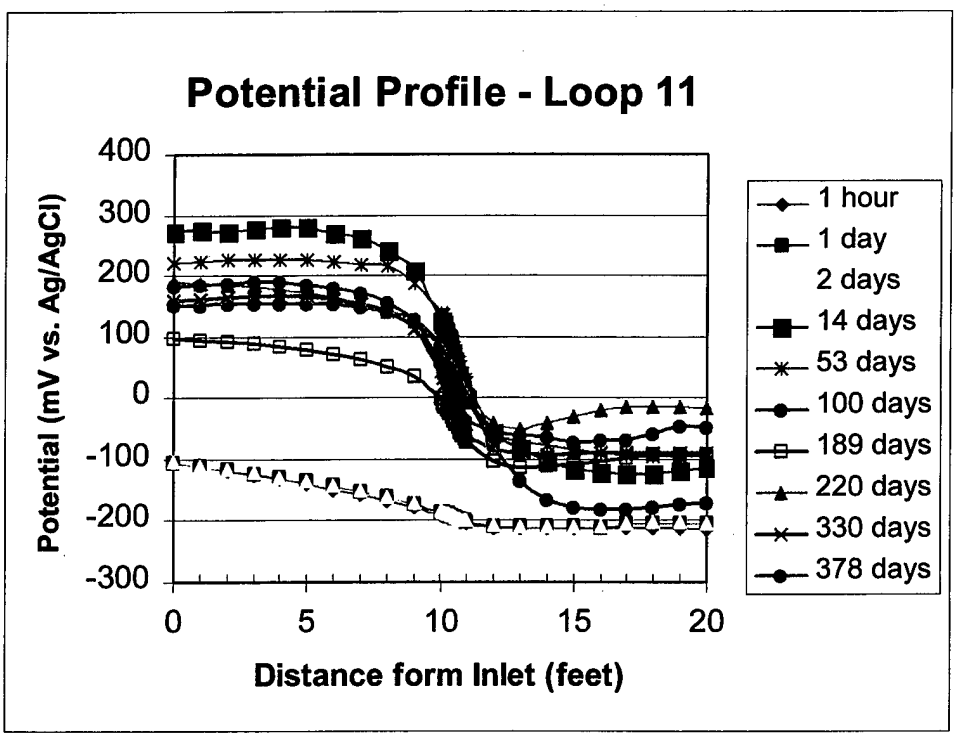

Figure 25 - Alloy 625/70:30 Copper-Nickel Piping Couple separated by a 10-in long PVC spacer – Loop 11. Potential profile shown as a function of time and location.

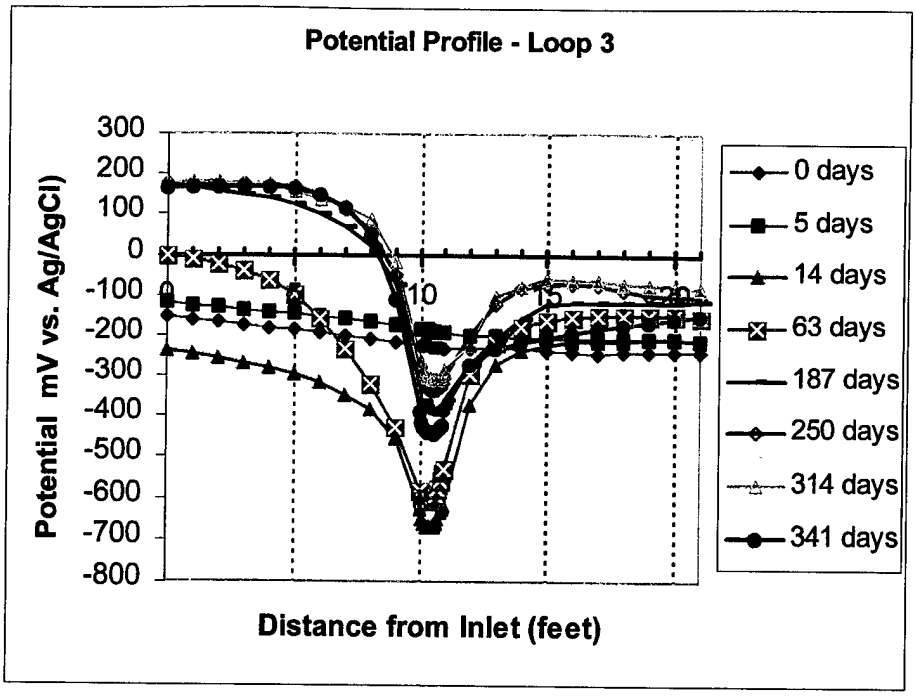

Figure 26 - Alloy 625/70:30 Copper-Nickel Piping Couple with bi-electrode in CP mode – Loop 3. Potential profile shown as a function of time and location.

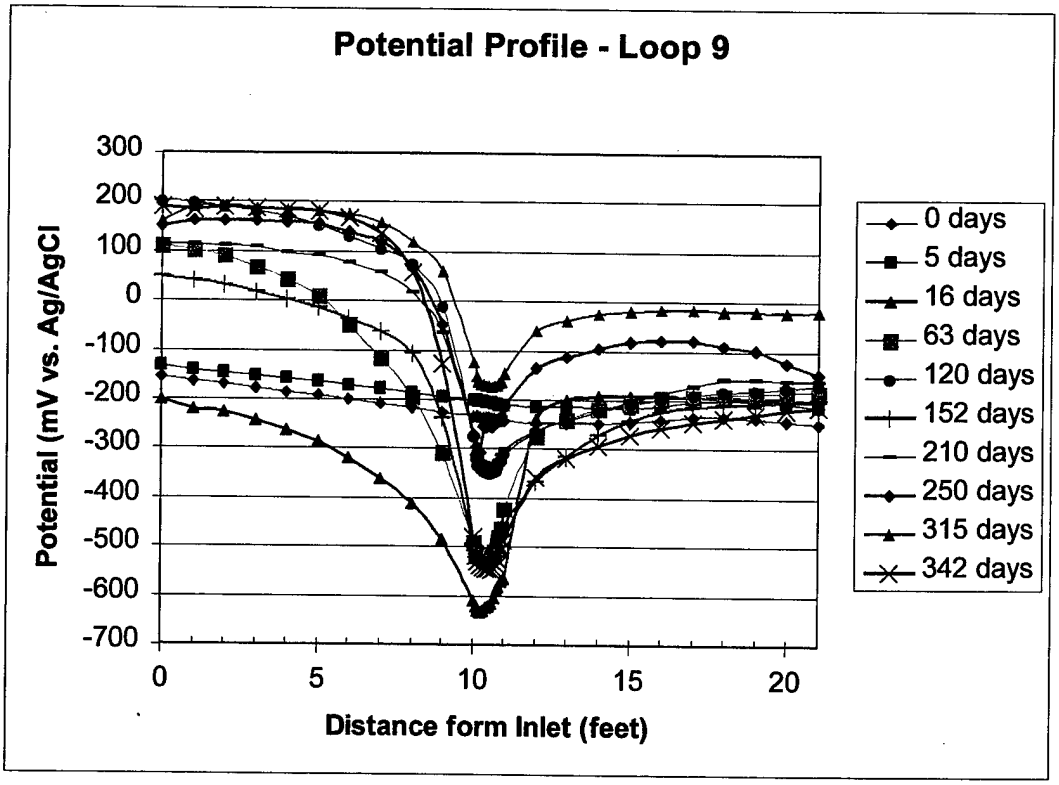

Figure 27 - Alloy 625/70:30 Copper-Nickel Piping Couple with bi-electrode in CP mode – Loop 9. Potential profile shown as a function of time and location.

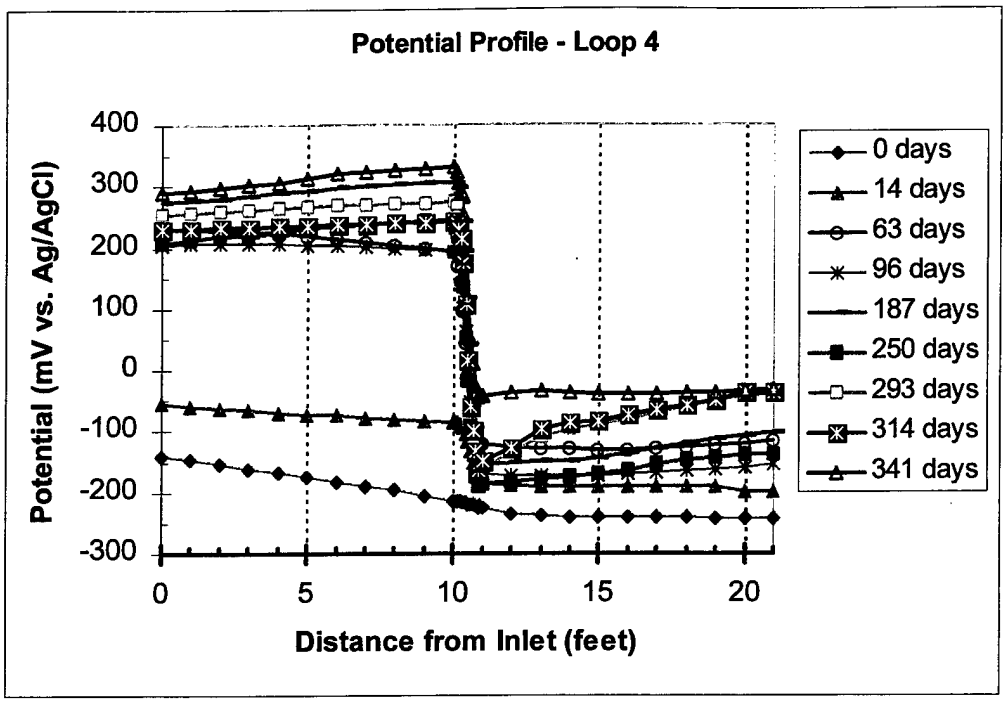

Figure 28 - Alloy 625/70:30 Copper-Nickel Piping Couple with bi-electrode – Loop 4. Potential profile shown as a function of time and location along the pipe.

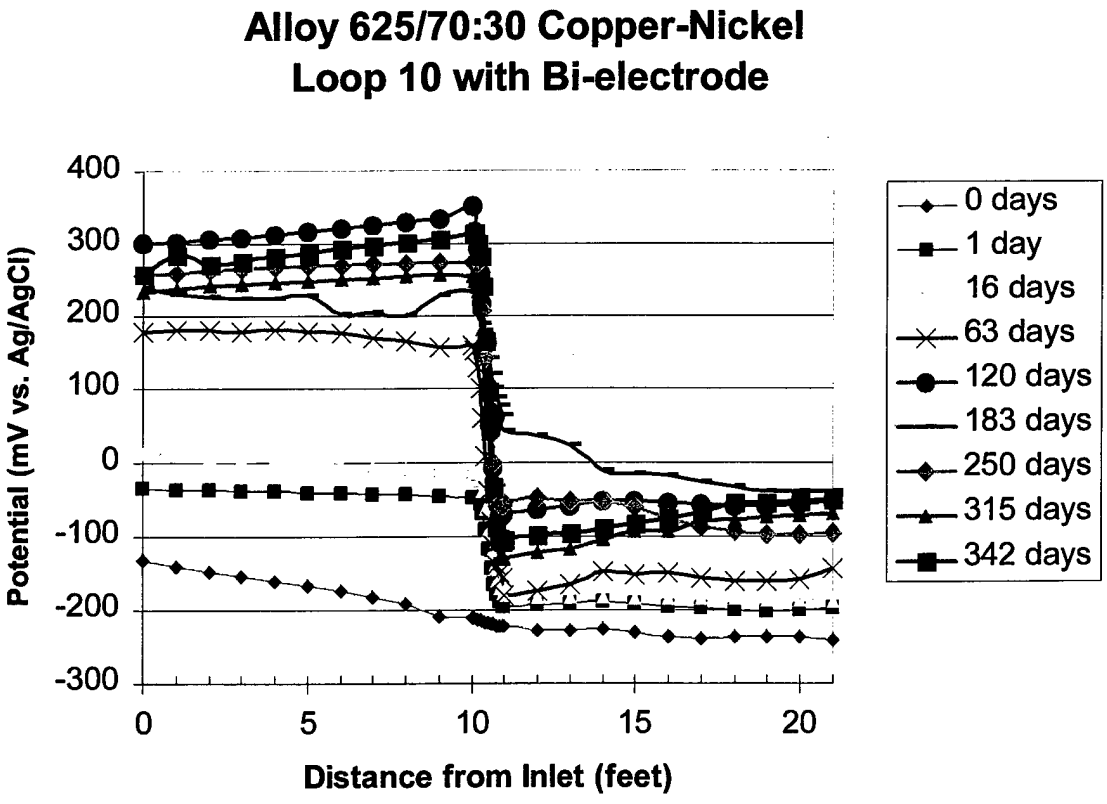

Figure 29 - Alloy 625/70:30 Copper-Nickel Piping Couple with bi-electrode – Loop 10. Potential profile shown as a function of time and location along the pipe

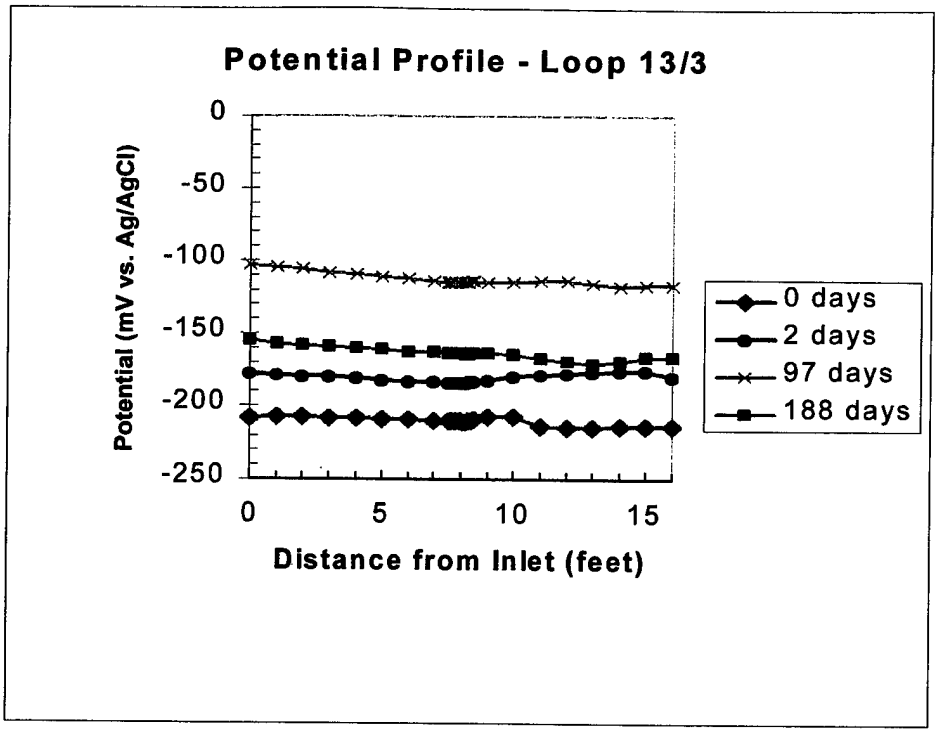

Figure 30 - Urethane-based coated Titanium/70:30 copper-nickel piping couple - Loop 13/3. Potential profile shown as a function of time and location along the pipe.

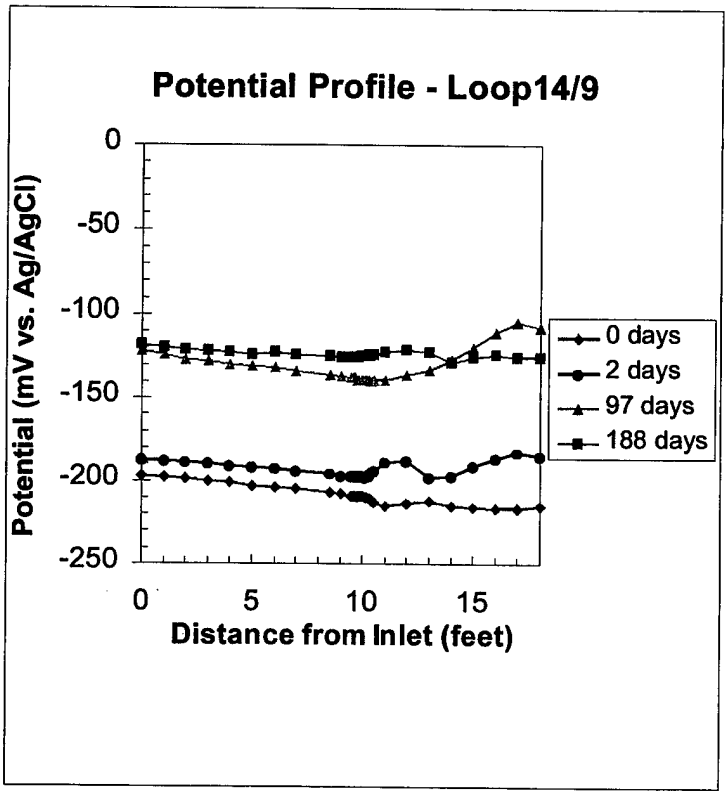

Figure 31 - Tiodize™ Type IV Titanium/70:30 copper-nickel piping couple - Loop 14/9. Potential profile shown as a function of time.

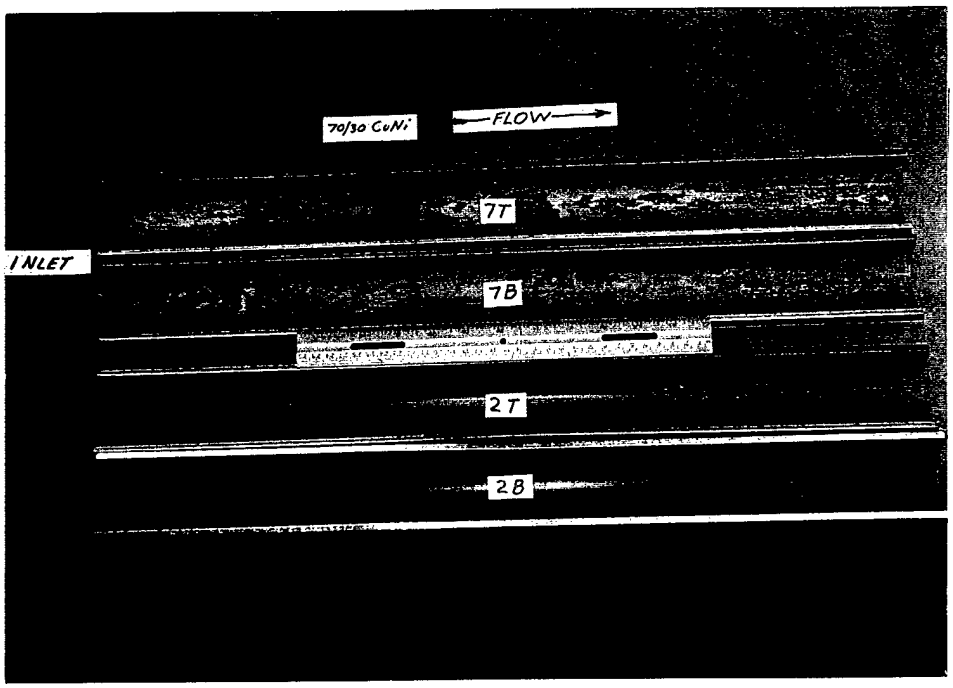

Figure 32 - Copper-nickel pipes coupled to titanium from mockup loops 2 (calcareous deposit coating) and 7 (bare alloy) after about one year seawater exposure. Pipes have been cleaned. Inlet is at junction with titanium. Pipes sectioned into top (T) and bottom (B) section as exposed.

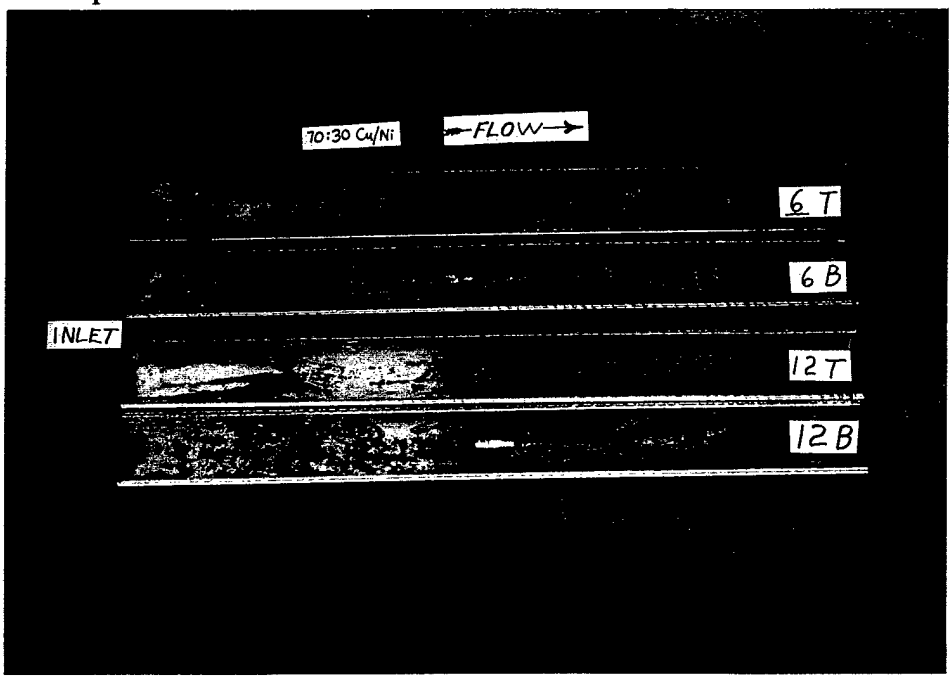

Figure 33 - Copper-nickel pipe sections coupled to Alloy 625 from mockup loops 6 and 12 after about one year seawater exposure. Inlet is at junction with the cathodic 625 section. Heavy copper deposits on copper alloy surfaces, particularly at inlet.

Figure 34 - Top and bottom sections of copper-nickel pipe section coupled to Alloy 625 (loop 12). Inlet (left side) is at junction with the cathodic 625 section. Heavy copper deposits on copper alloy surfaces, particularly along the bottom of pipe (lower tube half).

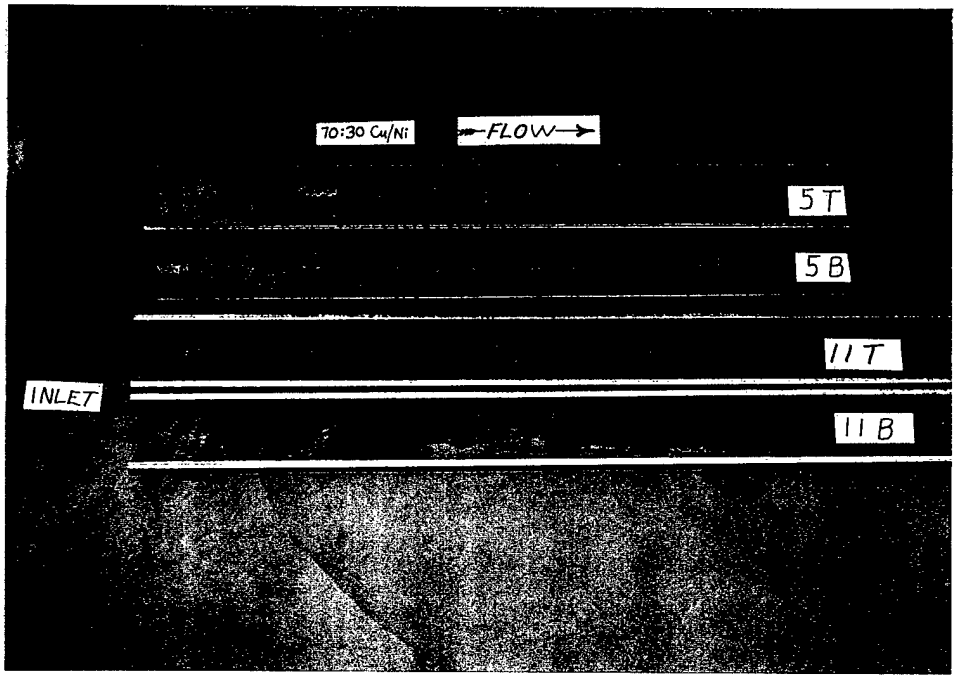

Figure 35 - Copper-nickel pipe sections coupled to a 10-in long PVC spacer and Alloy 625 from mockup loops 5 and 11 after about one year seawater exposure. Inlet is at junction with the cathodic 625 section.

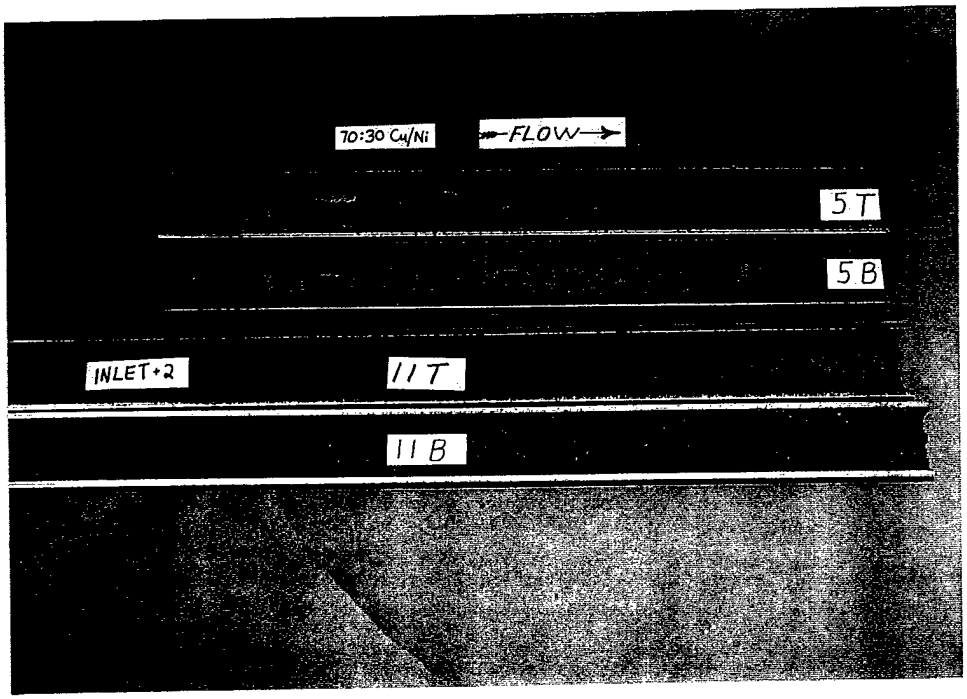

Figure 36 - Copper-nickel pipe sections coupled to a 10-in long PVC spacer and Alloy 625 from mockup loops 5 and 11 after about one year seawater exposure. Bottom of loop 11 displayed some macrofouling about 4 feet (120 cm) from the copper-nickel inlet.

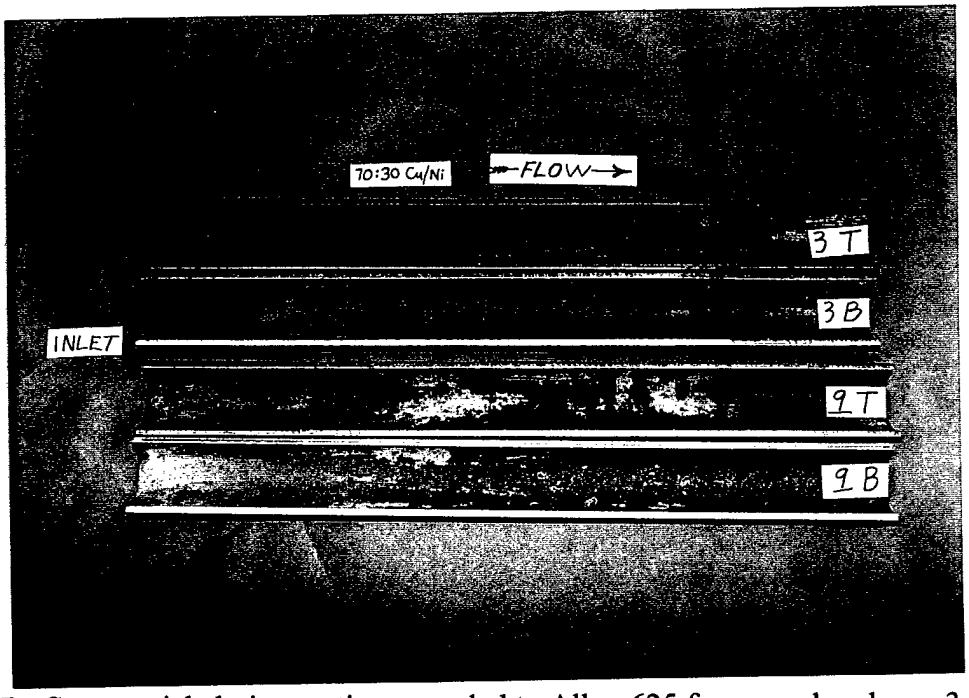

Figure 37 - Copper-nickel pipe sections coupled to Alloy 625 from mockup loops 3 and 9 under the influence of cathodic protection after about one year seawater exposure "as received". Surfaces appeared to have formed a scale over most the top and bottom surfaces.

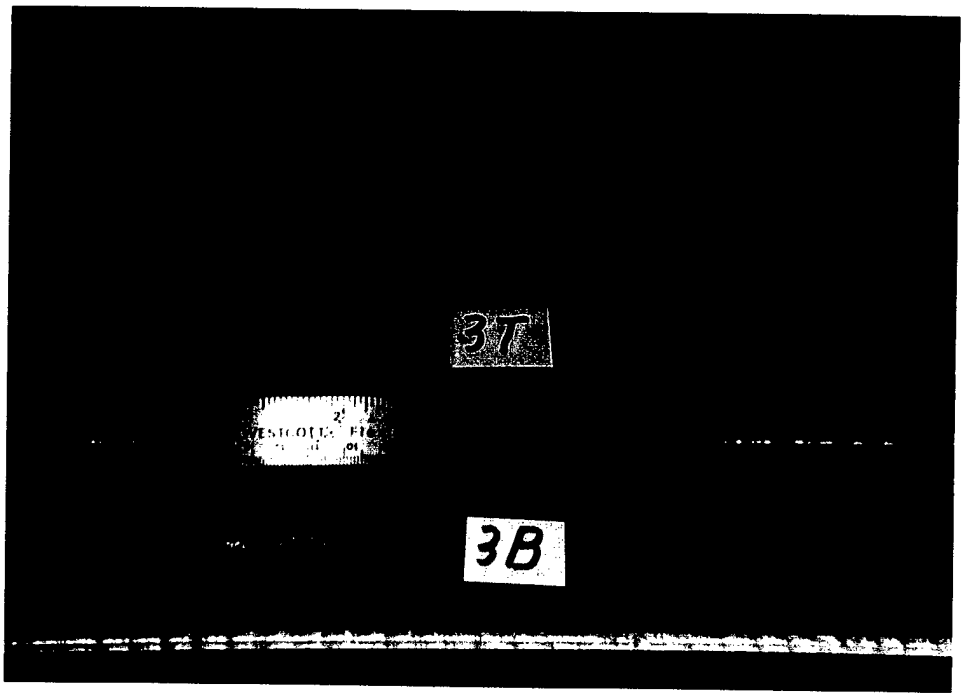

Figure 38 - Some cleaning of the top and bottom sections of copper-nickel piping (loop 3) discloses that the calcareous deposit has formed on the waterside surfaces as a result of the cathodic protection.

Figure 39 - Closeup of bottom calcareous deposit formed 12 to 16-in. from junction with CP device on copper-nickel pipe 9. Deposit a result of impressed current from cathodic protection.

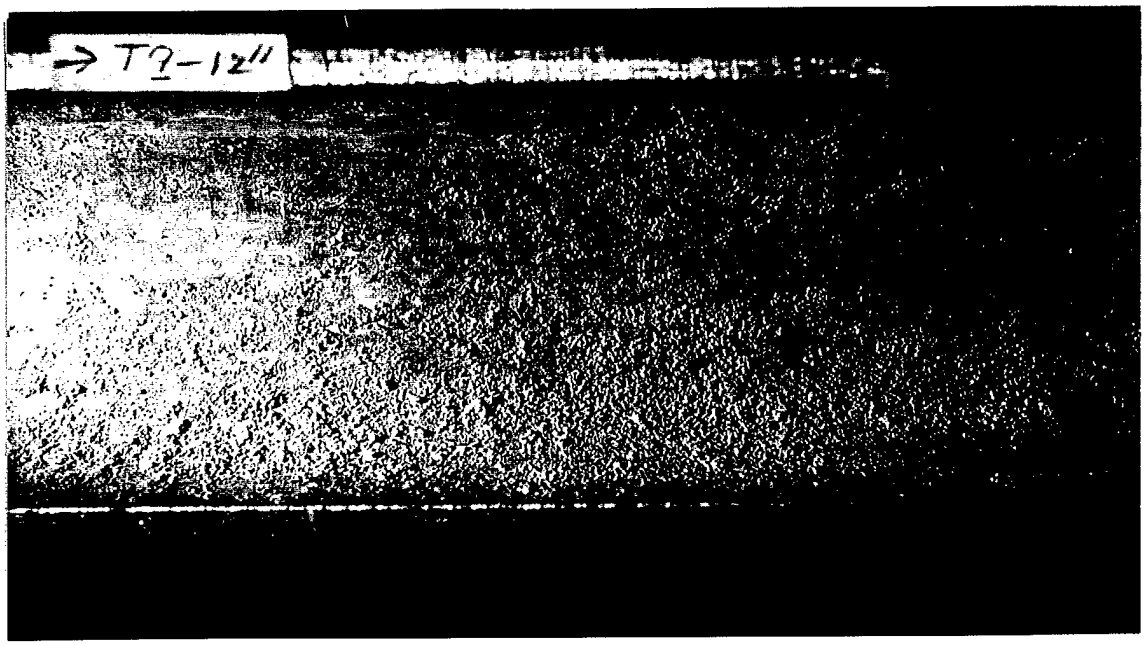

Figure 40 - Top side, nonuniform calcareous deposit formed 12 to 16-in. from junction with CP device on copper-nickel pipe 9. Deposit a result of impressed current from cathodic protection.

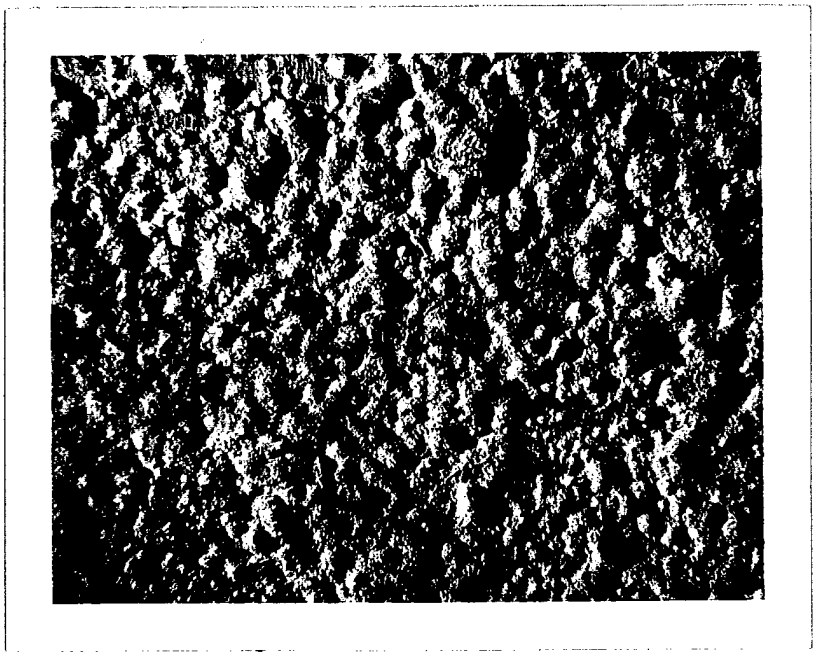

Figure 41 - Copper-nickel piping surface (loop 3) discloses the nature of the calcareous deposit which has formed as a result of the applied current from the cathodic protection.

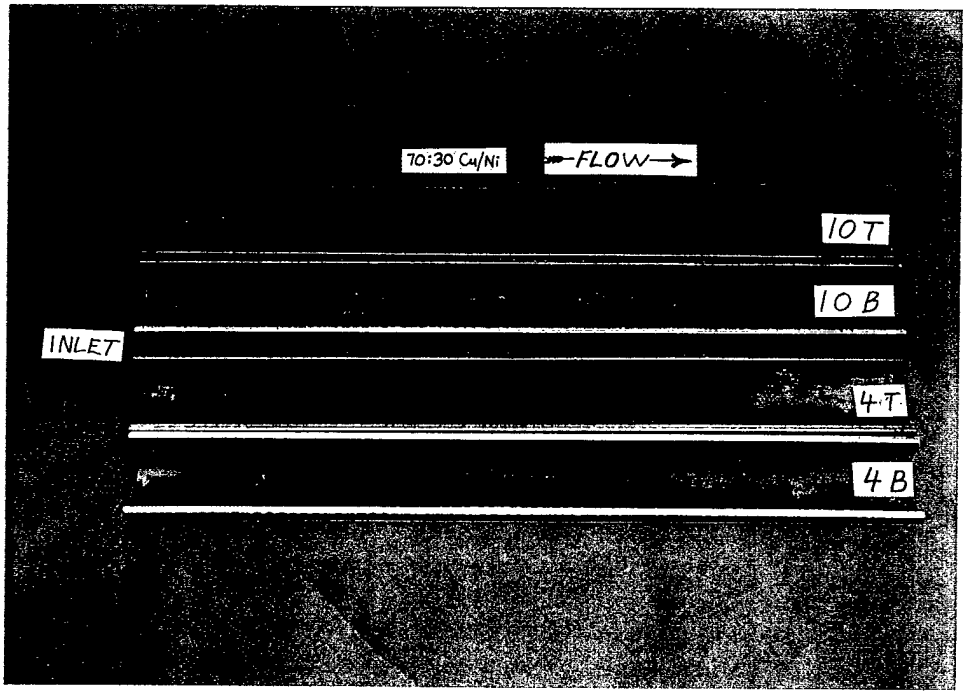

Figure 42 - Copper-nickel pipe sections coupled to Alloy 625 from mockup loops 4 and 10 under the influence of the bi-electrode after about one year seawater exposure "as received". Surfaces appeared to have little scale on either the top or bottom surfaces.

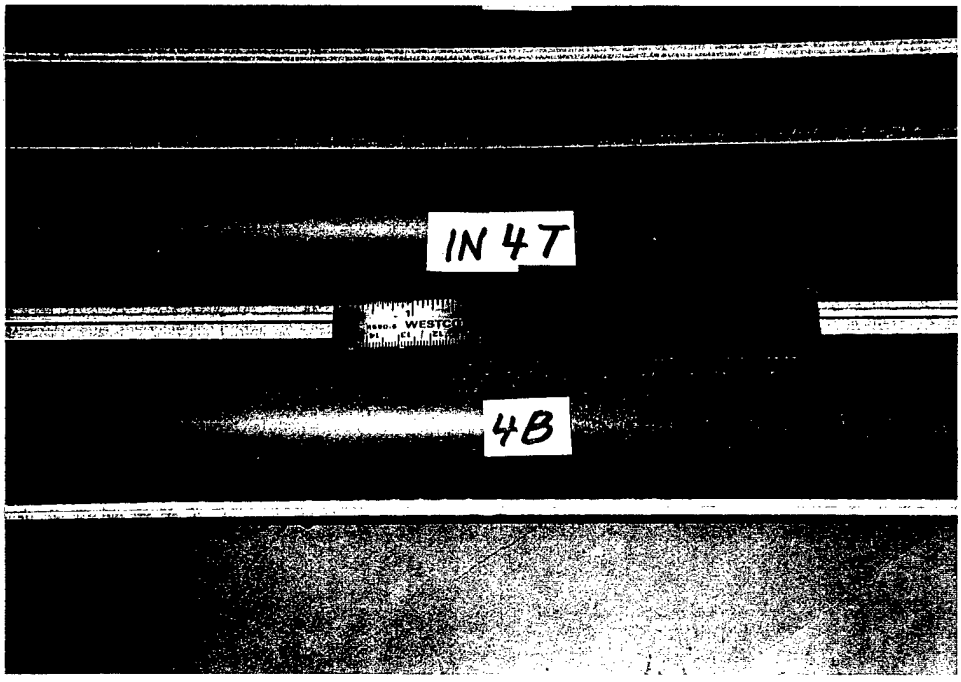

Figure 43 - Closer examination of the copper-nickel section from loop 4 revealed no apparent pitting of the waterside surfaces after slight cleaning.

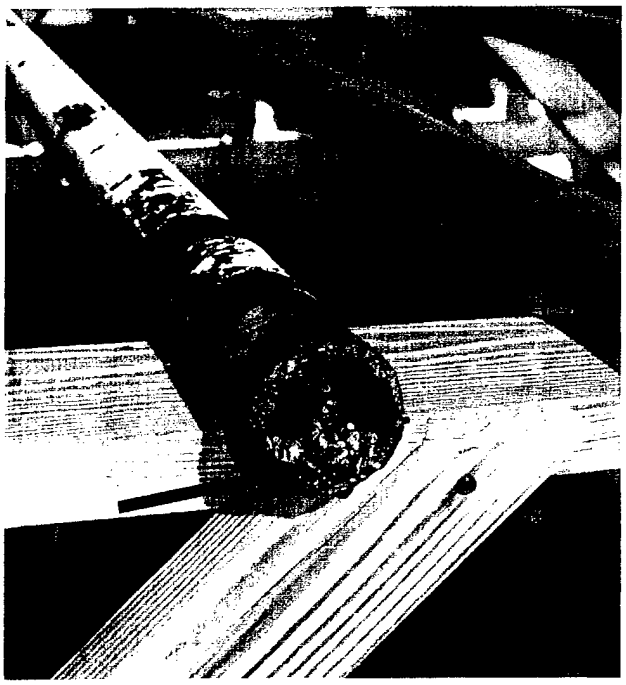

Figure 44 - Macrofouling of titanium piping viewed (at arrow) during one of the inspections during the one-year exposure using filtered natural seawater flowing at 1.8 m/s.

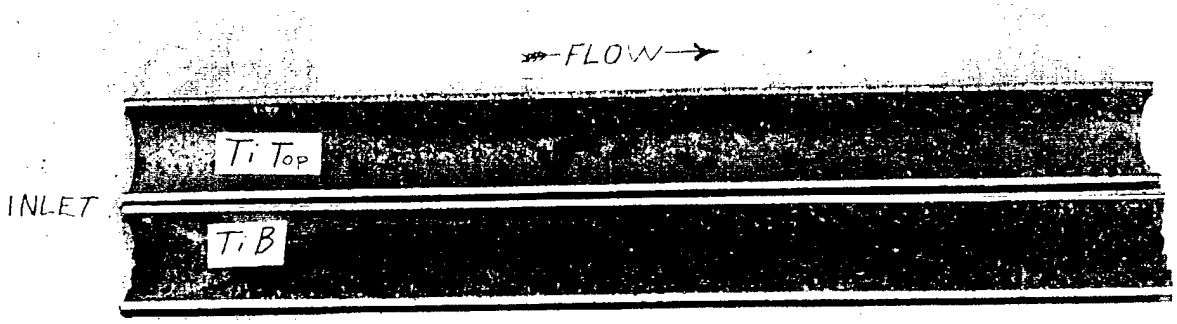

Figure 45 - Distribution of the macrofouling at the inlet end of the titanium pipe shows that heaviest concentration is on bottom half.

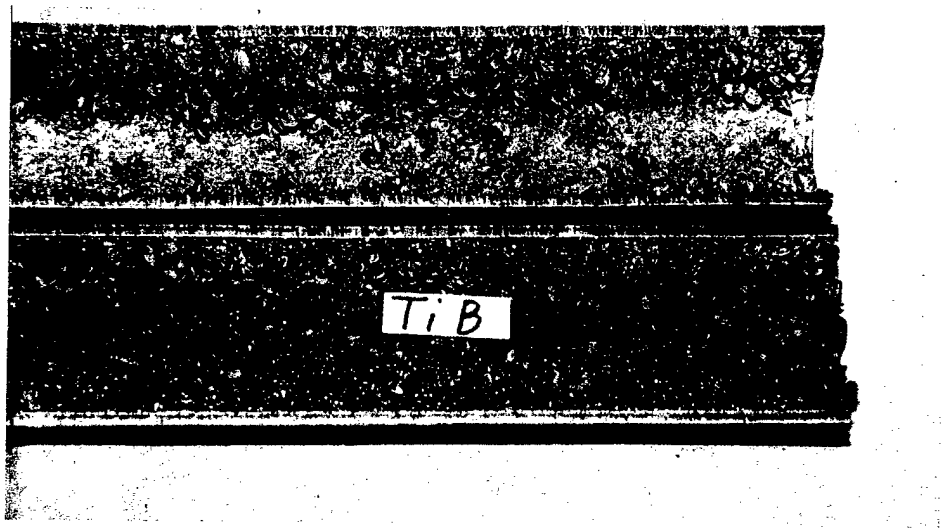

Enlarged view of the macrofouling on titanium shows small mussels
form ping surface.

Figure 47 - Biofouling at the outlet of a Alloy 625 section viewed during one of the inspections during the one-year exposure in flowing, filtered natural seawater.

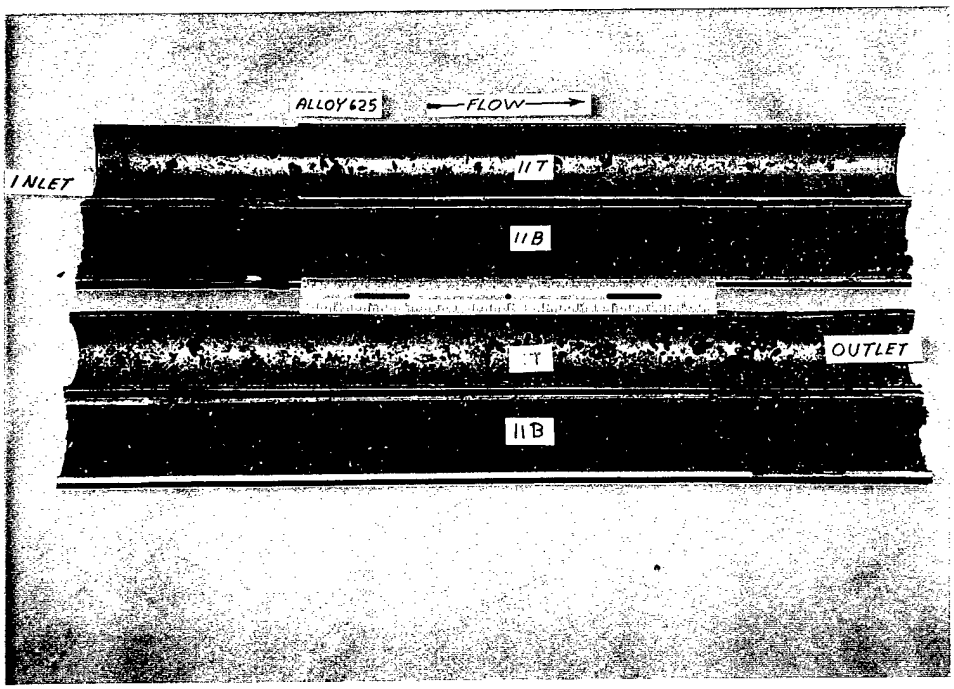

Figure 48 - Distribution of the macrofouling at the outlet end of an Alloy 625 pipe also shows that heaviest concentration is on bottom half.

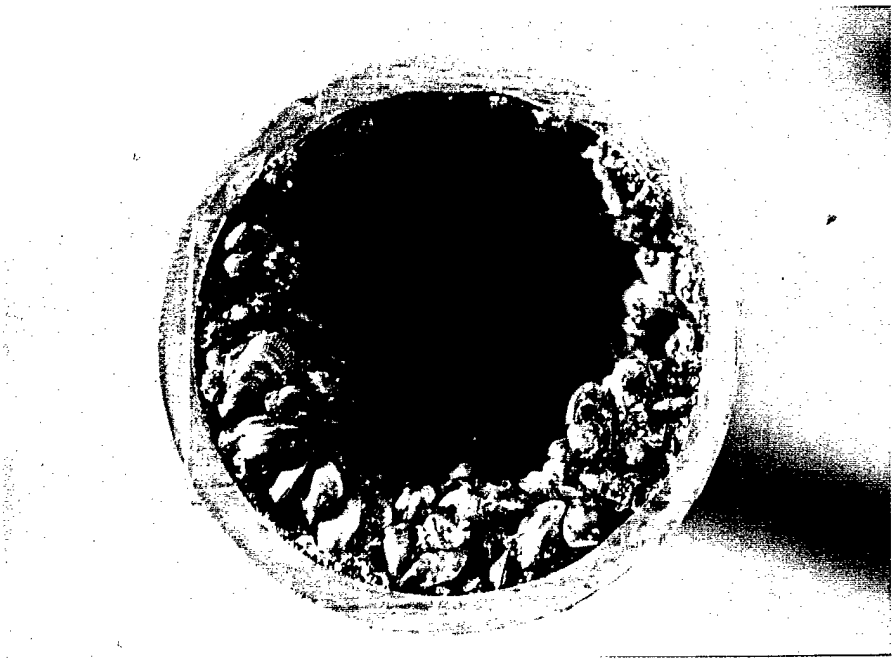

Figure 49 - Cross-section of the macrofouling after six months of exposure. Reduction of cross-sectional area increases effective flow downstream of restictions,

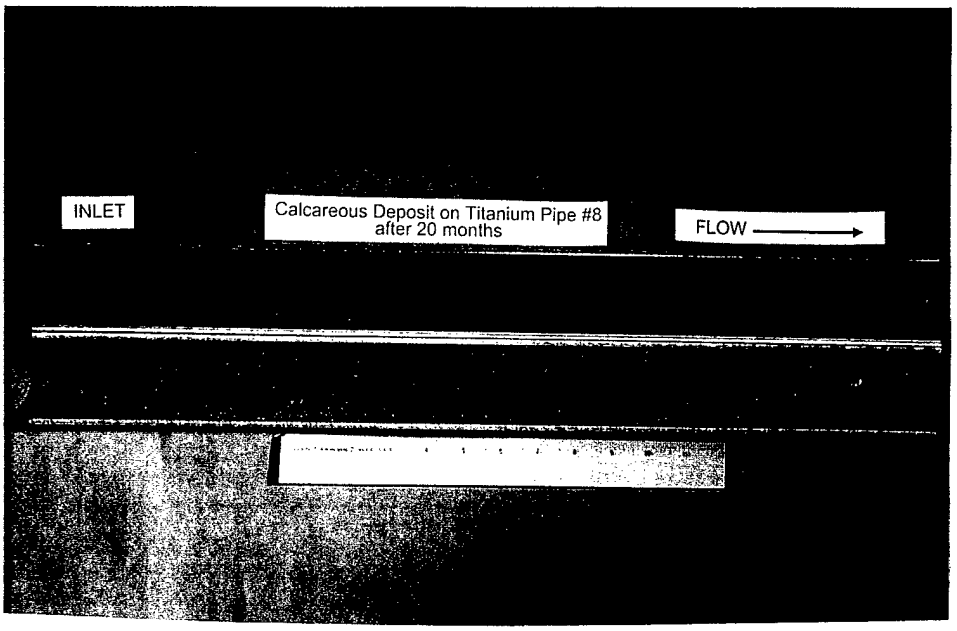

Figure 50 - Condition of calcareous deposit coated titanium pipe after 20 months exposure. Macrofouling along bottom half of pipe.

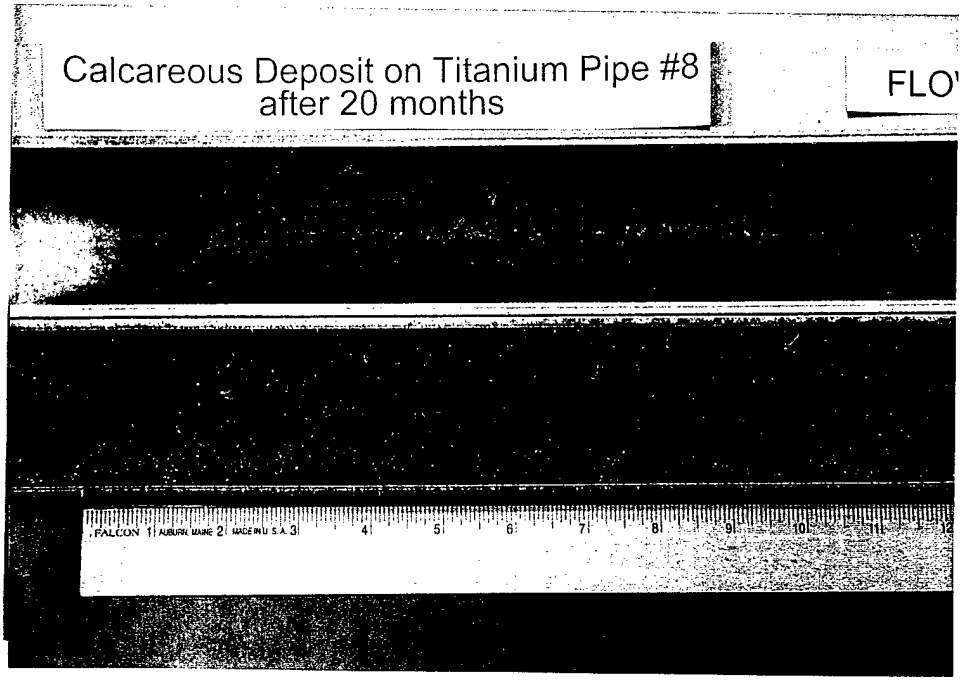

Figure 51 - Magnified view of top and bottom of titanium pipe after 20 months of exposure.

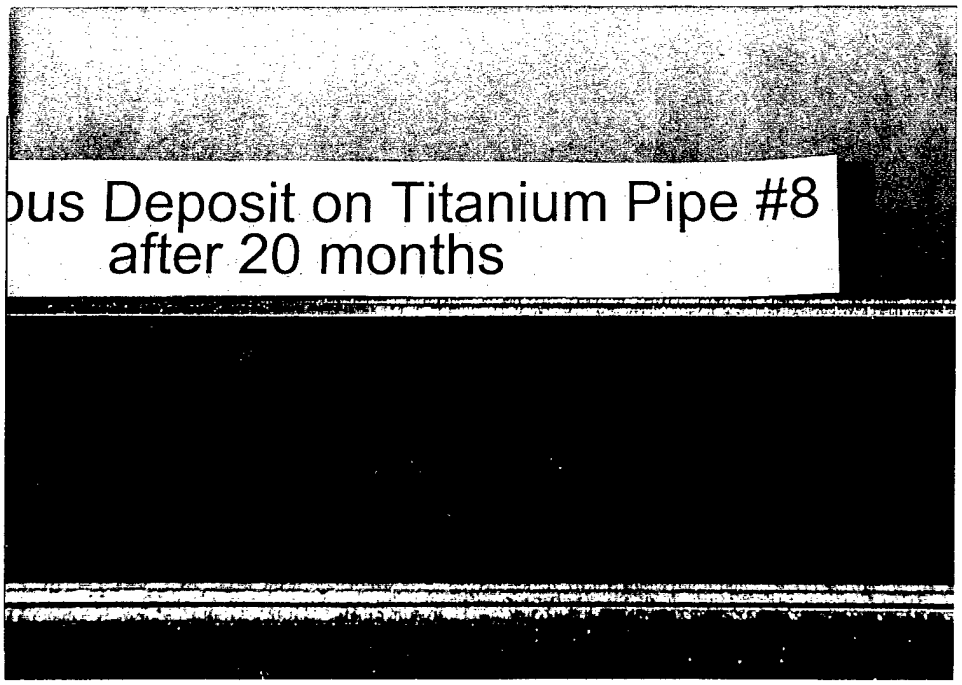

Figure 52 - Calcareous deposit remains on titanium piping surface, but there is some flaking and thinning of the deposit after 20 months of exposure.

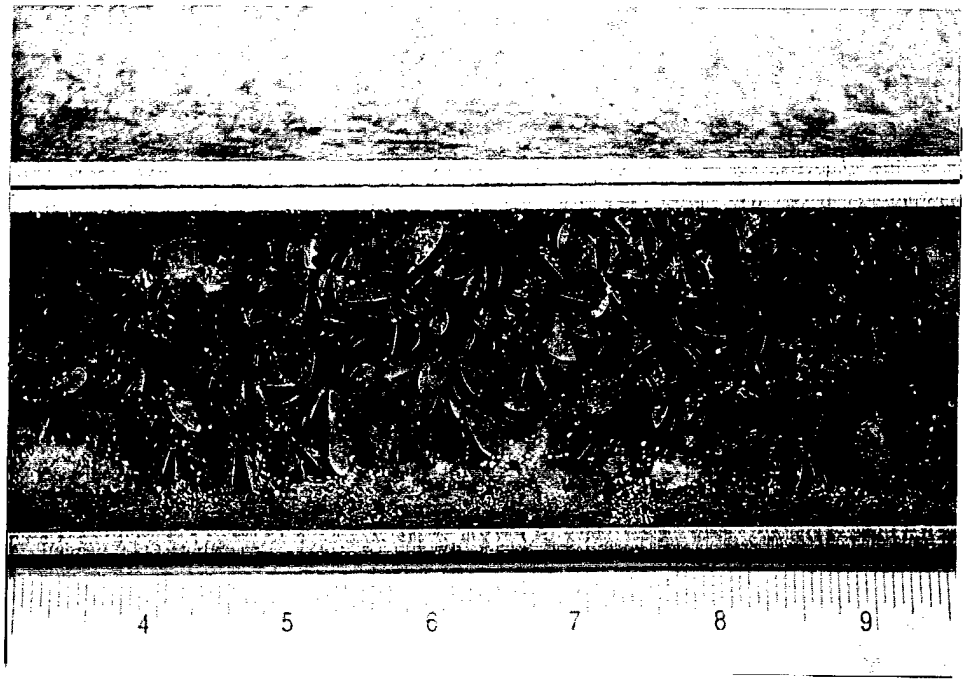

Figure 53 - Small mussels about 3-5 months old have formed over the bottom titanium pipe despite using flowing (1.8m/s) filtered natural seawater.

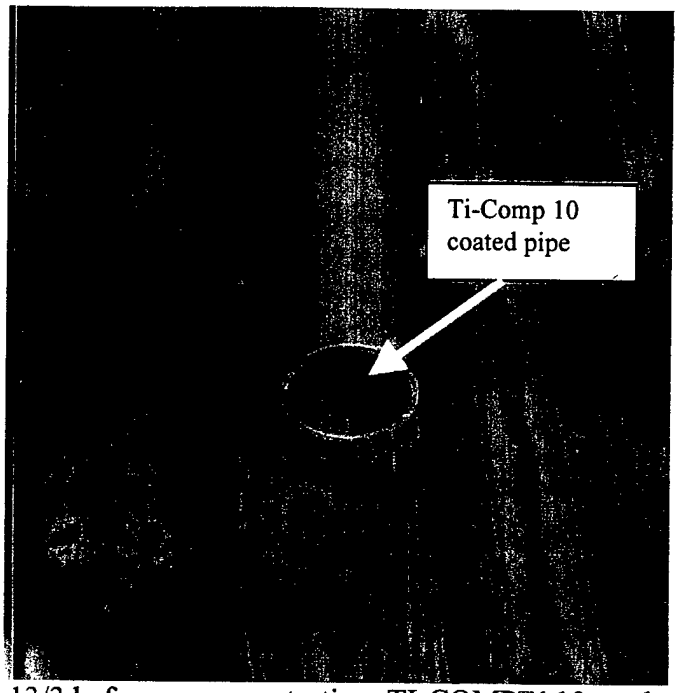

Figure 54 - Pipe 13/3 before exposure testing. TI-COMP™ 10 urethane-based coating was applied on both inner and outer surfaces of titanium pipe after thorough cleaning.

Figure 55 - TI-COMP™ 10 coated titanium pipe after 6 months exposure. Interior deposit and sludge during the exposure period could easily be removed.

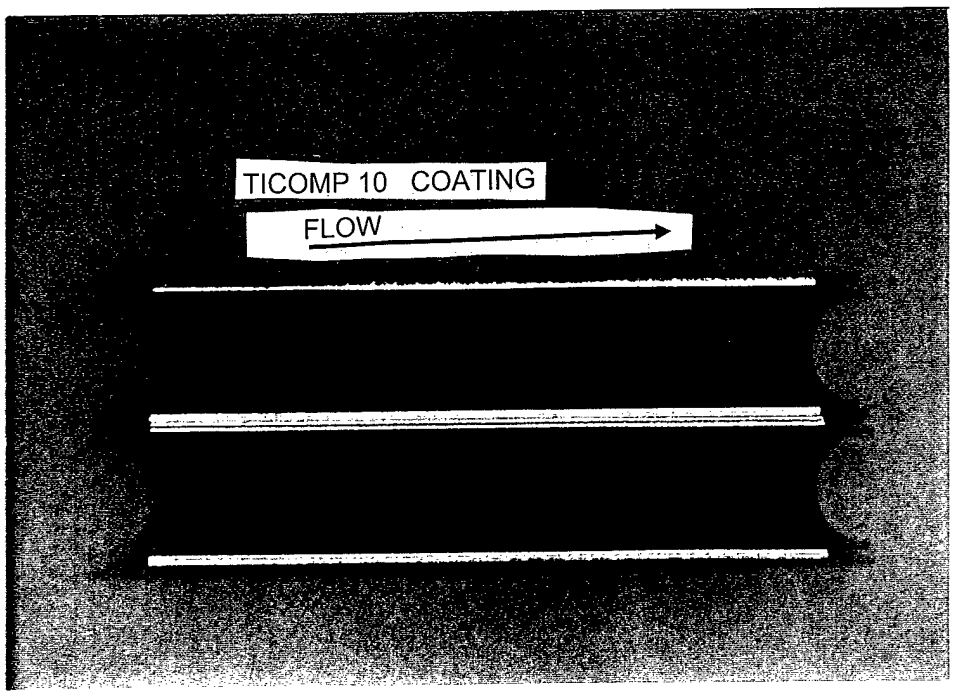

Figure 56 - Loose deposits found along a segment (1-ft long) titanium pipe with TI-COMP™ 10 urethane-based coating.

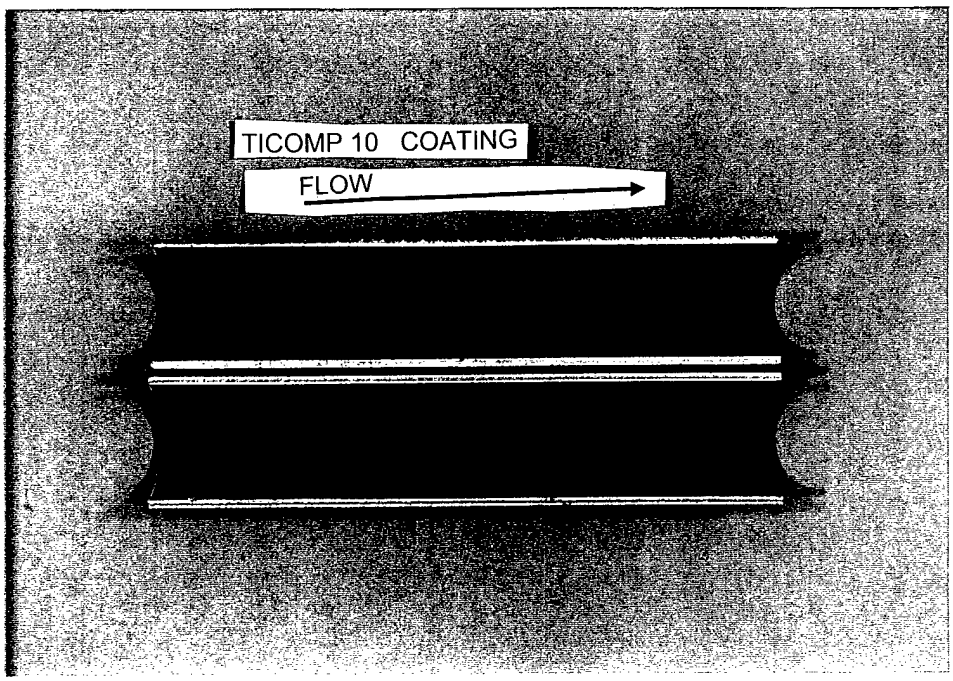

Figure 57 - After removal of sludge and deposits along the TI-COMP™ 10 coated titanium pipe, coating appeared intact after the 6 months exposure.

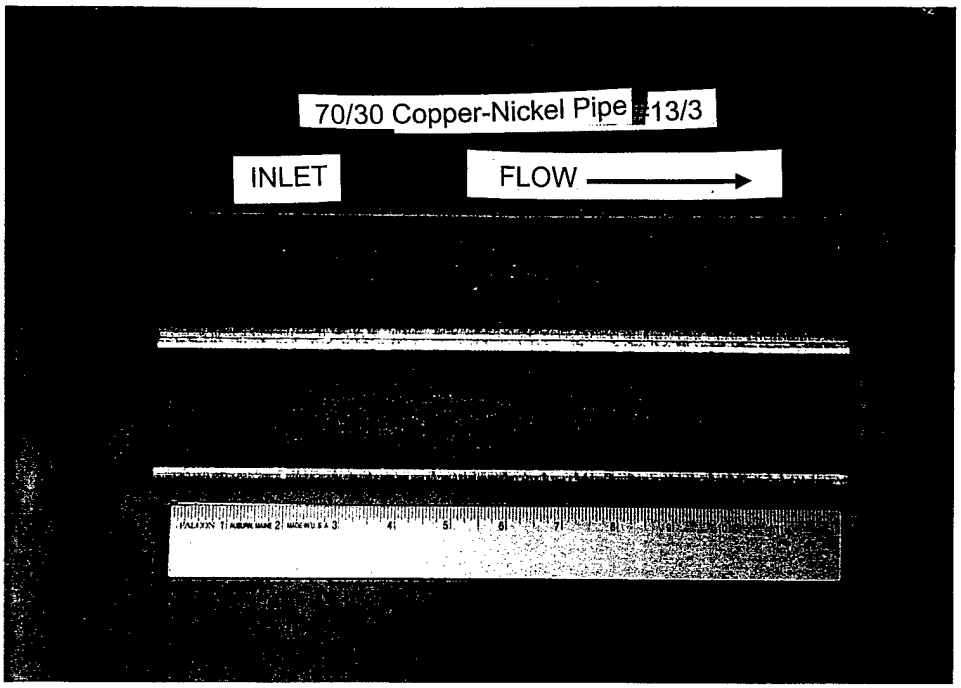

Figure 58 - Copper-nickel section after 6 months exposure to adjacent TI-COMP™ 10 coated titanium pipe. Small macrofouling site located on bottom half of copper-nickel surface. No visible corrosion of copper-nickel observed.

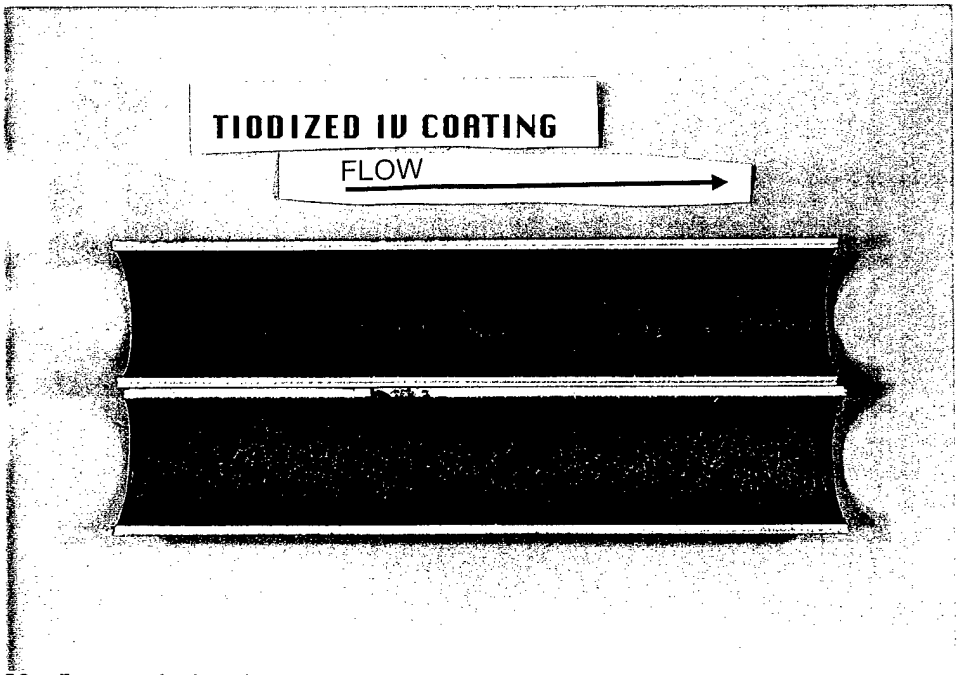

Figure 59 - Loose sludge found on anodized titanium piping (loop 14/9) section after 6 months of exposure in flowing seawater.

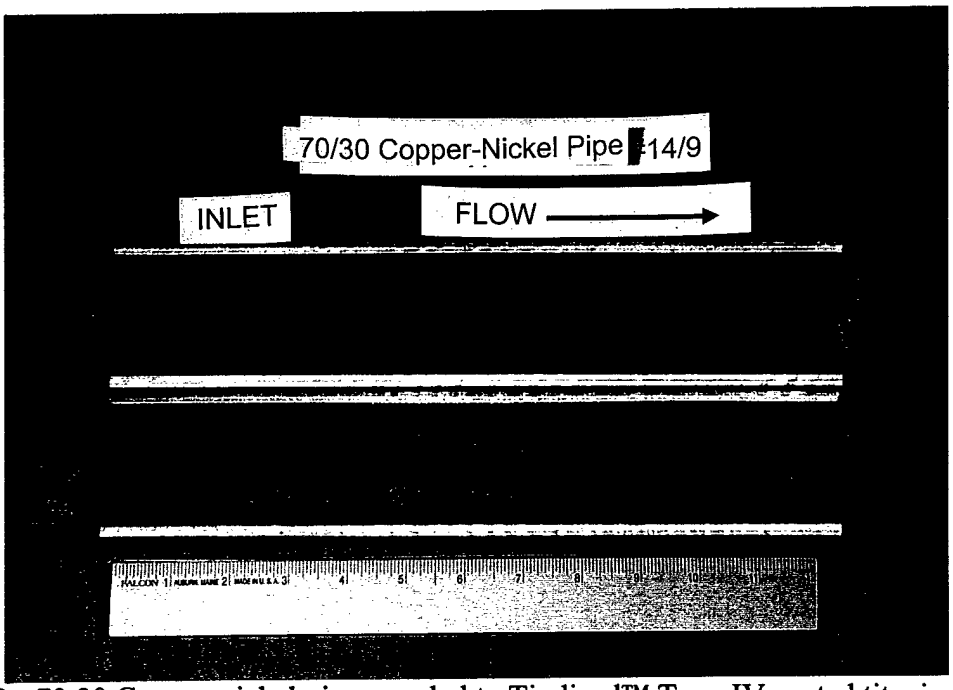

Figure 60 - 70:30 Copper-nickel pipe coupled to Tiodized™ Type IV coated titanium pipe (loop 14/9). No visible corrosion observed.

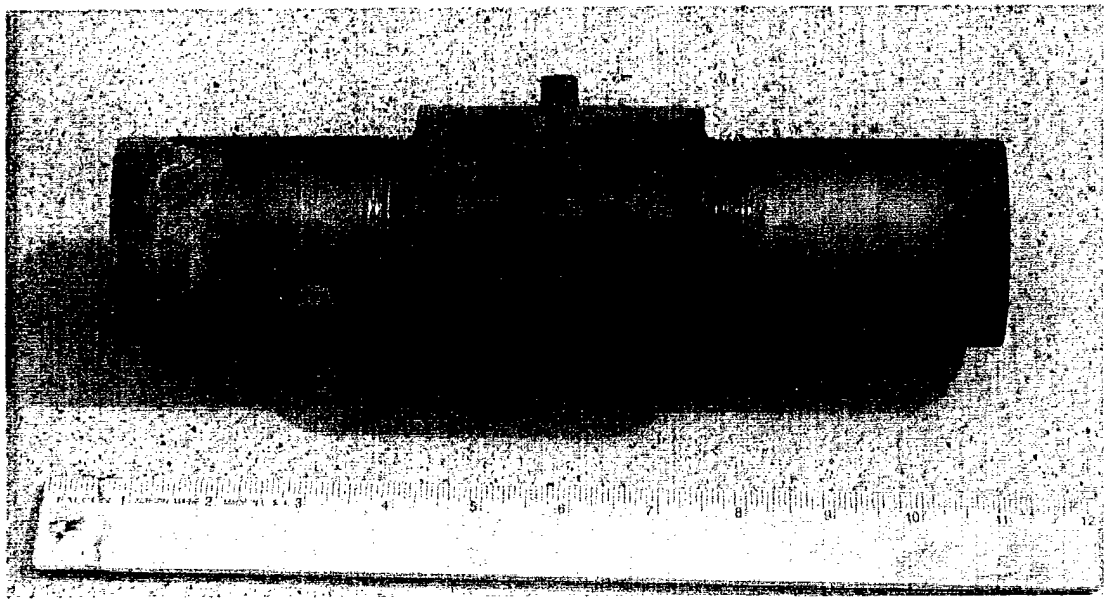

Figure 61 - Bi-electrode used in LCCT piping mockup tests in natural seawater to control galvanic currents between Alloy 625/70:30 copper-nickel piping sections. Two 4-in long titanium pipe nipples were platinized on interior surfaces and connected to PVC coupler.

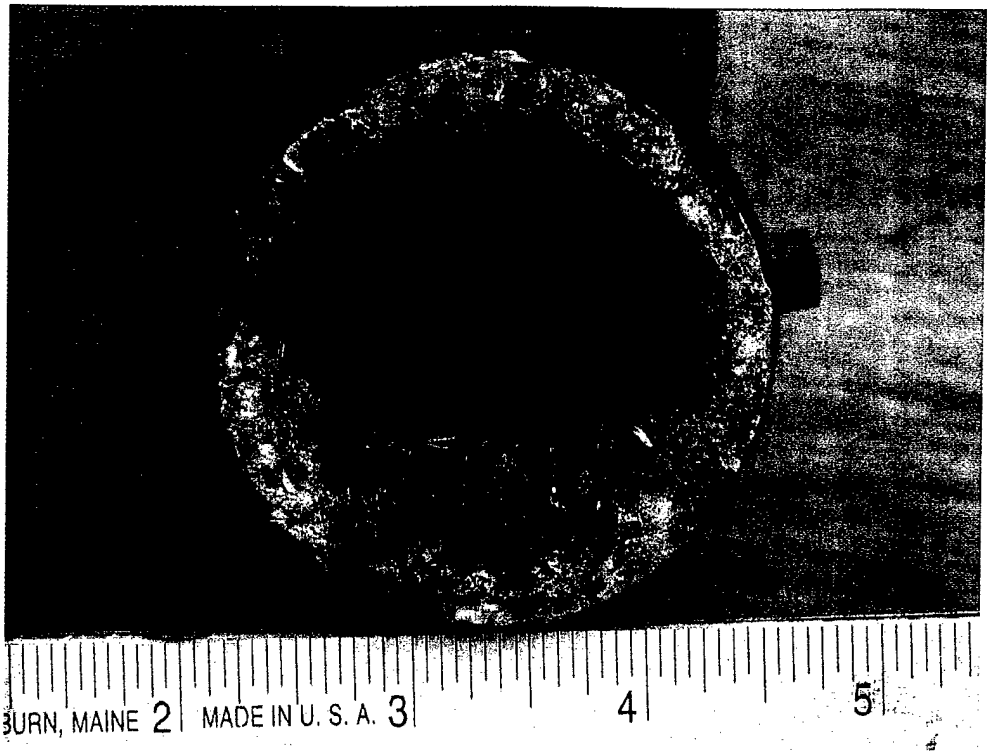

Figure 62 - Bi-electrode end adjacent to the Alloy 625 piping section displayed calcareous deposits and macrofouling on platinized electrode.

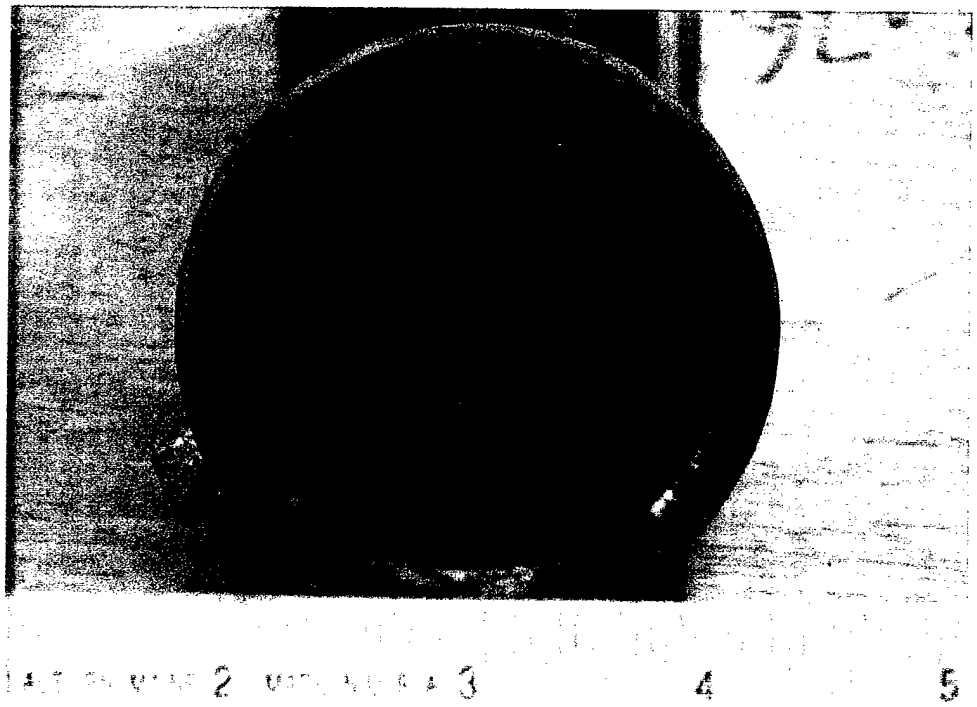

Figure 63 - Bi-electrode end adjacent to the 70:30 copper-nickel piping section displayed a clean platinized electrode with no deposits or macrofouling.

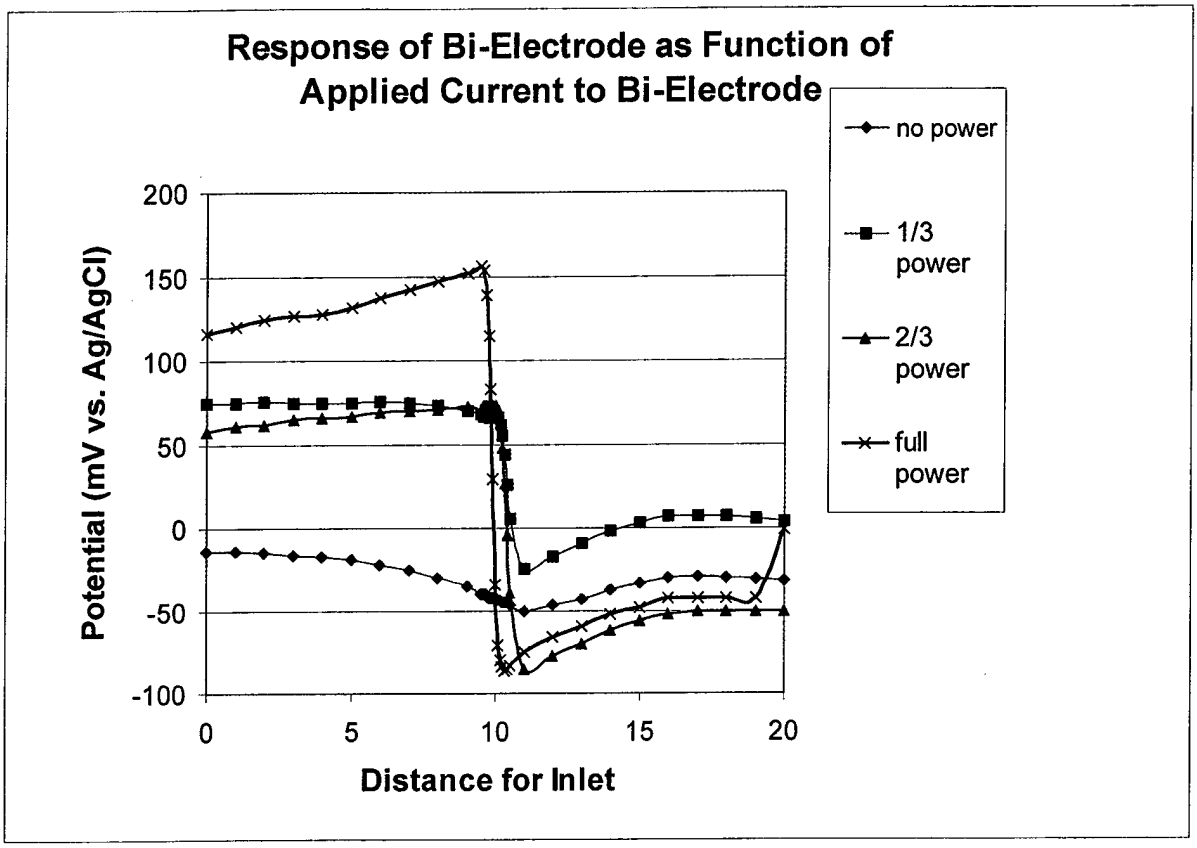

Figure 64 - Effects of the bi-electrode (BED) on titanium (0 to 10-ft) and 70:30 copper-nickel as a function of applied current (power). Full power is the applied current required to completely counteract the normal galvanic current flow. As the power to the bi-electrode is increased, the potential of the titanium adjacent to the BED becomes more electropositive than steady state potential of titanium and the copper-nickel adjacent to the BED becomes more electronegative than the steady state potential of Cu-Ni.

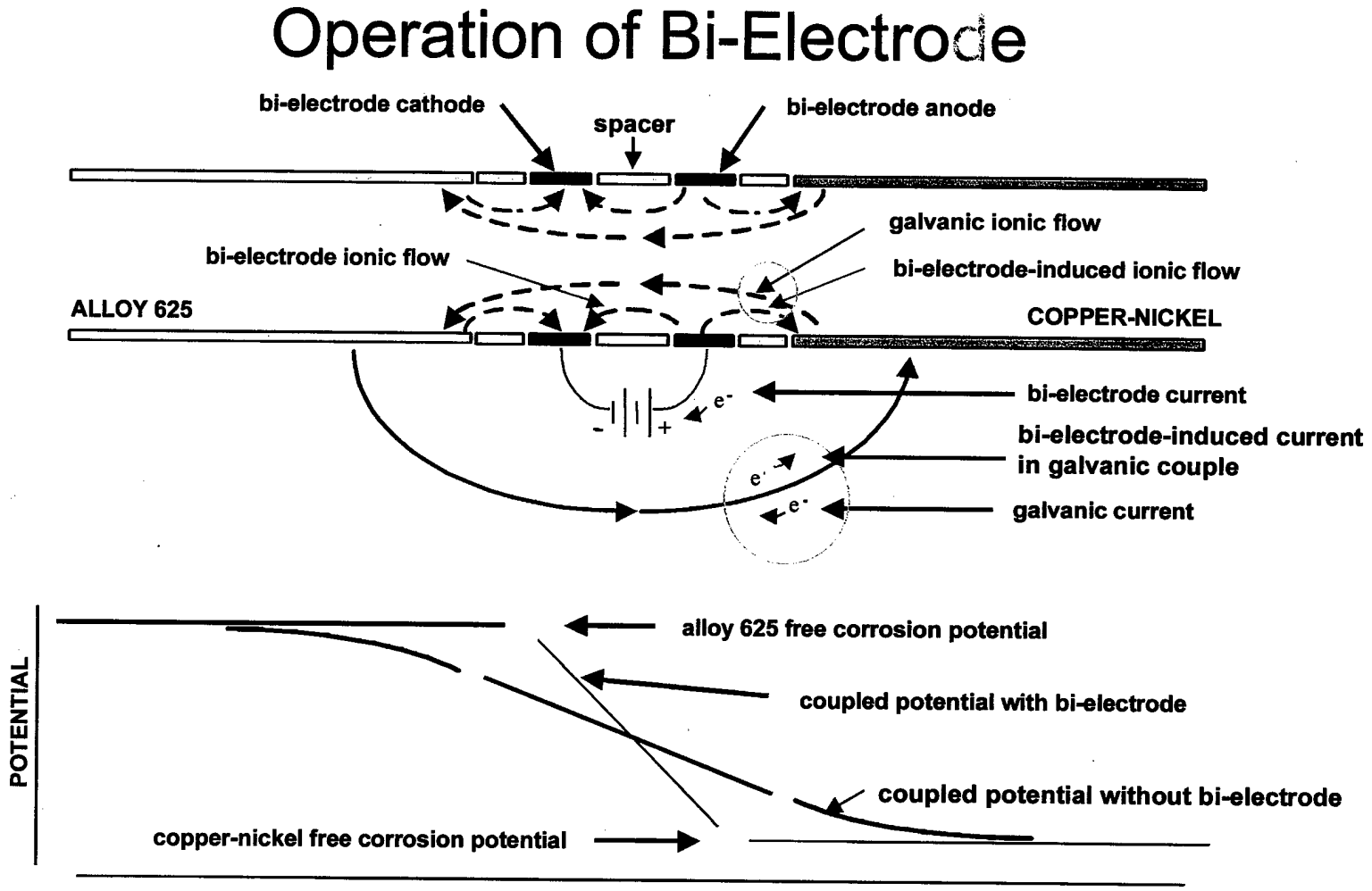

Figure 65 - Bi-electrode device operation as supported by visual observations and mockup piping loop testing.

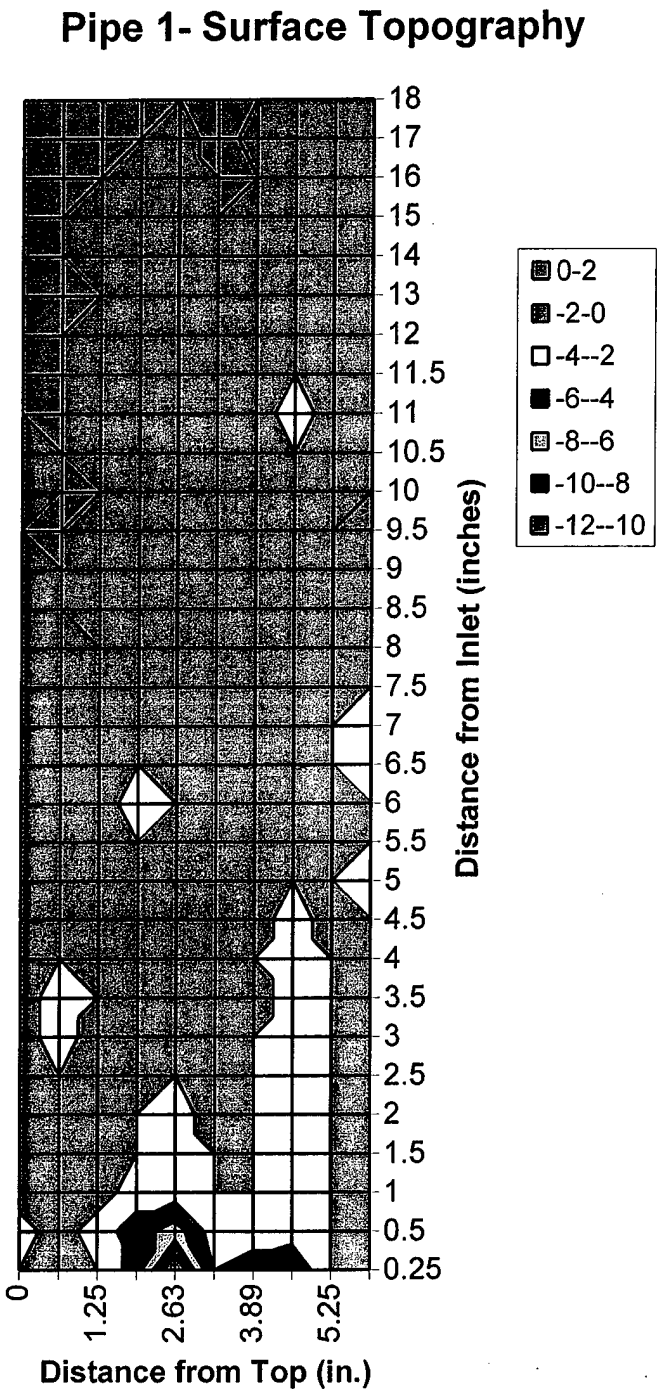

Figure 66 - Titanium/70:30 copper-nickel couple, mockup loop 1 after 637 days exposure. Surface topography of copper-nickel section as function of pipe clockwise orientation and distance from titanium. Legend denotes depth of corrosion/pitting in mils (0.001").

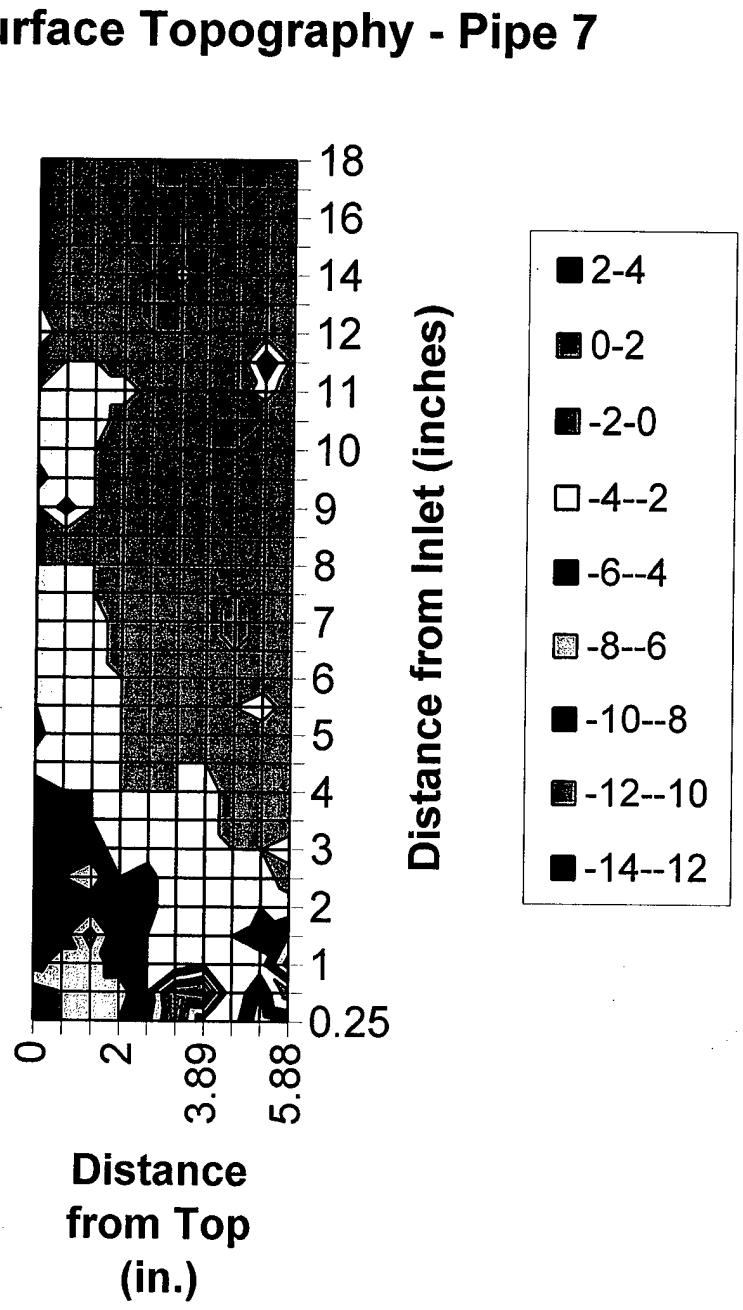

Figure 67 - Titanium/70:30 copper-nickel couple, mockup loop 7 after 379 days exposure. Surface topography of copper-nickel section as function of pipe clockwise orientation and distance from titanium. Legend denotes depth of corrosion/pitting in mils (0.001").

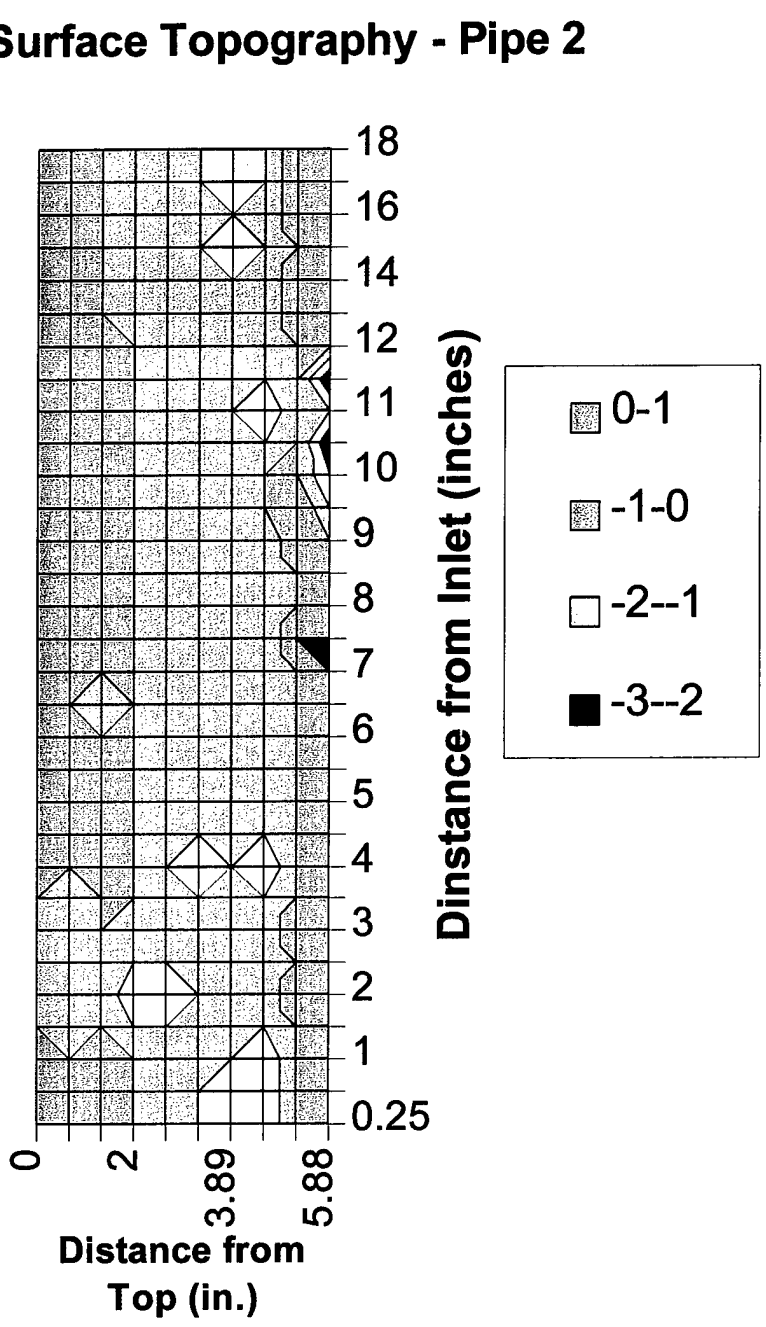

Figure 68 - Calcareous deposit coated Titanium/70:30 copper-nickel couple, mockup loop 2 after 365 days exposure. Surface topography of copper-nickel section as function of pipe clockwise orientation and distance from titanium. Legend denotes depth of corrosion/pitting in mils (0.001").

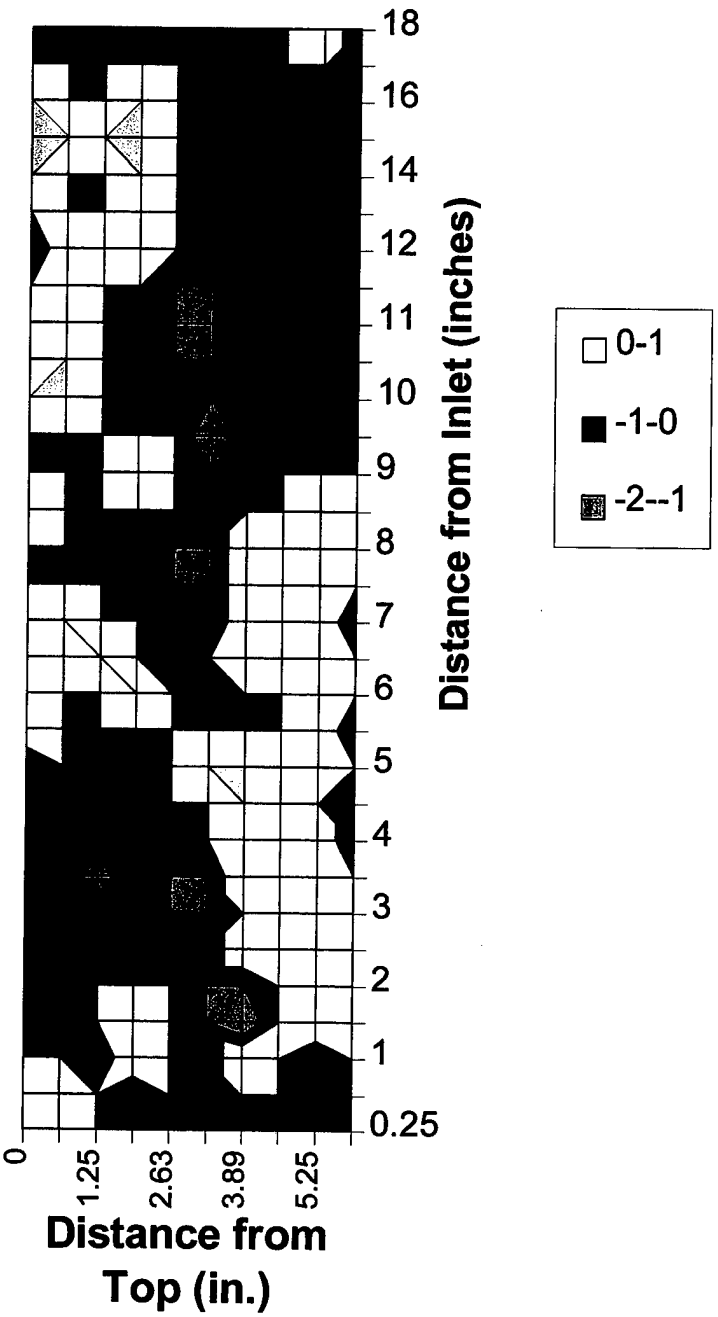

Figure 69 - Calcareous deposit coated Titanium/70:30 copper-nickel couple, mockup loop 8 after 623 days exposure. Surface topography of copper-nickel section as function of pipe clockwise orientation and distance from titanium. Legend denotes depth of corrosion/pitting in mils (0.001").

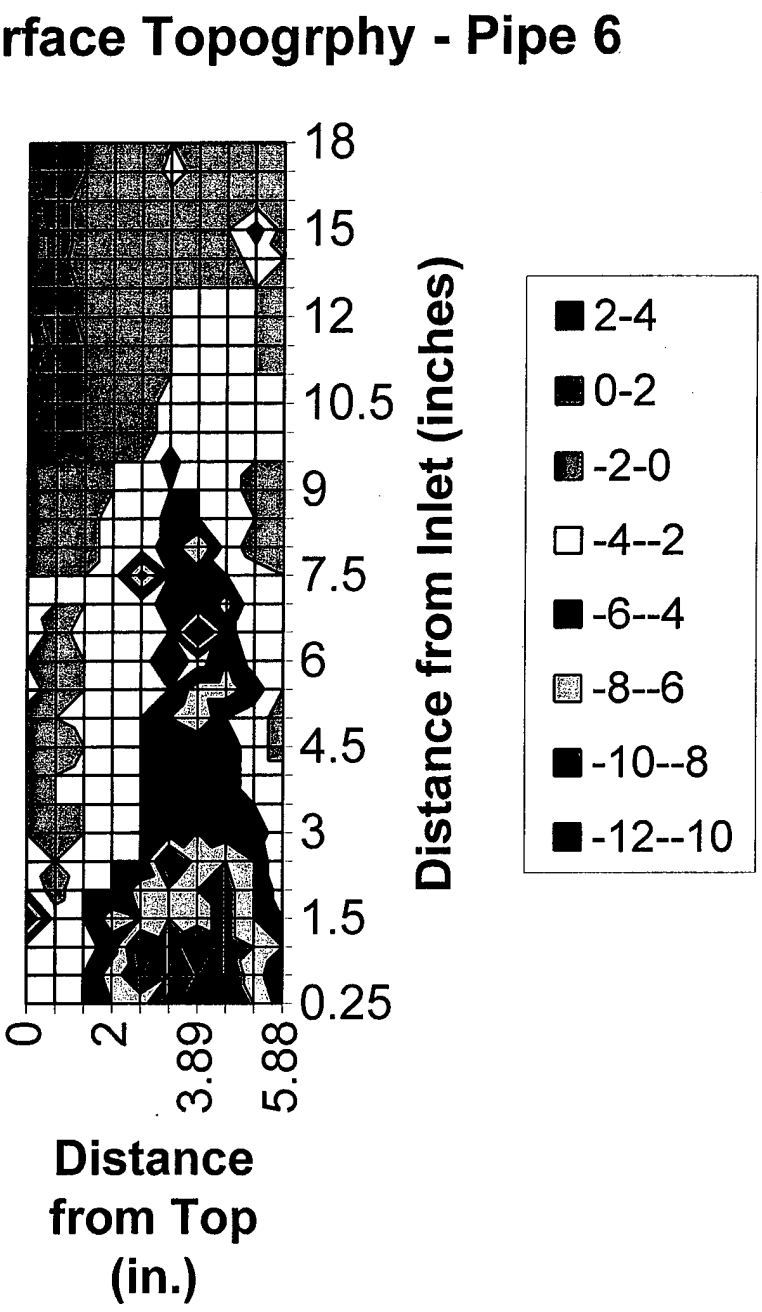

Figure 70 - Alloy 625/70:30 copper-nickel couple, mockup loop 6 after 379 days exposure. Surface topography of copper-nickel section as function of pipe clockwise orientation and distance from titanium. Legend denotes depth of corrosion/pitting in mils (0.001").

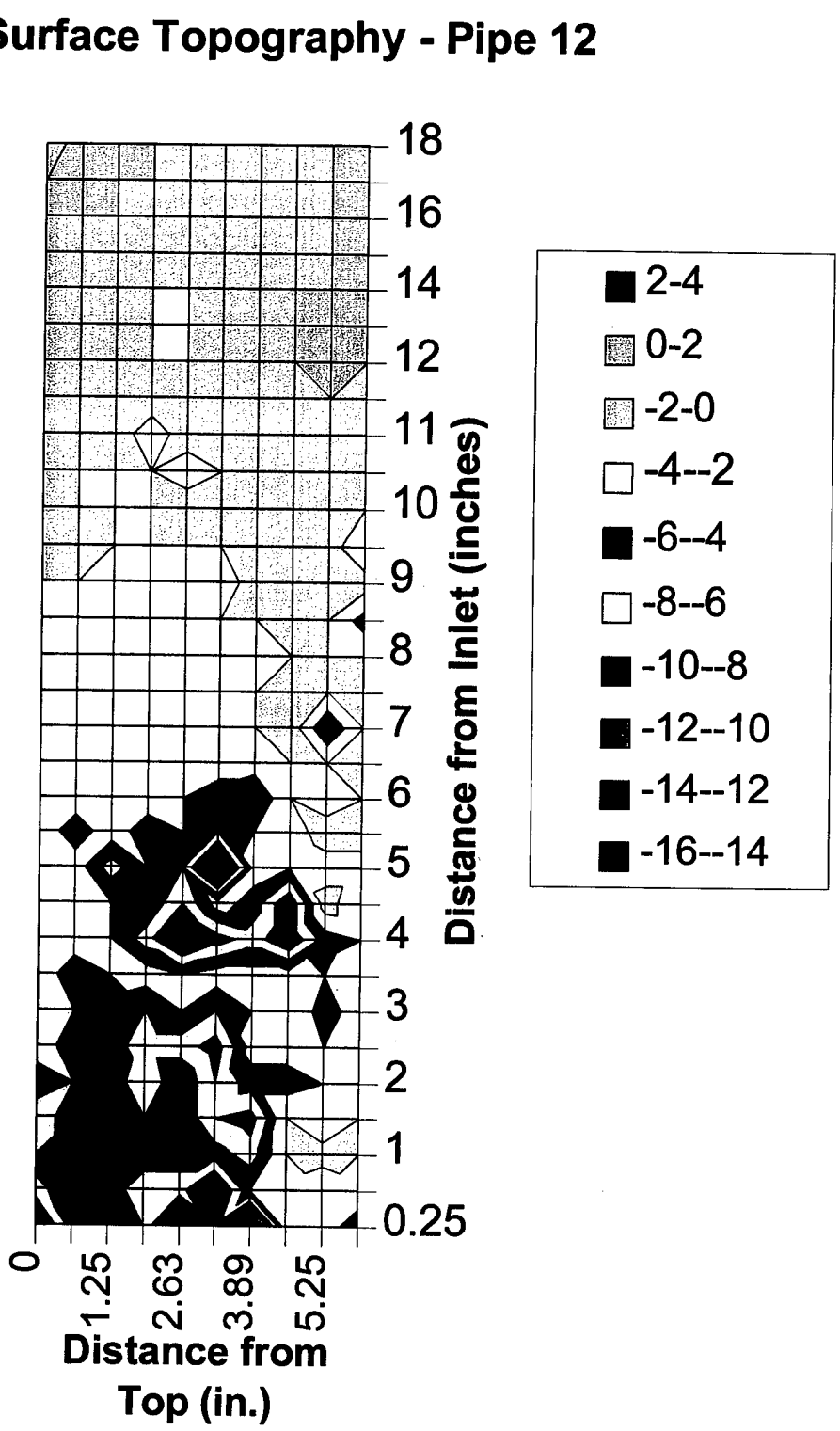

Figure 71 - Alloy 625/70:30 copper-nickel couple, mockup loop 12 after 379 days exposure. Surface topography of copper-nickel section as function of pipe clockwise orientation and distance from titanium. Legend denotes depth of corrosion/pitting in mils (0.001").

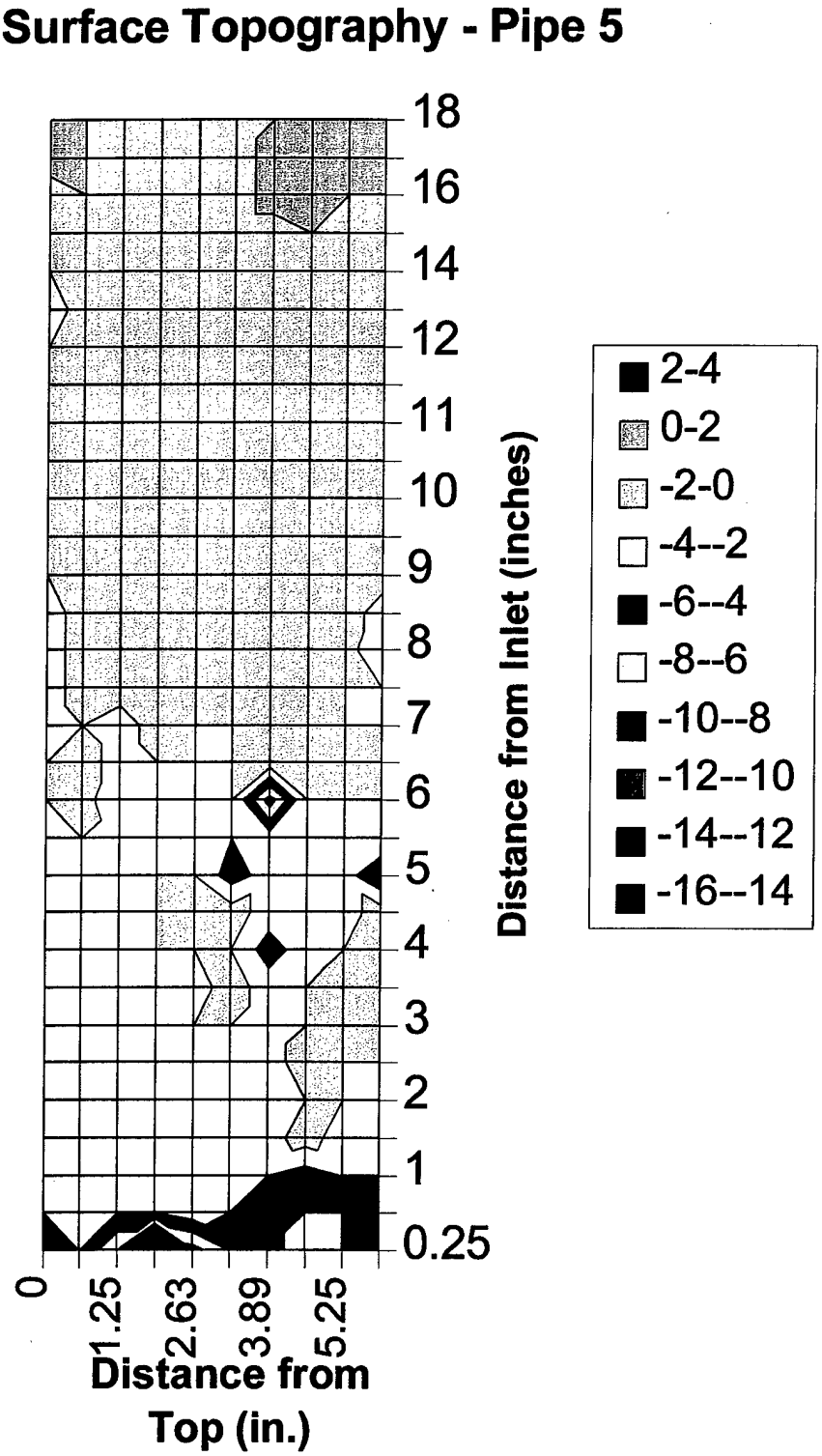

Figure 72 - Alloy 625/70:30 copper-nickel couple, mockup loop 5 after 379 days exposure with 10-in long PVC spacer between dissimilar alloy sections. Surface topography of copper-nickel section as function of pipe clockwise orientation and distance from titanium. Legend denotes depth of corrosion in mils (0.001").

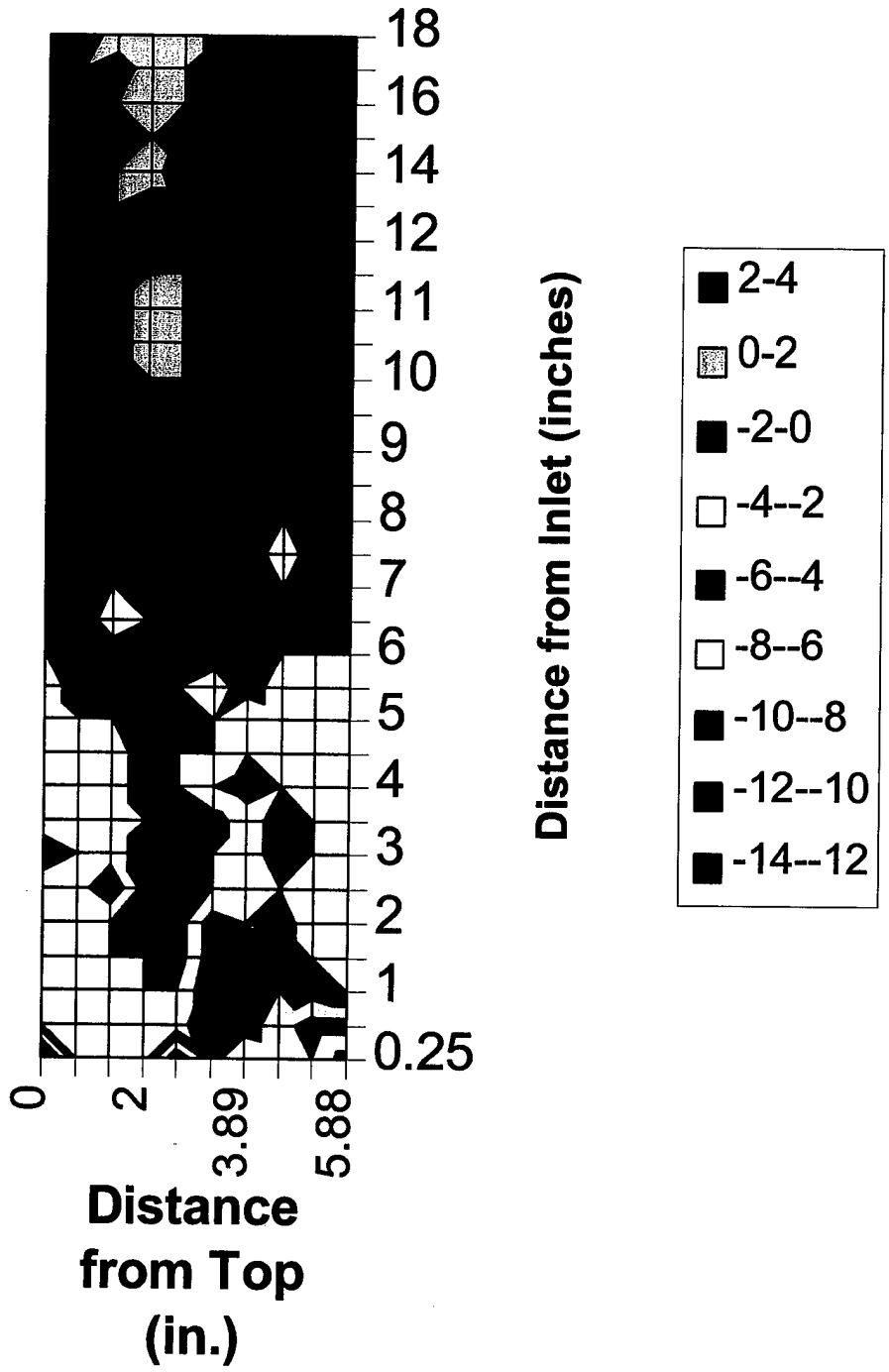

Figure 73 - Alloy 625/70:30 copper-nickel couple, mockup loop 11 after 379 days exposure with 10-in long PVC spacer between dissimilar alloy sections. Surface topography of copper-nickel section as function of pipe clockwise orientation and distance from titanium. Legend denotes depth of corrosion in mils (0.001").

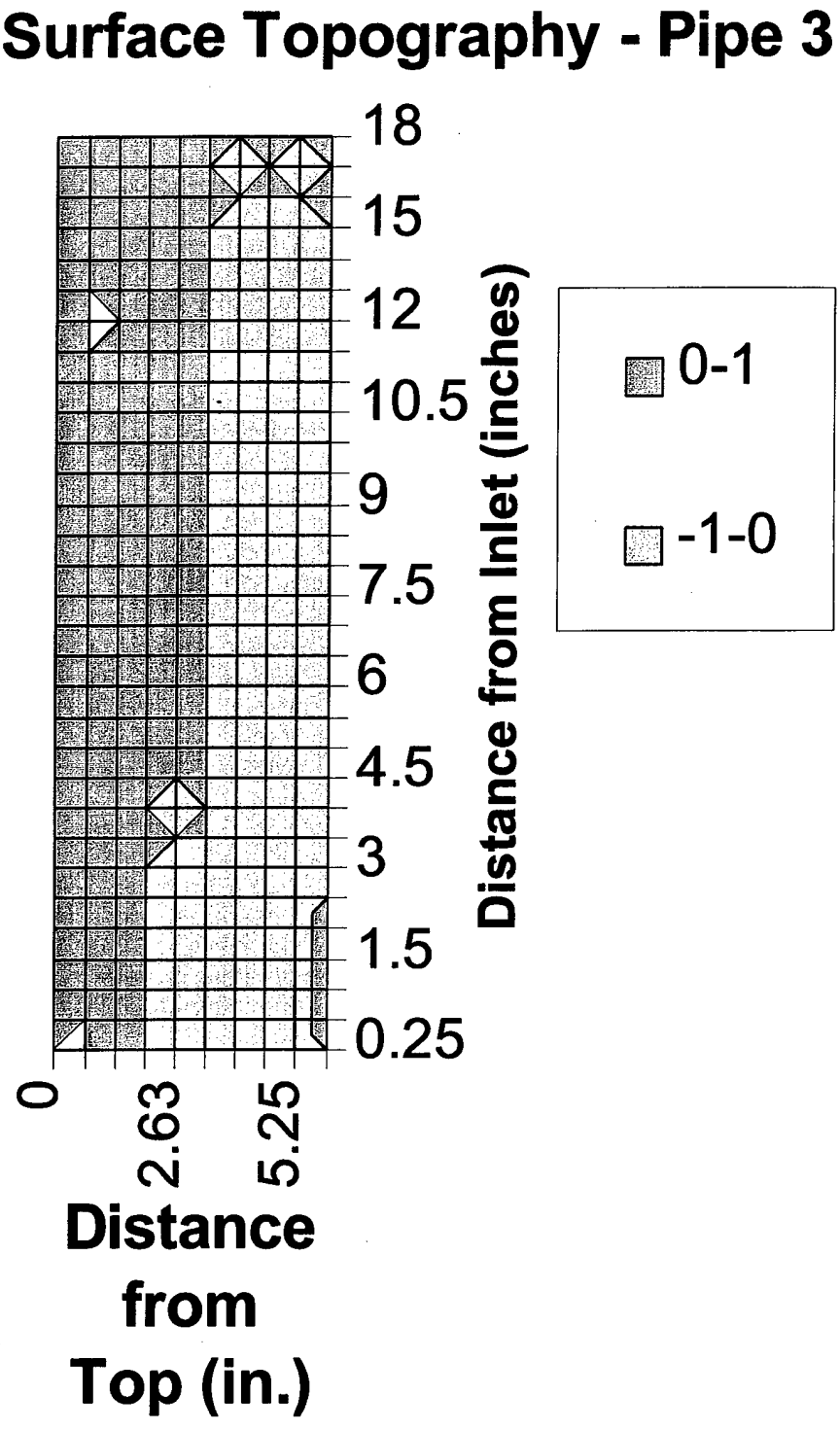

Figure 74 - Alloy 625/70:30 copper-nickel couple, mockup loop 3 after 340 days exposure under influence of CP. Surface topography of copper-nickel section as function of pipe clockwise orientation and distance from titanium. Legend denotes depth of corrosion/pitting in mils (0.001").

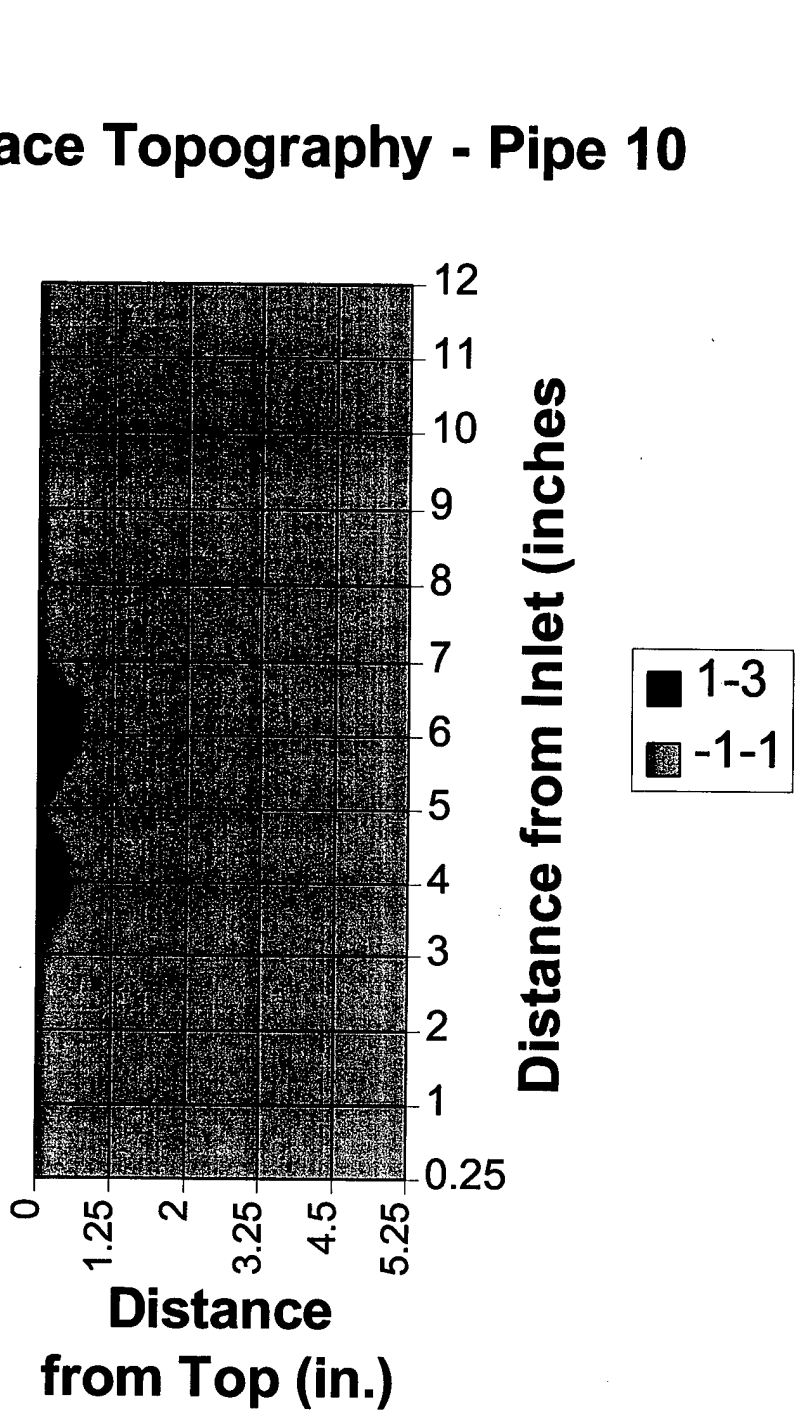

Figure 75 - Alloy 625/70:30 copper-nickel couple, mockup loop 10 after 343 days exposure under the influence bi-electrode device. Surface topography of copper-nickel section as function of pipe clockwise orientation and distance from titanium. Legend denotes depth of corrosion/pitting in mils (0.001").

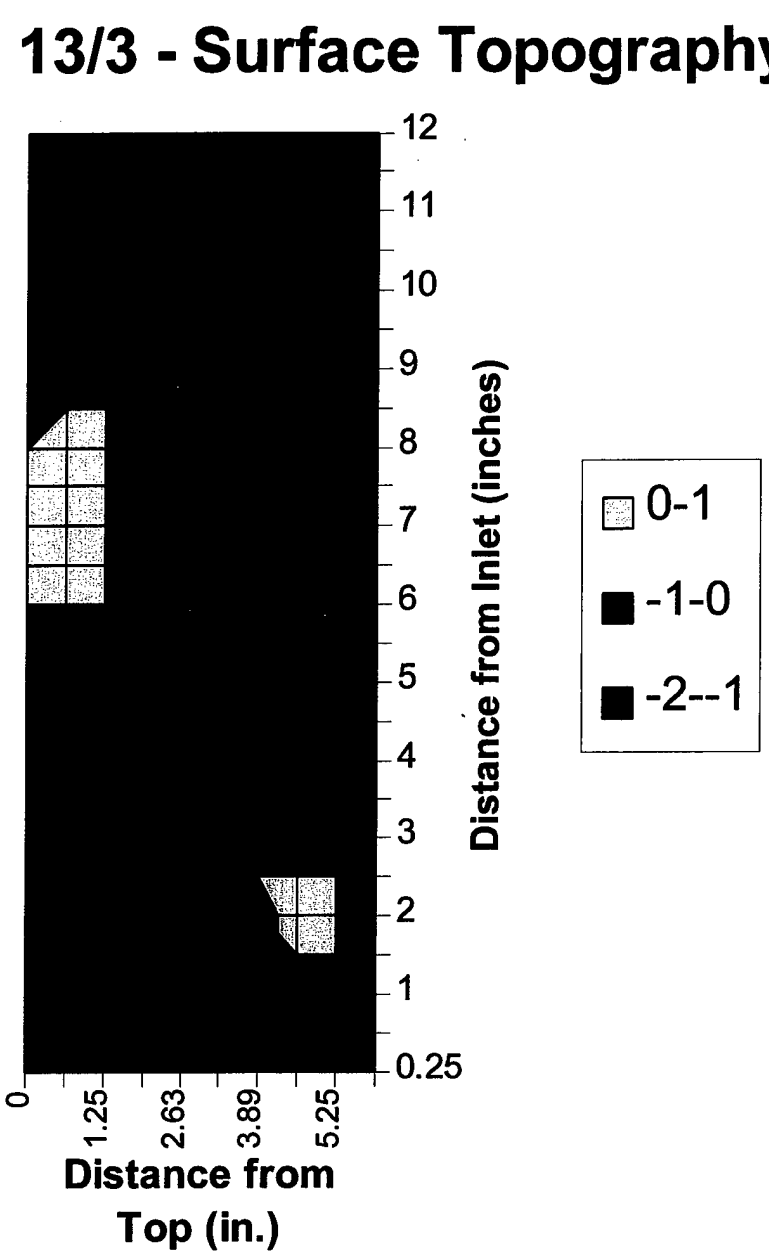

Figure 76 - Urethane-based coated titanium/70:30 copper-nickel couple, mockup loop 13/3 after 188 days exposure. Surface topography of copper-nickel section as function of pipe clockwise orientation and distance from titanium. Legend denotes depth of corrosion/pitting in mils (0.001"). Further examination revealed no surface pitting. Pipe 14/9 displayed similar behavior.

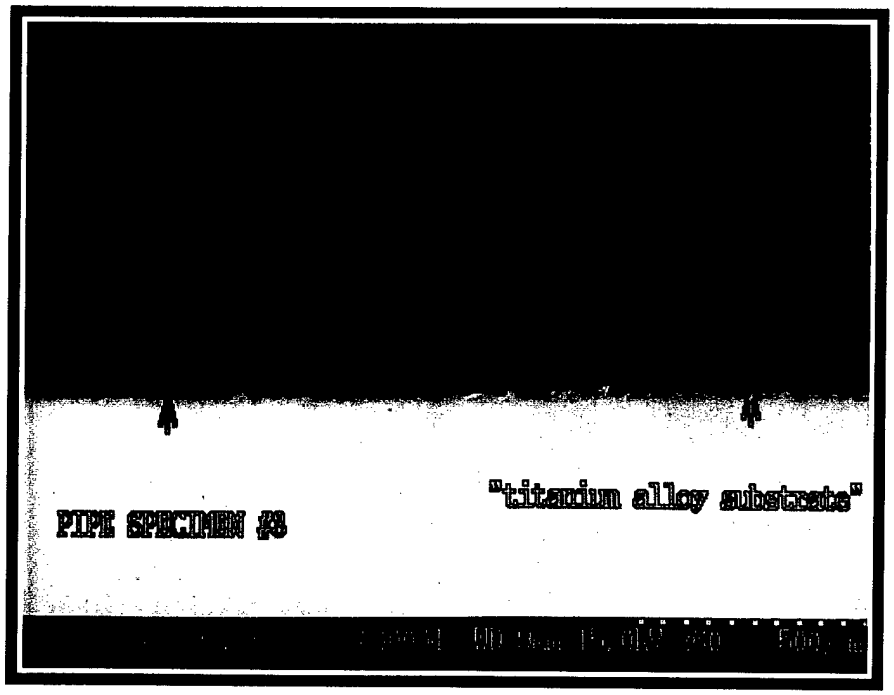

Figure 77 - SEM photomicrograph of urethane-based coating on titanium after the 188 day exposure. Coating is 420 μm thick and free of porosity. No delamination or decohesion observed.

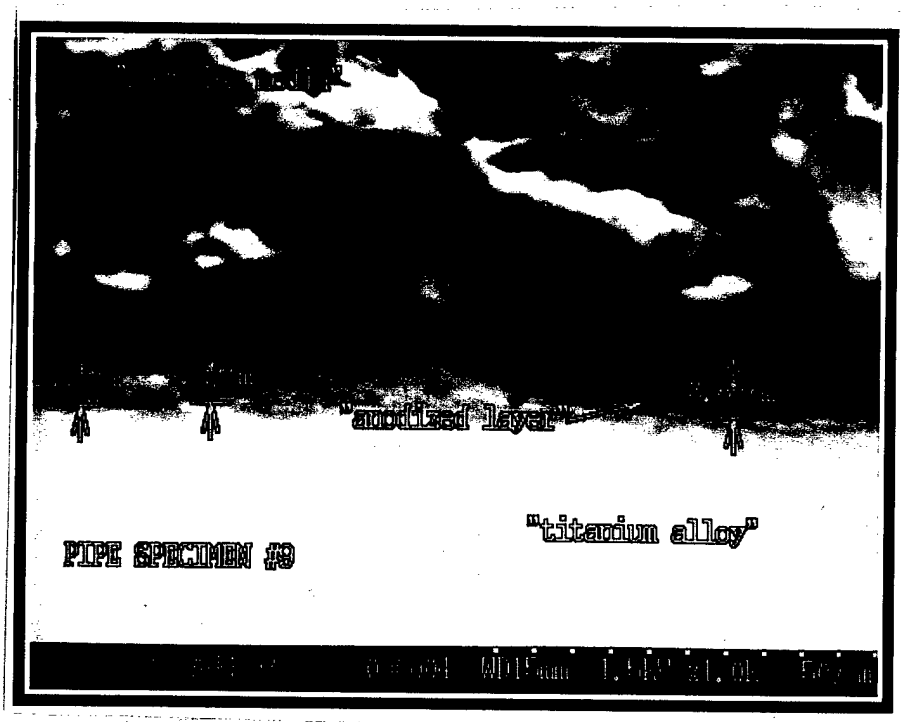

Figure 78 - SEM photomicrograph of anodized layer on titanium after the 188 day exposure. Anodized coating is 4 μm thick and free of porosity. No discontinuities at the titanium/anodized layer.

COATED TITANIUM SPECIMEN #3, 50X MAGNIFICATION

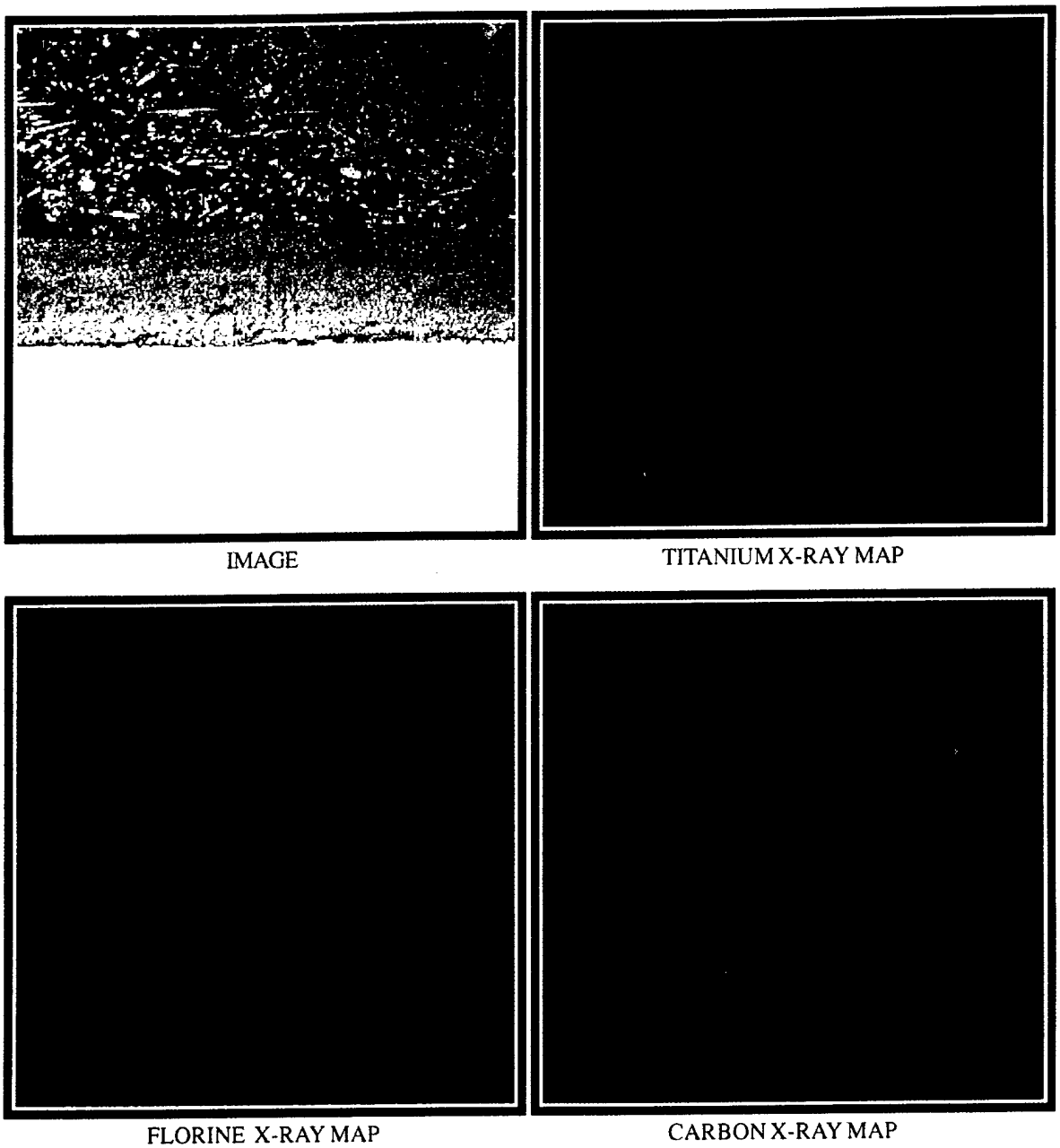

IMAGE | TITANIUM X-RAY MAP

FLORINE X-RAY MAP | CARBON X-RAY MAP

Figure 79 - Elemental X-ray maps of components of the urethane-based TICOMP ™ 10 organic coating on titanium.

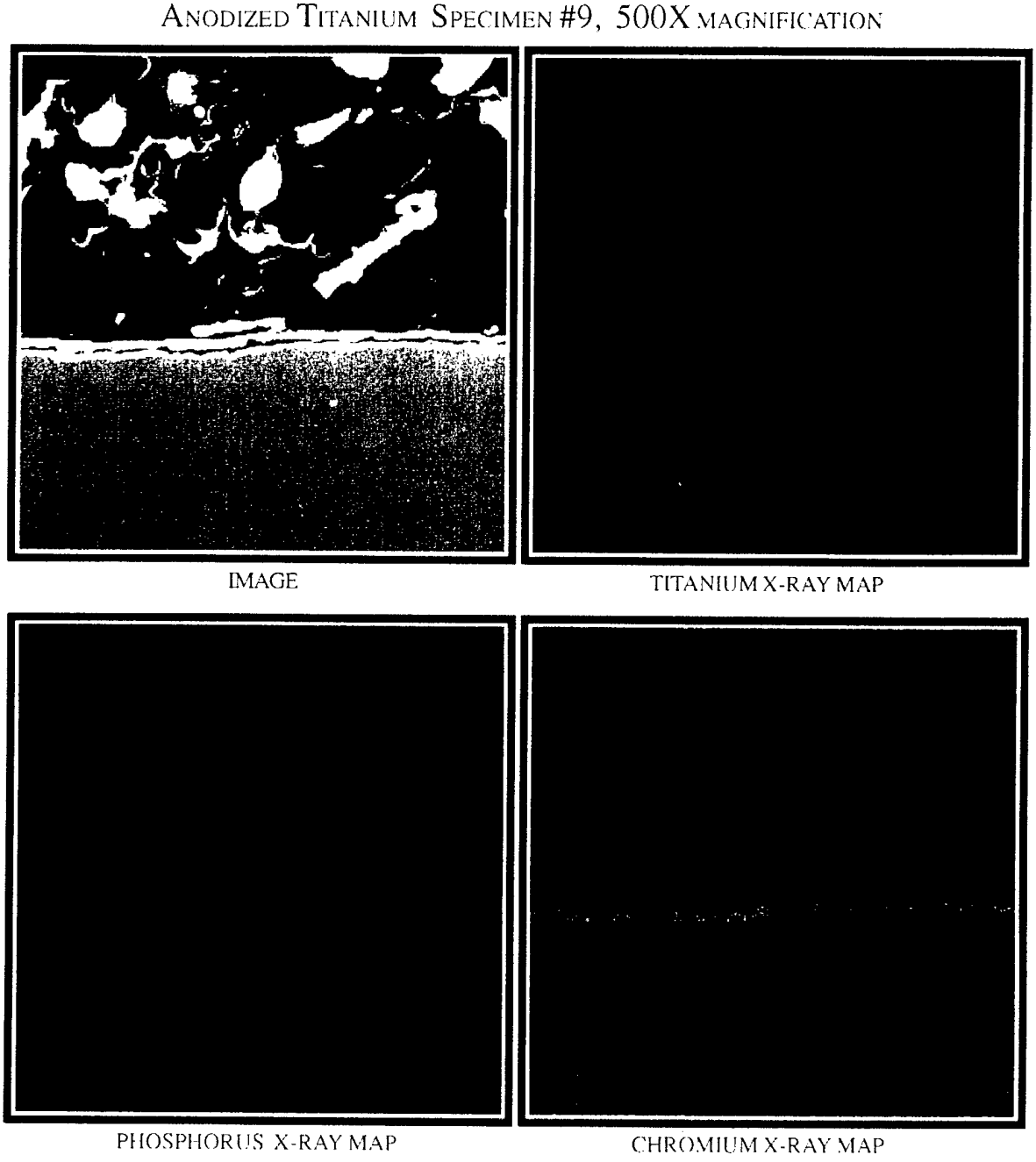

Figure 80 - Elemental X-ray maps of components of the sealed anodized TIODIZE ™ Type IV coating on titanium.

ANODIZED TITANIUM SPECIMEN #9, 500X MAGNIFICATION

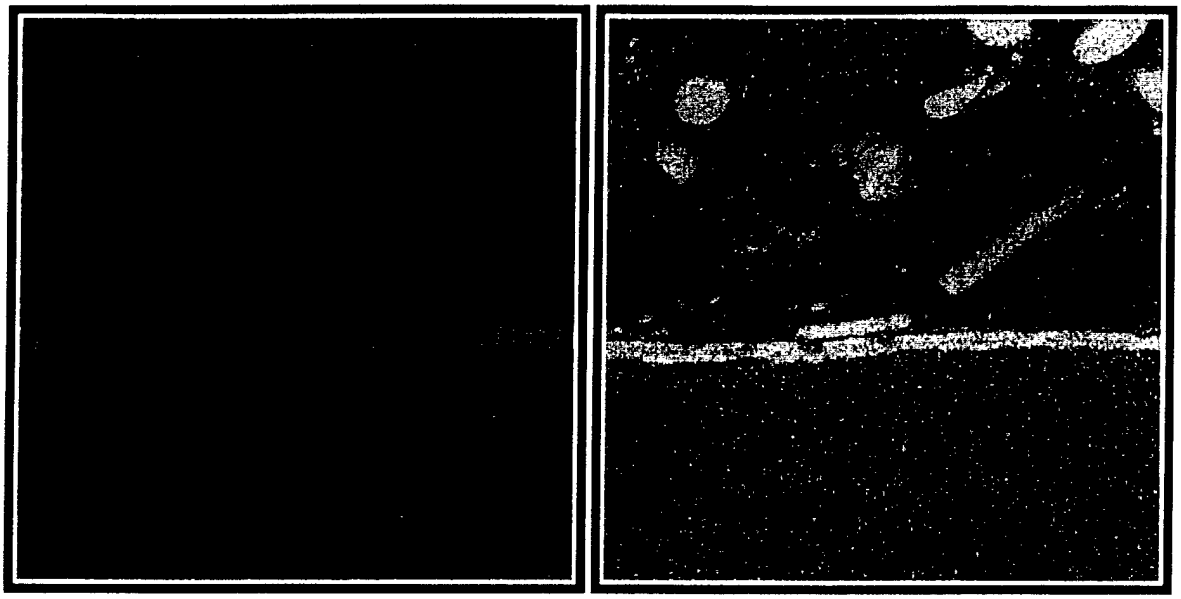

FLUORINE X-RAY MAP

OXYGEN X-RAY MAP

Figure 81 - Additional elemental X-ray maps of components of the sealed anodized TIODIZE ™ Type IV coating on titanium.

INITIAL DISTRIBUTION

Copies

4 Commander, Naval Sea Systems Command
2531 Jefferson Davis Hwy.
Arlington VA 22242-5167
1 - 03M (Kaznoff)
1 - 03M1 (Brinckerhoff)
1 - 03U3
1 - 03P

2 Office of Naval Research
1 - 332 (Pohanka)
1 - 332 (Sedriks)

1 Naval Research Laboratory
1 Code 6310 (Thomas)

2 DTIC

CENTER DISTRIBUTION

Copies

27 Commander, Naval Surface Warfare Center
Carderock Division
Bethesda, MD 20084-5000
1 Code 011 (Messick)
1 Code 0113
1 Code 0114
1 Code 60 (Morton)
1 Code 602
1 Code 603 (Cavallaro)
1 Code 61 (Holsberg)
1 Code 61s (Report Archive)
1 Code 612 (Aprigliano)
2 Code 613 (Ferrara)
1 Code 613 (Aylor)
1 Code 613 (Hays)
10 Code 613 (Shifler)
1 Code 614 (Montemarano)
1 Code 615 (DeNale)
1 Code 64 (Fischer)

Commanding Officer
Carderock Division
Naval Surface Warfare Center
Naval Ship Systems Engineering Station
Philadelphia, PA 19112-5083

1 Code 62 (Eichinger)